Title

The Role of Transcription Factors in RGC Development, Maintenance, and Survival

Author

Abed, Sadaf

Publication Date

2023

UNIVERSITY OF CALIFORNIA
SANTA CRUZ

THE ROLE OF TRANSCRIPTION FACTORS IN RETINAL GANGLION CELL DEVELOPMENT, MAINTENANCE, AND SURVIVAL

A dissertation submitted in partial satisfaction
of the requirements for the degree of

DOCTOR OF PHILOSOPHY

in

MOLECULAR, CELL AND DEVELOPMENTAL BIOLOGY

by

Sadaf Abed

December 2023

The Dissertation of Sadaf Abed is approved:

_____
Professor David A. Feldheim, chair

_____
Professor Bin Chen

_____
Professor Euiseok Kim

_____
Peter Biehl
Vice Provost and Dean of Graduate Studies

Table of Contents

List of Figures ..... *v*

Abstract ..... *vii*

Dedication ..... *ix*

Acknowledgements ..... *x*

Chapter 1: General Introduction 1

1.1 Vision 1

1.2 The Retina 2

1.3 Retina Development 4

1.4 Retinal ganglion cell subtype classification 8

1.5 Retinal ganglion cell development 12

1.6 Bibliography 23

Chapter 2: Adult Expression of Tbr2 is required for the maintenance but not survival of intrinsically photosensitive retinal ganglion cells 35

2.1 Abstract 36

2.2 Introduction 37

2.3 Results 39

2.4 Discussion 55

2.6 Materials and Methods 61

2.5 Supplementary Figures 67

2.7 Bibliography 70

Chapter 3: Isl2 is required in RPCs and RGCs for the survival of Isl2$^+$ RGC subtypes but not for eye-specific axon-pathfinding 77

3.1 Abstract 77

3.2 Introduction 78

3.3 Results 81

3.4 Discussion 93

3.5 Materials and Methods 99

3.6 Supplementary Figures 107

3.7 Bibliography 108

List of Figures

CHAPTER 1

FIGURE 1.1 SCHEMATIC OF THE MOUSE EYE AND RETINA 3

FIGURE 1.2 MODES OF RPC DIVISION DURING RETINA DEVELOPMENT 5

FIGURE 1.3 THE BIRTH ORDER OF CELLS IN THE MOUSE RETINA 6

FIGURE 1.4 SCHEMATIC OF RETINORECIPIENT REGIONS OF THE MOUSE BRAIN 11

FIGURE 1.5 VISUAL PATHWAY DEVELOPMENT 16

CHAPTER 2

FIGURE 2.1 CHARACTERIZATION OF TBR2^{CreER} EXPRESSION VISUALIZED BY TDTOMATO REPORTER IN WILDTYPE AND *TBR2^{KO}* RETINAS AND BRAINS 41

FIGURE 2.2 LOSS OF TBR2 IN ADULTHOOD RESULTS IN LOSS OF MELANOPSIN EXPRESSION BUT NOT CELL DEATH OF TOMATO^{+} RGCS. 45

FIGURE 2.3 ECTOPIC EXPRESSION OF TBR2 DOES NOT INDUCE MELANOPSIN EXPRESSION IN NON-TBR2 RGCS 48

FIGURE 2.4 TBR2-EXPRESSING RGCS PREFERENTIALLY SURVIVE OPTIC NERVE INJURY AND TBR2 INFLUENCES THEIR SURVIVAL 51

FIGURE 2.5 MEIS2 IS EXPRESSED IN THE MAJORITY OF TBR2-EXPRESSING DISPLACED AMACRINE CELLS AND IN A SUBSET OF TBR2-EXPRESSING RGCS 55

FIGURE S2.1 TBR2 IS NOT REQUIRED FOR TOMATO^{+} AC AND RGC DENDRITIC LAMINATION 67

FIGURE S2.2 MANY RGCS ARE INFECTED WITH TBR2-GFP-AAV2 BUT DO NOT EXPRESS MELANOPSIN 68

FIGURE S2. 3 *ISL1*^{CRE};*TBR2*$^{FLOX/FLOX}$ MICE LACK IPRGCS 68

FIGURE S2.4 MEIS2 LABELS MANY CELLS IN THE INL AND GCL 69

CHAPTER 3

FIGURE 3.1 GENERATION AND VALIDATION OF *ISL2* CONDITIONAL KNOCKOUT MICE... 83

FIGURE 3.2 EYE-SPECIFIC RETINOGENICULATE PROJECTIONS ARE UNAFFECTED IN ADULT *ISL1*^{CRE};*ISL2*$^{FLOX/FLOX}$ MICE..... 85

FIGURE 3.3 EYE-SPECIFIC RETINOGENICULATE PROJECTIONS ARE UNAFFECTED IN P0 *ISL1*^{CRE};*ISL2*$^{FLOX/FLOX}$ MICE 87

FIGURE 3.4 ISL2 IS REQUIRED FOR THE EXPRESSION OF ISL2-RGC SUBTYPE MARKERS FOXP2, ZIC1, AND TUSC5 90

FIGURE 3.5 THERE ARE FEWER RGCS IN THE ADULT ACCOMPANIED BY INCREASED APOPTOSIS AT P0, BUT MARKERS OF NON-ISL2 RGCS ARE UNAFFECTED IN *ISL2*^{CKO} 92

FIGURE S3.1 EYE-SPECIFIC RGC AXON TRACING TO THE SC AND THROUGH THE OPTIC TRACT 107

Abstract

The Role of Transcription Factors in RGC Development, Maintenance, and Survival

Sadaf Abed

Neurons in the mammalian central nervous system must be maintained throughout the lifetime of an organism because they are unable to regenerate. Retinal ganglion cells (RGCs) are the projection neurons of the retina that project directly to and form connections with the brain. Injury and disease can damage RGC axons, ultimately leading to RGC death and resulting in blindness. Learning how to protect these cells from dying and how to regenerate them after loss remain critical goals of vision neuroscientists; these endeavors aim to prevent blindness in those at risk and to restore vision in individuals already blind or visually impaired. Transcription factors regulate the development, maintenance, and survival of neurons. In this dissertation, I explore the roles of two transcription factors, Tbr2 and Isl2, in these important processes. My lab has previously demonstrated that Tbr2 is required during development for the formation and survival of intrinsically photosensitive RGCs (ipRGCs), a unique class of RGCs that are resilient to injury. The persistent expression of Tbr2 in a subset of adult RGCs, including all ipRGCs, led to the hypothesis that it is required for their maintenance and survival. In this dissertation, I establish that Tbr2 is indeed necessary for maintaining the defining aspect of ipRGC identity–the expression of the photopigment melanopsin, which enables them to directly respond to light. However, Tbr2 is not essential for the survival of adult ipRGCs. Additionally, I show that after optic nerve injury, ipRGCs lacking Tbr2 continue to survive better than non-ipRGCs,

albeit to a lesser extent than wildtype ipRGCs. The function of Isl2 in RGC development has not previously been elucidated because *Isl2* knockout mice die shortly after birth. Therefore, I designed an Isl2-flox mouse and subsequently generated *Isl2* conditional knockout mice in which *Isl2* is specifically removed from the retina. I demonstrate that Isl2 is required for the survival of Isl2-expressing RGC subtypes. My work uncovers important roles for Tbr2 and Isl2 in RGC development, maintenance, and survival. Additionally, the generation of a mouse with an *Isl2* conditional knockout allele provides a new tool that can be used to study the development of other cell types in which Isl2 is expressed.

Dedication

To my parents and grandparents.

To all the women and girls in Afghanistan, my ancestral homeland.

Acknowledgements

My PI, David Feldheim—thank you for giving me the opportunity to pursue my PhD in your lab, for teaching me most of the techniques I used in this dissertation, for allowing me independence, and for being a good person. You have shown me grace during some of the most difficult times of my life and I want you to know that I've appreciated it immensely.

Members of the Feldheim lab—thank you for making lab a warm and welcoming environment. I'd like to especially thank Jena Yamada, Yufei Si, and Brian Mullen for their moral support and friendship over the years. Jena, my fellow orange-lover, crybaby, and smoothie—thank you for your support as a friend and as a lab manager, you've helped me when I've needed it without me having to ask for it. I cherish all the meaningful talks that we've had. Yufei, you've been a joy to work with. Thank you for being so thoughtful and always providing a positive spin on things. Brian, thank you for making this introvert feel welcome at UCSC when I was a newcomer and chatting with me at MCD events. I am glad that you decided to postdoc in the Feldheim lab and that I've had the good fortune of working with you. I'd also like to thank my one and only undergrad during my time at UCSC, Nixuan Cai. I am excited for what the future has in store for you.

Bin Chen and Euiseok Kim—thank you for serving on my thesis advisory committee and for your helpful feedback.

James Ackman, Yi Zuo, Scott Lokey, and Melissa Jurica—thank you for serving on my qualifying exam committee. James, thank you for helping me assess the

feasibility of my initial proposal. I'm grateful for your approachability and advice over the years. Yi, thank you for challenging me during my rotation in your lab and in preparation for and during my qualifying exam. Your enthusiasm for science is inspirational. Scott, thank you for meeting with me before my exam and providing helpful feedback. Melissa, thank you for stepping in last minute.

Sasha Sher, I enjoyed my time as a roton in your lab. It was exciting to work on a project outside of my comfort zone and I thank you for your guidance.

I am grateful for the friends that I've made during grad school. We've had some of the best times together and some of the worst—I'm glad that we had each other. Hannah, thank you for being the type A to my type B and always offering a helping hand.

I'd like to acknowledge my undergrad and masters PI, Dr. Rachael French (I am still used to calling you Dr. French). Thank you for giving me a shot and for believing in me. The French lab holds a special place in my heart.

I'd like to thank my friends outside of school, who have provided unwavering love and support. I owe my sanity to y'all. Luis—TKM. Yazan—blade. Patty and Amanda, thank you for being my ride-or-dies and for making trips out to Santa Cruz to spend time with me. Maram and Sabrina, thank you for listening to my woes, for letting me practice my talks with you, and for always being down to have a good time.

My baby sisters Mina and Marjan have been here through it all. They were my first friends (and they had no choice in the matter ;)). I love you both. Thank you for

always being there for me and for believing in me...even when I didn't believe in myself.

None of this would have been possible without my parents, Abdul Rehim and Khalida. They have made tremendous sacrifices to provide me with the opportunity to pursue this trajectory, including risking their lives to leave Afghanistan during the Cold War. Today, women and girls in Afghanistan are unable to attend school…my heart breaks for them. I would have faced the same fate if my parents didn't have the courage to try to leave when they did. Mom and Dad, I love you dearly and I am so proud to be your daughter. Mom, I am in awe of your ability to do it all—thank you for all that you have done and continue to do to support me. I am lucky to have a mom that I know I can always count on and one that has served as an example of strength and bravery. Dad, you always pushed me to challenge myself and I am so grateful for it. Thank you for giving me a head start in my education by taking the time to teach me math before I was taught it in school…I still attribute my success in academics to this.

My husband David has been my rock and my best friend, without him I would not have made it through the last few years of this program. Thank you for encouraging me to be the best version of myself and for taking care of me both emotionally and physically. I know it hasn't been easy and I appreciate the sacrifices you've made to ensure my success. I love you so much and am beyond lucky to have such a supportive partner by my side.

Lastly, I'd like to acknowledge my grandparents who have all passed away but have each served as sources of inspiration. My maternal grandfather Mohammad

Solaiman was blind, and he is the reason I chose to pursue research of the visual system. My maternal grandmother Sultana Solaiman was the kindest women I knew, and I am grateful for her love. Sadly, I did not get the chance to meet my paternal grandparents. My paternal grandfather, Abdul Rahman Abed, was an academic and I am honored to follow in his footsteps. My paternal grandmother, Maryam Abed, lived the last few years of her life without an eye due to cancer and this further motivated me to study vision.

It really did take a village to get me here and I am eternally grateful to everyone that's played a role in helping me succeed.

The text of this dissertation includes a modified reprint of the following previously published material:

Abed S, Reilly A, Arnold SJ, Feldheim DA. 2022. Adult Expression of Tbr2 Is Required for the Maintenance but Not Survival of Intrinsically Photosensitive Retinal Ganglion Cells. Front Cell Neurosci. 16:1–13. doi:10.3389/fncel.2022.826590.

Author contributions for this publication are as follows: DF, AR, and SA conceived of and designed experiments. AR performed initial experiments not included in the manuscript. SA performed all experiments included in the manuscript, analyzed and interpreted the data, and wrote the manuscript with support from DF. SJA provided the Tbr2CreER mice. All authors discussed and commented on the results and approved of the submitted version of the manuscript.

Chapter 1: General Introduction

1.1 Vision

We use our senses to navigate and interact with the world around us. Our sense of vision is particularly important for effectively performing many of the ordinary tasks required in our daily lives. Activities such as preparing food, dressing oneself, maneuvering through the environment, reading, and driving become exceedingly difficult or impossible for the blind, leading to a reduced quality of life. Recent reports estimate that 43.3 million people worldwide are blind (Bourne et al., 2021a). With modernity's increasing life expectancies comes a rise in age-related forms of blindness; it is estimated that 61 million people will be blind by the year 2050 (Bourne et al., 2021a). Age-related forms of blindness such as glaucoma, age-related macular degeneration, and diabetic retinopathy are neurodegenerative and consequently irreversible. Neurons of the mammalian central nervous system (CNS) lack an inherent capacity to regenerate making their loss in neurodegenerative diseases permanent (Ramón y Cajal 1928; David and Aguayo 1981; Schwab and Thoenen 1985; Fawcett 1992; Ming and Song 2005; Curcio and Bradke 2018; Williams et al., 2020; Dyer and Cepko, 2000; Karl et al., 2008). Most forms of irreversible blindness involve the retina, an extension of the brain located in the eye, the structure in which visual processing begins.

1.2 The Retina

> "*In the study of this membrane [the retina] I for the first time felt my faith in Darwinism (hypothesis of natural selection) weakened, being amazed and confounded by the supreme constructive ingenuity revealed not only in the retina and in the dioptric apparatus of the vertebrates but even in the meanest insect eye... I felt more profoundly than in any other subject of study the shuddering sensation of the unfathomable mystery of life.*"
>
> -Santiago Ramón y Cajal

The retina is a layered, light-sensitive and responsive structure that lines the back of the eye (**Fig. 1.1**). It comprises three nuclear layers inhabited by the somata of 6 neuronal types and a glial cell type, separated by two plexiform layers where synapses form between the neurons (**Fig. 1.1B**). The photoreceptors (rods and cones) reside in the outer nuclear layer (ONL), the interneurons (horizontal cells, HCs; bipolar cells, BCs; and amacrine cells, ACs) reside in the inner nuclear layer (INL), the projection neurons (retinal ganglion cells, RGCs) reside in the ganglion cell layer (GCL), and the glial cells (Müller glia) span the entire depth of the retina with their cell bodies localized to the INL. Some RGCs and ACs are displaced and are found in the INL and GCL, respectively. Photons of light are first detected by photoreceptors and are transformed into electrical signals that are communicated to BCs and HCs in the outer plexiform layer (OPL). BCs go on to transmit this signal to RGCs directly via synapses formed between their axons and RGC dendrites in the inner plexiform layer (IPL) or indirectly via ACs. HCs and ACs modulate activity at the level of the OPL and IPL, respectively. RGCs are the sole output neurons of the retina making them responsible for transmitting visual information to the brain; they do so by extending their axons out of

the eye, through the optic nerve, and to various brain regions (Morin and Studholme et al., 2014; Martersteck et al. 2017).

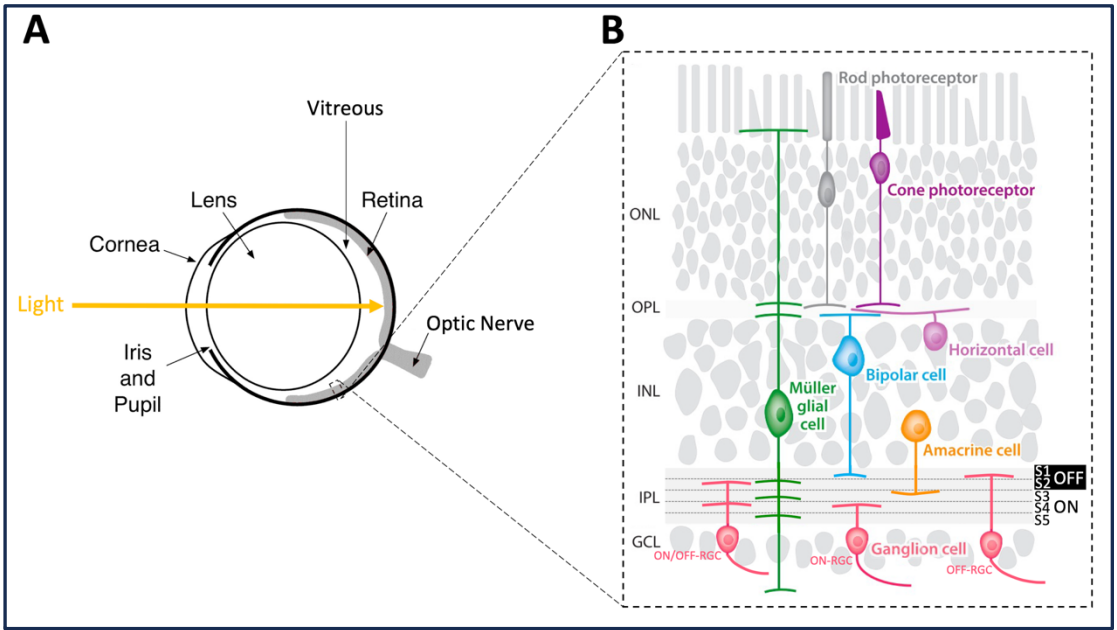

Figure 1.1 Schematic of the mouse eye and retina

(**A)** Light enters the eye and is detected by photoreceptors located at the back of the retina. (adapted from Nylen 2010) **(B)** RGCs that respond to light decrements have dendrites that laminate within OFF sublaminae of the IPL (S1-S2) and those that respond to light increments have dendrites that laminate within ON sublaminae (S4-S5). INL=inner nuclear layer; IPL=inner plexiform layer; ONL=outer nuclear layer; OPL=outer plexiform layer. (adapted from Petridou and Godinho 2022)

Glaucoma is the leading cause of irreversible blindness worldwide (Bourne et al., 2021b) and is a condition in which RGCs degenerate, severing the communication pathway between the eye and the brain. To be able to one day treat irreversible blindness via replacement of lost cell types, it is imperative that we learn how to generate them. We can gain insights by turning towards development and understanding how nature achieves this. This dissertation will focus on RGCs.

1.3 Retina Development

A common multipotent retinal progenitor cell (RPC) gives rise to all the cell types of the retina (Young 1983, 1985; Turner and Cepko 1987; Turner et al., 1990). RPCs initially undergo symmetric mitotic divisions to expand the RPC pool (**Fig. 1.2**) (Livesey and Cepko 2001; Petridou and Godinho 2022). After the expansion phase, they divide asymmetrically to produce one post-mitotic cell and one mitotic RPC. By late retinal development, RPCs undergo symmetric post-mitotic divisions, producing two differentiated cells that can be of the same class or of different classes (i.e. one rod and one Müller glia or two rods). Different retinal cell types are generated in sequential but overlapping waves with RGCs being the first born type, and Müller glia being the latest born type (**Fig. 1.3**). The birth order of cells in the retina is mostly conserved across vertebrate species (Jacobson 1968; Young 1985; Holt et al., 1988; Prada et al., 1991; La Vaile et al., 1991). Several studies have sought to determine what contributes to an RPC's production of one cell type over another, finding that intrinsic factors confer competence for generating distinct types and that extrinsic factors can influence their decision/outcome. Classic heterochronic transplantation studies showed that RPCs have intrinsically different potentials: when early RPCs from the embryonic retina are placed in a postnatal retinal environment, they continue to generate early cell types (Belliveau & Cepko 1999, Rapaport et al. 2001) and when late RPCs from the postnatal retina are placed in an embryonic retinal environment, they continue to generate late cell types (Belliveau et al., 2000). Additionally, when RPCs are cultured in the absence of other retinal cells, they continue to generate cell types in accordance

with their temporal identity (Reh and Kijavin, 1989; Cayouette et al., 2003). In an experiment performed in chick, RPCs cultured with older retinal cells did not produce RGCs unless RGCs were removed from the culture, demonstrating extrinsic influence on fate (Waid and McLoon 1997). This finding suggests that RGCs can provide feedback inhibition to RPCs, and indeed it was later determined that they do so by producing sonic hedgehog (shh; Wang et al., 2005)—a signaling molecule that regulates the development of many tissues (Carballo et al., 2018).

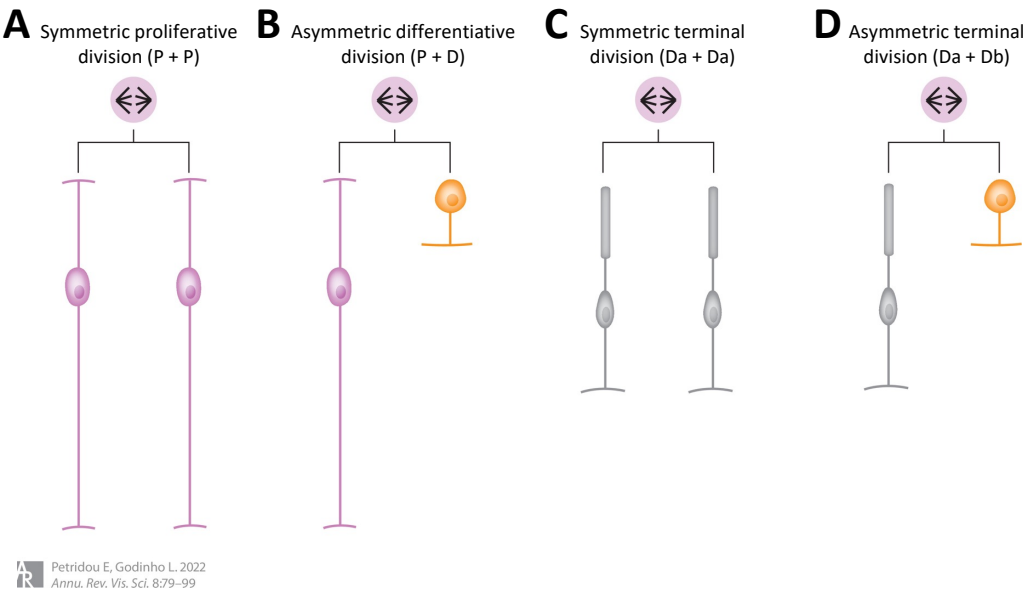

Figure 1.2 Modes of RPC division during retina development

RPCs can divide symmetrically to produce two progenitor cells **(A)** or two differentiated cells of the same type **(C)**; they can also divide asymmetrically to produce one progenitor cell and one differentiated cell **(B)** or two differentiated cells of different types **(D)**. P= progenitor cell, D= postmitotic differentiated cell (neuron or Müller glia). (adapted from Petridou and Godinho 2022)

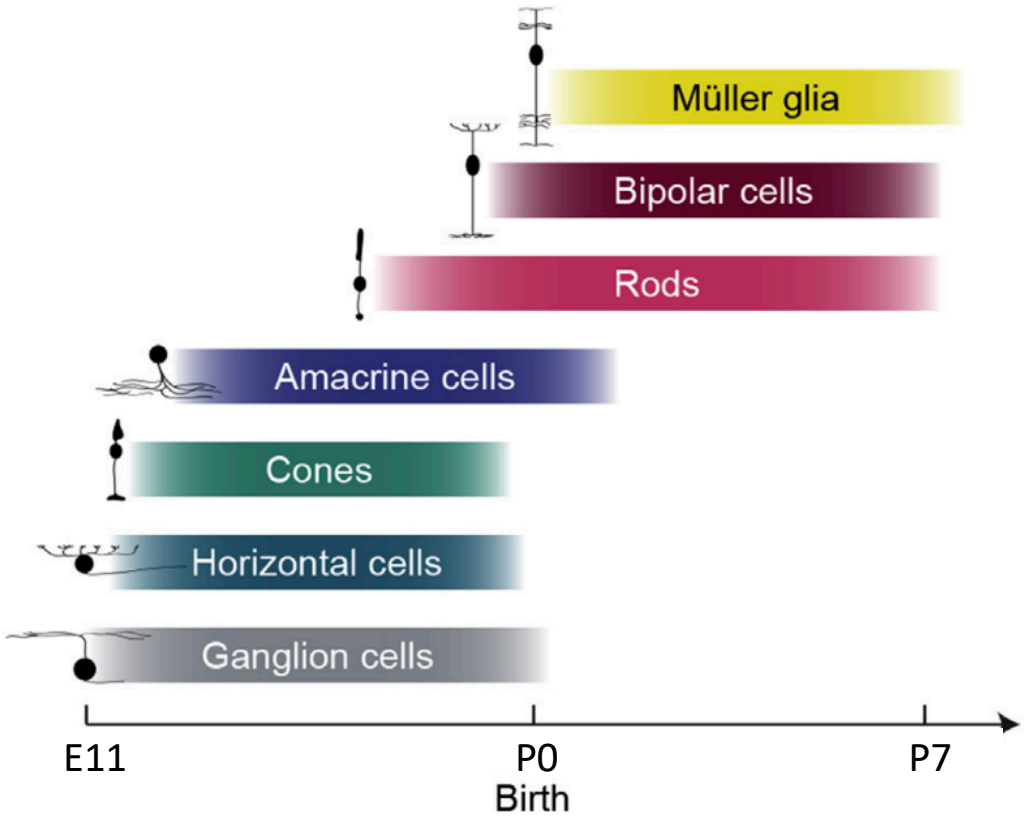

Figure 1.3 The birth order of cells in the mouse retina

Retinal neurogenesis begins with the birth of RGCs on embryonic day 11 (E11) and continues through the first postnatal (P) week. (adapted from Kerschensteiner 2020)

Intrinsic differences in RPC competence can be ascribed to the varied expression of transcription factors termed "temporal identity factors" or "TIFs" (reviewed in Santos-França et al., 2022). These factors act upstream of transcription factor networks that specify cell fate. Ikaros (Ikzf1) is a TIF that is required for the generation of early cell types including RGCs but is dispensable for the generation of late cell types, as demonstrated by loss of function analysis (Elliott et al., 2008). Casz1 is a TIF that induces the production of mid and late-born types when misexpressed and

whose function is to suppress the generation of early-born types (Mattar et al., 2015); its expression is inhibited by Ikzf1. Pou2f1 is a recently discovered TIF that is sufficient for the production of cones and also acts to inhibit Casz1 (Javed et al., 2020). Select transcription factors confer proliferative competence to RPCs–Pax6, Chx10, Sox2, Lhx2–and when genetically ablated, there are insufficient numbers of RPCs leading to underdeveloped retinas (Burmeister et al., 1996; Marquardt et al., 2001; Taranova et al., 2006; Gordon et al., 2013). Single-cell RNA sequencing (scRNAseq) of mouse RPCs at different stages throughout development has shown that they can be broadly divided into "primary" or "neurogenic" and within these two classes, subdivided into early or late RPCs (Clark et al., 2019). Primary RPCs express cell cycle related genes whereas the neurogenic class express proneural transcription factors. Results gleaned from this study support the findings of previous work; the TIFs I introduced earlier, Casz1 and Pou2f1, are expressed in RPCs isolated at timepoints that are consistent with when cells that they provide competence for are generated (cones and rods, respectively). Neurogenic RPCs were found to express the basic helix-loop-helix (BHLH) transcription factors Atoh7 (also known as Math5), Neurog2, and Olig2, reinforcing findings from lineage tracing studies that indicate these factors promote terminal neurogenic divisions (Brzezinski et al., 2011; Hafler et al., 2012). Neurogenic BHLH factors regulate the expression of master regulatory transcription factors that define cell fate, such as Otx2, which specifies a photoreceptor identity (Nishida et al., 2003). Master regulatory transcription factors activate the expression of factors that lead to the differentiation of one cell type while repressing factors that specify other

types. For example, Otx2 has a cross-inhibitory relationship with the transcription factors Dlx1/2, master regulators of a late-born RGC fate (de Melo et al., 2005): Otx2 represses Dlx1/2 (Ghinia Tegla et al., 2020) and Dlx1/2 reciprocally repress Otx2 (de Melo et al., 2005). While many factors that contribute to the specification of the 7 retinal cell types have been uncovered, far less is known about how subtypes within these classes are generated. RGCs make up the smallest proportion of retinal cells, amounting to about 1% of the total population, but are remarkably diverse with over 40 subtypes identified in mice (Tran et al., 2019; Goetz et al., 2022). A major goal in the field is dissecting the intricacies of each subtype and understanding how such diversity of cell types is generated.

1.4 Retinal ganglion cell subtype classification

RGC subtypes have been classified based on their differences in morphology, physiology, and molecular properties (Sanes and Masland 2015; Bae et al., 2018; Baden et al., 2016; Rheaume et al., 2018; Tran et al., 2019; Goetz et al., 2022). Morphologically, RGC subtypes differ in their soma and dendritic arbor sizes as well as in the complexity and stratification pattern within the IPL of their dendritic arbors (Bae et al., 2018; Goetz et al., 2022). An RGC's dendritic lamination pattern is related to its physiology (Goetz et al., 2022) and its dendritic field size is linked to its receptive field size (Lefebvre et al., 2015). Physiologically, they differ in the type and size of stimulus they respond to, and the temporal dynamics of their responses (i.e. transient or sustained responses). Broadly, some subtypes respond to light increments (ON-RGCs), others to light decrements (OFF-RGCs), and others to both increments and

decrements of light (ON-OFF RGCs). ON-RGCs have dendrites that laminate closer to the GCL in sublamina 4 or 5 (S4,S5) of the IPL, OFF-RGCs have dendrites that laminate closer to the INL in S1-S2, and ON-OFF RGCs have dendrites that are bistratified or that laminate within S3 (**Fig. 1.1B**). Additionally, different molecules are expressed in each RGC subtype and can be used to distinguish them from one another. ScRNAseq has allowed for the large-scale classification of RGCs by their unique molecular signatures, each subtype being defined by its expression of a combination of transcripts, and very rarely by a single factor (Tran et al., 2019). Recently, Goetz et al. (2022) profiled RGCs using all 3 criteria and aligned their data to large-scale morphological (Bae et al., 2018) and molecular (Tran et al., 2019) datasets to generate a unified RGC atlas.

Each RGC subtype is tuned to a particular visual feature (reviewed in Kerschensteiner 2022) and tiles the retina to form a mosaic such that the cells within a subtype exhibit regular spacing, ensuring that each part of the visual field is sampled (Wässle and Riemann 1978; reviewed in Sanes and Masland 2015). RGCs can be broadly functionally divided into image-forming and non-image-forming. Image-forming RGCs include those that detect visual features such as contrast or motion direction, with the latter types designated direction-selective ganglion cells (DSGCs); DSGC subtypes respond to motion in one of the four cardinal directions (up, down, backward, forward). Non-image-forming RGCs are involved in subconscious aspects of vision; this class includes luminance detectors that participate in circadian photoentrainment, a behavior that is mediated by RGCs that are intrinsically

photosensitive RGCs (ipRGCs). RGCs project to >50 subcortical regions of the brain, each responsible for mediating unique functions (**Fig. 1.4**) (Morin and Studholme et al., 2014; Martersteck et al., 2017). There are 2 major retinorecipient regions of the brain, both of which mediate image-forming vision: the superior colliculus (SC) receives projections from 85-90% RGCs (Ellis et al., 2016) and the dorsal lateral geniculate nucleus (dLGN) of the thalamus is innervated by ~30% of RGCs (Martin 1986), the majority of which also innervate the SC (Ellis et al., 2016). The superior colliculus is a midbrain structure where sensory information of multiple modalities is integrated and used to direct behavioral outputs such as eye and head movements in the direction of salient stimuli (Ito and Feldheim 2018). The dLGN relays information from the retina to the visual cortex and is involved in conscious image formation (Guido 2018). Non-image-forming RGCs project to regions such as the suprachiasmatic nucleus of the hypothalamus (SCN) and the olivary pretectal nucleus (OPN), responsible for circadian photoentrainment and the pupillary light reflex, respectively (**Fig. 1.4**). The generation of this vast diversity in RGC subtypes is not well-understood and remains a critical area of research. What do we know about RGC development and how does a newly postmitotic immature RGC differentiate into one of the >40 unique subtypes?

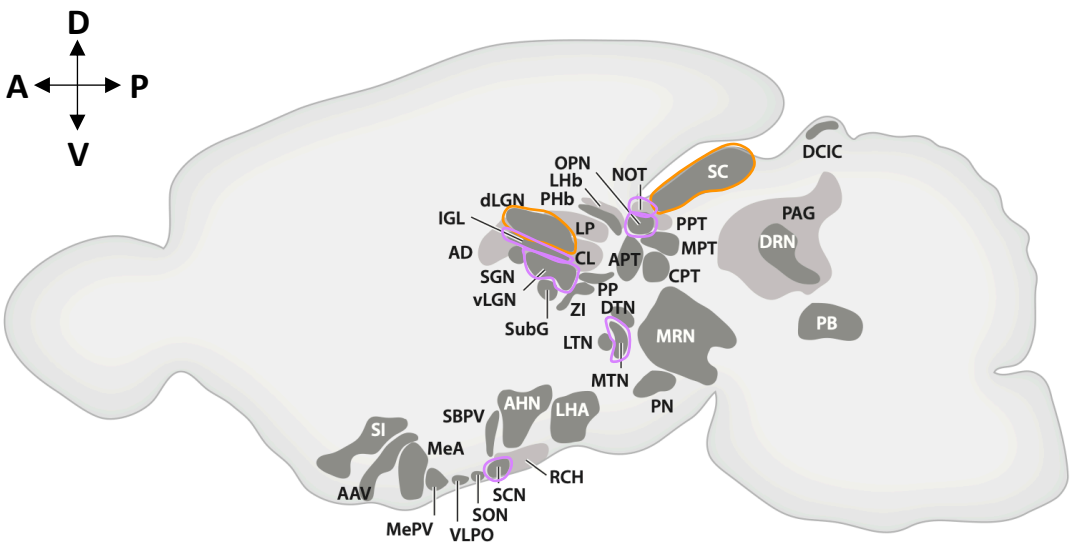

Figure 1.4 Schematic of retinorecipient regions of the mouse brain

Most RGCs innervate the major image-forming regions, highlighted in orange. Non-image-forming regions are highlighted in lavender. Abbreviations: D, dorsal; V, ventral; A, anterior; P, posterior; AAV, anterior amygdaloid area, ventral; AD, anterodorsal thalamic nucleus; AHN, anterior hypothalamic area; APT, anterior pretectal nucleus; CL, centrolateral thalamic nucleus; CPT, commissural pretectal nucleus; DCIC, dorsal cortex of the inferior colliculus; dLGN, dorsolateral geniculate nucleus of the thalamus; DRN, dorsal raphe nucleus; DTN, dorsal terminal nucleus; IGL, intergeniculate leaflet; LHA, lateral hypothalamic area; LHb, lateral habenula; LP, lateral posterior nucleus of the thalamus; LTN, lateral terminal nucleus; MeA, medial amygdala, anterior; MePV, medial amygdala, posteroventral; MPT, medial pretectal nucleus; MRN, midbrain reticular nucleus; MTN, medial terminal nucleus; NOT, nucleus of the optic tract; OPN, olivary pretectal nucleus; PAG, periaqueductal gray; PB, parabrachial nucleus; PHb, perihabenular nucleus; PN, paranigral nucleus; PP, peripeduncular nucleus; PPT, posterior pretectal nucleus; RCH, retrochiasmatic area; RGC, retinal ganglion cell; SBPV, subparaventricular zone; SC, superior colliculus; SCN, suprachiasmatic nucleus; SGN, suprageniculate nucleus; SI, substantia innominate; SON, supraoptic nucleus; SubG, subgeniculate nucleus; vLGN, ventrolateral geniculate nucleus; VLPO, ventrolateral preoptic area; ZI, zona incerta. (adapted from Kerschensteiner 2022)

1.5 Retinal ganglion cell development

1.5.1 Molecular factors involved in differentiation and specification

The BHLH transcription factor Atoh7 is transiently expressed in RPCs and is necessary for RGC development; Atoh7-null mice display an almost complete loss of RGCs (>95% reduction) and lack optic nerves (Brown et al., 1998; Brown et al., 2001; Wang et al., 2001). Lineage analysis studies have revealed that only 11% of Atoh7^{+} RPCs become RGCs, with the remainder giving rise to ACs, HCs, and photoreceptors, and that only 50% of RGCs are from the Atoh7 lineage (Yang et al., 2003; Feng et al., 2010; Brzezinski et al., 2012). These data suggest that Atoh7 does not specify an RGC fate, but rather acts as a competence factor that permits an RGC fate. Two transcription factors downstream of Atoh7, Islet1 (Isl1) and Brn3b (also known as Pou4f2), are able to rescue the loss of RGCs in Atoh7-null mice when expressed together in its place suggesting that Atoh7 activates the transcription of downstream factors that lead to RGC differentiation (Wu et al., 2015). Data from a recent study where researchers inactivated the proapoptotic gene Bax in Atoh7-null mice provide a new explanation for Atoh7's role in RGC development (Brodie-Kommit et al., 2021). With cell death inhibited in Atoh7-null mice, there is only a 20% reduction in RGCs relative to Bax-null controls and the surviving RGCs express normal levels of Isl1 and Brn3b. However, these mice display severe defects in axon guidance and vasculature development. Their results suggest that Atoh7 acts as a pro-survival factor that is required for RGC viability and for directing axons to the optic nerve head (Brodie-Kommit et al., 2021).

The SoxC family of transcription factors regulate RGC specification. Loss of function of Sox4 or Sox11 alone modestly impacts RGC development, but Sox4/11 double mutants display a significant loss of RGCs (Jiang et al., 2013). There is an even greater effect on RGC development when Sox12 is additionally deleted in triple knockout mice (Kuwajima et al., 2017).

Dlx1 and Dlx2 are necessary for the specification of late-born RGCs; Dlx1/2 double knockout mice show a selective loss of late-born RGCs, amounting to a loss of about 33% (de Melo et al., 2005; Zhang et al., 2017). Dlx1 and Dlx2 directly activate the expression of Brn3b (Zhang et al., 2017). When Brn3b is also knocked out in Dlx1/2 mutants to produce triple knockout mice, there is a 95% loss of $Brn3a^{+}$ RGCs at embryonic day 18 (E18) accompanied by an increase in amacrine cell production (Zhang et al., 2017).

Brn3b and Isl1 are co-expressed in newly post-mitotic RGCs before they acquire subtype identity. They are both required for RGC differentiation and are downstream of Atoh7 and SoxC transcription factors (Yang et al., 2003; Jiang et al., 2013). Both Brn3b-null mice and Isl1-(retina)null mice display defects in RGC differentiation and survival but not specification (Gan et al., 1999; Mu et al., 2008). ~70% of RGCs undergo apoptosis in both Brn3b-null mice (Gan et al., 1996; Erkman et al., 1996) and in Isl1-(retina)null mice (Pan et al., 2008). In retinas in which both Brn3b and Isl1 are knocked out, there is recapitulation of the phenotype observed in Atoh7-null mice, where >95% of RGCs undergo apoptosis (Pan et al., 2008).

T-box transcription factors are important for RGC subtype specification. The T-box transcription factor Tbr2 (also known as EOMES) is expressed in newly postmitotic RGCs and in mature RGCs (Mao et al., 2008; Mao et al., 2014; Sweeney et al., 2014; Sweeney et al., 2017). Our lab and others have shown that Tbr2 is necessary during development for the formation and survival of ipRGCs (Mao et al., 2008; Sweeney et al., 2014; Mao et al., 2014); loss of Tbr2 in developing RGCs results in an absence of ipRGCs, increased apoptosis, and defective optic nerve myelination. A study in which scRNAseq was performed on developing RGCs at multiple timepoints identified Tbr2-expressing RGCs as a fate-restricted class (Shekhar et al., 2022), supporting our findings. Tbr1 is a closely related transcription factor that is expressed in the adult retina in 4 types of OFF RGCs (Liu et al, 2018; Kiyama et al., 2019). When Tbr1 is removed from RPCs, Liu et al. (2018) found no effect on RGC survival or morphology, whereas Kiyama et al. (2019) found increased apoptosis, the absence of 2 OFF-RGC classes, and aberrant dendritic morphology. When Tbr1 is ablated during RGC dendritogenesis, the former study observed aberrant dendritic morphology (Liu et al., 2018). Another T-box transcription factor, Tbx5, was recently found to be required for the formation of ON-DSGCs that detect upward motion (Al-Khindi et al, 2022).

Satb1 (special AT-rich sequence-binding protein 1) is another transcription factor that is expressed in developing and mature RGCs and plays a role in dendrite patterning (Peng et al., 2017). It is expressed in two types of ON-OFF DSGCs (ooDSGCs), which as their name implies, have bistratified dendrites. In Satb1-null

mice, the ON arbors of ooDSGCs are lost, leading to an absence of ON-responses. The researchers further demonstrated that the homophilic adhesion molecule, Contactin 5 (Cntn5), is expressed in Satb1 RGCs and in the interneurons that their dendrites connect with. They found that loss of Cntn5 in ooDSGCs partially phenocopies loss of Satb1.

1.5.2 Retinal ganglion cell axon guidance

How do RGCs know which side of the brain to project to and, given that there are >50 subcortical targets, which region to project to?

1.5.2a Intraretinal guidance and exit

Axon outgrowth occurs prior to RGC subtype specification and begins in newly postmitotic RGCs (Herrera et al., 2019). RGC axons must first navigate through the retina into the optic fiber layer and then extend towards the optic disc (**Fig. 1.5A**). Inhibitory Slit/Robo signaling and expression of the secreted frizzled proteins Sfrp1/Sfrp2 have been shown to play an important role in these steps (Niclou et al., 2000; Marcos et al., 2015). Both sets of molecules inhibit the growth of axons into the outer retina. Netrin-1 is expressed in glial cells at the optic disc and is necessary for RGC axon exit from the eye (Deiner et al., 1997). Slit2 and Sema5a are inhibitory signals that restrict the axons to the optic nerve as they make their way through it and towards the optic chiasm. Vax1 attracts and guides RGC axons to the optic chiasm, without which they stall before reaching the chiasm (Kim et al., 2014).

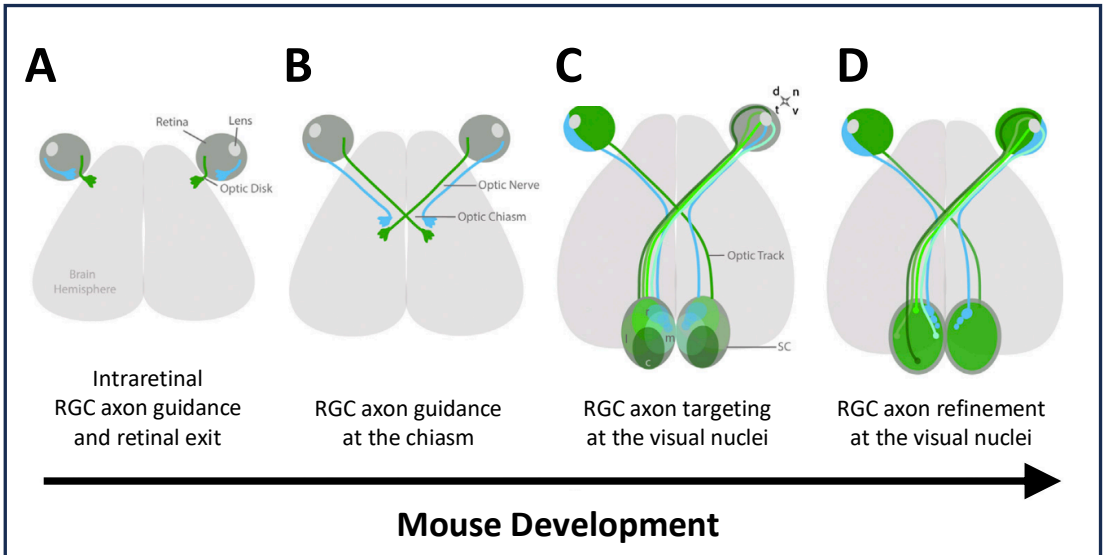

Figure 1.5 Visual pathway development

RGC axons must find their way through the retina **(A)**, towards the correct side of the brain at the optic chiasm **(B)**, to the appropriate visual nuclei **(C)**, and to the correct region within nuclei **(D)**. (Adapted from Herrera et al., 2019)

1.5.2b Guidance at the chiasm

Upon reaching the optic chiasm, RGC axons either cross at the midline to grow towards the contralateral (opposite) hemisphere of the brain, or avoid crossing to grow towards the ipsilateral (same) side of the brain (**Fig. 1.5B**). The proportion of RGCs that project ipsilaterally varies among different vertebrate species, correlating with their degree of binocularity. Mice have eyes that are situated on the sides of their heads resulting in minimally overlapping visual fields. The vast majority of RGCs in mice (~97%) project contralaterally and convey monocular information. The ~3% of ipsilaterally projecting RGCs allow for binocular vision and reside in the ventrotemporal quadrant of the retina termed the ventrotemporal crescent (VTC) (Dräger and Olsen 1980). Different genes are expressed in contralateral and ipsilateral

RGCs that allow them to respond to molecular cues in their environment in distinct manners and thus take the appropriate trajectory at the optic chiasm (Wang et al., 2016; Herrera et al., 2019).

Ipsilaterally projecting RGCs avoid midline crossing at the chiasm due to their expression of Zic2 (zinc-finger protein of the cerebellum 2), a transcription factor selectively expressed in RGCs of the VTC during development. Loss-of-function and gain-of-function analyses have shown that Zic2 is both necessary and sufficient for specifying an ipsilateral axon trajectory; in its absence, there is a loss of ipsilateral axons at the optic chiasm (Herrera et al., 2003) and when it is ectopically expressed in contralateral RGCs, axons are directed ipsilaterally (Garcia-Frigola et al., 2008). Zic2 activates expression of EphB1, a receptor tyrosine kinase that is expressed in ipsilateral RGC axons (Garcia-Frigola et al., 2008). Its ligand, ephrinB2, is expressed in radial glial cells at the midline and acts as a repulsive signal, causing EphB1-expressing axons to turn ipsilaterally (Williams et al., 2003; Petros et al., 2009). Ten-m2, a member of the Teneurin family of adhesion molecules, has also been shown to be involved in this process. In its absence, there is a reduction in EphB1 expression and a 40% reduction in ipsilateral projections, with no effect on Zic2 expression (Young et al., 2013). Transaxonal shh signaling is additionally implicated in RGC midline avoidance at the chiasm; shh is expressed in contralateral axons and repels ipsilateral axons that express the shh receptor Boc (Fabre et al., 2010; Peng et al., 2018).

The transcription factor Islet2 (Isl2) is expressed in ~40% of RGCs, all of which project contralaterally (Pak et al., 2004; Triplett et al., 2014). Pak et al. (2004) found

that Isl2 specifies a contralateral trajectory in a small population of RGCs in the VTC by repressing Zic2; the vast majority of contralateral RGCs in the Isl2-null mice used in their study display normal laterality. The SoxC transcription factors mentioned earlier in section 1.5.1 (Sox4, Sox11, and Sox12) are involved in contralateral RGC fate specification (Kuwajima et al., 2017). In SoxC triple mutants, there is decreased expression of the guidance receptors Plexin-A1 and Nr-CAM that are normally expressed in contralateral RGCs (Williams et al., 2006). These guidance receptors interact with semaphorin6D (sema6D) and Nr-CAM expressing radial glia as well as Plexin-A1-expressing neurons at the optic chiasm to promote axon growth contralaterally (Kuwajima et al., 2012); sema6D repels contralateral RGC axons in the absence of Nr-CAM and Plexin-A1. Contralateral RGCs from SoxC triple mutants display reduced neurite outgrowth on chiasm cells in vitro and some fail to cross at the midline in vivo, instead growing ipsilaterally. These mutant RGC axons are unable to invade the ipsilateral dLGN or SC despite aberrantly projecting ipsilaterally.

1.5.2c Targeting visual nuclei

RGC axons are guided towards their correct target (**Fig. 1.5C**) by molecular cues within and surrounding the visual pathway. Different RGC subtypes express transcription factors that inform the expression of distinct combinations of receptors for these molecular cues, facilitating guidance to specific brain areas. The homophilic cell adhesion molecule cadherin-6 (cdh6) is expressed in RGCs that project to non-image-forming brain regions as well as within these regions themselves, facilitating axon-target connectivity (Osterhout et al., 2011). The extracellular matrix glycoprotein

reelin is also involved in targeting of non-image-forming nuclei; it is expressed in the vLGN and IGL and is required for ipRGC innervation of these areas (Su et al., 2011). Studies using transgenic mouse lines expressing GFP in discrete RGC subtypes have revealed different strategies for axon target-matching depending on the timing of RGC birth and axon outgrowth (Osterhout et al., 2014). Early-born and early-extending RGCs appear to sample multiple brain areas before stabilizing their projection in a particular target whereas late-born and late-extending RGCs make precise connections to their target destination. Additionally, Sema6A/PlexinA2/4 signaling is required for innervation of the MTN by ON-DSGCs (Sun et al., 2015).

1.5.2d Refinement

Axon terminals of RGCs are topographically aligned in their target structures such that RGCs that respond to the same area of space maintain their spatial relationship within their target, ensuring the appropriate transmission of spatial information (**Fig. 1.5D**; Feldheim and O'Leary 2010). Along the nasotemporal retinal axis, RGCs from the temporal retina project their axons to the anterior SC while those from the nasal retina project to the posterior SC. Along the dorsoventral axis, dorsal RGCs project to lateral SC and ventral RGCs to medial SC. Members of the Eph/ephrin family of receptor tyrosine kinases/ligands play an important role in the formation of these topographic maps. Both Eph receptors and ephrin ligands can be divided into A and B types and each of these categories contain multiple subclasses (Kullander and Klein 2002). These molecules are expressed in gradients across the retina and in visual targets and act as attractive/repulsive signals. EphA5/6 are highly expressed in

temporal RGCs and weakly expressed in nasal RGCs, while being highly expressed in the anterior SC and weakly in the posterior SC (Brown et al., 2000; Feldheim et al., 2000). There is a counter-gradient of ephrin-A5 in both structures such that ephrin-A5 is highly expressed in the nasal retina and posterior SC, and weakly expressed in the temporal retina and posterior SC. Unlike the nasotemporal axis, RGCs along the dorsoventral axis exhibit pre-target sorting so that RGC axons from the dorsal and ventral regions of the retina are already segregated within the optic tract prior to arriving to the SC (Plas et al., 2005). However, EphB/ephrinB signaling has been shown to play a role in topographic refinement along this axis. RGC axons form interstitial branches that grow bidirectionally along the medial-lateral axis towards their correct location. EphrinB1 is highly expressed in the medial SC and weakly expressed in the lateral SC, and EphB2/3 exhibit a high to low expression pattern from dorsal to ventral retina. In the absence of EphB2/3, ectopic terminal zones form in incorrect regions along the mediolateral axis (Hindges et al., 2002). Other factors implicated in topography and refinement include BDNF/TrkB signaling (in interstitial branching; Marler et al., 2014), Wnt3/Ryk signaling (opposing role to EphB/ephrinB signaling; Schmitt et al., 2006), Tenm3 (ipsilateral topography; Leamey et al., 2007; Dharmaratne et al., 2012; Leamey and Sawatari 2019). Lastly, in addition to molecular mechanisms, activity-dependent mechanisms also play a role in axon guidance, eye-specific segregation, and refinement. Retinal waves–the spontaneous bursts of retinal activity that occur during development prior to visual experience–are important for fine-scale refinement of terminal zones (Torborg and Feller 2005; Assali et al., 2014).

1.5.3 Developmental RGC death

"*By the time I was born, more of me had died than survived.*"

-Lewis Thomas

Programmed cell death ensures the proper development of various complex structures including the nervous system (Conradt et al., 2009; Oppenheim 1991; Buss et al., 2006). Cells are initially overproduced and subsequently eliminated to reveal a refined structure. There are two waves of apoptosis during retina development, the first wave occurs during neurogenesis and migration while the second wave coincides with synaptogenesis. Peak RGC death in rodents occurs between P2-P4, during synaptogenesis, and it is estimated that 50-70% are eliminated by P5 (Young 1984; Galli-Resta and Ensini 1996; Strom and Williams 1998; Farah and Easter 2005). The neurotrophic hypothesis posits that neuronal survival depends on the ability to compete for a limited supply of neurotrophic factors present in targets (Hamburger & Levi-Montalcini 1949; Purves et al., 1988). Several studies have supported this hypothesis showing that factors in both the postsynaptic and presynaptic environment contribute to a neuron's survival in a variety of nervous tissues (Hughes and McLoon 1979; Lindon and Perry 1982; Lipton 1986; Cui and Harvey 1995).

The neurotrophin superfamily of neurotrophic factors has been extensively studied and includes: nerve growth factor (NGF), brain-derived neurotrophic factor (BDNF), neurotrophin-3 (NT-3), and neurotrophin-4/5 (NT-4/5) (Gillespie 2003). Neurotrophins bind to the Trk family of receptor tyrosine kinases (TrkA, TrkB, TrkC) initiating signaling cascades that lead to survival and growth. They also bind to the P75

neurotrophin receptor, a member of the tumor necrosis factor-related molecules, and can induce apoptosis (Majdan et al., 1997). Injection of BDNF or NT-4/NT-5 into the developing eye or SC in rats reduces RGC death and application of BDNF to RGCs in culture prevents their death (Cui and Harvey, 1994, 1995; Ma et al., 1998). However, null mutations for BDNF, NT-4, and TrkB do not result in increased RGC death (Cellerino et al., 1997; Rohrer et al., 2001; Pollock et al., 2003); BDNF-null mice display thin, hypomyelinated RGC axons (Cellerino et al., 1997). In double mutant mice lacking both BDNF and NT-4/5, there is a delay in retinal development with a thicker GCL (Cellerino et al., 1997; Harada et al., 2005). These data suggest that there is compensation by other trophic factors and that individual trophic factors are not solely responsible for survival.

1.6 Bibliography

Al-Khindi T, Sherman MB, Kodama T, Gopal P, Pan Z, Kiraly JK, Zhang H, Goff LA, du Lac S, Kolodkin AL. 2022. The transcription factor Tbx5 regulates direction-selective retinal ganglion cell development and image stabilization. Curr Biol. 32(19):4286-4298.e5. doi:10.1016/j.cub.2022.07.064.

Baden T, Berens P, Franke K, Román Rosón M, Bethge M, Euler T. 2016. The functional diversity of retinal ganglion cells in the mouse. Nature. 529(7586):345–350. doi:10.1038/nature16468.

Bae JA, Mu S, Kim JS, Turner NL, Tartavull I, Kemnitz N, Jordan CS, Norton AD, Silversmith WM, Prentki R, et al. 2018. Digital Museum of Retinal Ganglion Cells with Dense Anatomy and Physiology. Cell. 173(5):1293-1306.e19. doi:10.1016/j.cell.2018.04.040.

Belliveau MJ, Cepko CL. 1999. Extrinsic and intrinsic factors control the genesis of amacrine and cone cells in the rat retina. Development. 126:555–566.

Belliveau MJ, Young TL, Cepko CL. 2000. Late retinal progenitor cells show intrinsic limitations in the production of cell types and the kinetics of opsin synthesis. J Neurosci. 20(6):2247–2254. doi:10.1523/jneurosci.20-06-02247.2000.

Bourne RRA, Steinmetz JD, Flaxman S, Briant PS, Taylor HR, Resnikoff S, Casson RJ, Abdoli A, Abu-Gharbieh E, Afshin A, et al. 2021(a). Trends in prevalence of blindness and distance and near vision impairment over 30 years: An analysis for the Global Burden of Disease Study. Lancet Glob Heal. 9(2):e130–e143. doi:10.1016/S2214-109X(20)30425-3.

Bourne RRA, Steinmetz JD, Saylan M, Mersha AM, Weldemariam AH, Wondmeneh TG, Sreeramareddy CT, Pinheiro M, Yaseri M, Yu C, et al. 2021(b). Causes of blindness and vision impairment in 2020 and trends over 30 years, and prevalence of avoidable blindness in relation to VISION 2020: The Right to Sight: An analysis for the Global Burden of Disease Study. Lancet Glob Heal. 9(2):e144–e160. doi:10.1016/S2214-109X(20)30489-7.

Brodie-Kommit J, Clark BS, Shi Q, Shiau F, Kim DW, Langel J, Sheely C, Ruzycki PA, Fries M, Javed A, et al. 2021. Atoh7-independent specification of retinal ganglion cell identity. Sci Adv. 7(11):eabe4983. doi:10.1126/sciadv.abe4983.

Brown NL, Kanekar S, Vetter ML, Tucker PK, Gemza DL, Glaser T. 1998. Math5 encodes a murine basic helix-loop-helix transcription factor expressed during early stages of retinal neurogenesis. Development. 125(23):4821–4833. doi:10.1242/dev.125.23.4821.

Brown A, Yates PA, Burrola P, Ortuñ D, Vaidya A, Jessell TM, Pfaff SL, O'Leary DDM, Lemke G. 2000. Topographic Mapping from the Retina to the Midbrain Is Controlled by Relative but Not Absolute Levels of EphA Receptor Signaling. Cell. 102(1):77–88. doi:10.1016/s0092-8674(00)00012-x.

Brown NL, Patel S, Brzezinski J, Glaser T. 2001. Math5 is required for retinal ganglion cell and optic nerve formation. Development. 128(13):2497–2508.

Brzezinski JA, Kim EJ, Johnson JE, Reh TA. 2011. Ascl1 expression defines a subpopulation of lineage-restricted progenitors in the mammalian retina. Development. 138(16):3519–3531. doi:10.1242/dev.064006.

Brzezinski JA, Prasov L, Glaser T. 2012. Math5 defines the ganglion cell competence state in a subpopulation of retinal progenitor cells exiting the cell cycle. Dev Biol. 365(2):395–413. doi:10.1016/j.ydbio.2012.03.006.

Burmeister M, Novak J, Liang M, Basu S, Ploder L, Hawes NL, Vidgen D, Hoover F, Goldman D, Kalnins VI, et al. 1996. Ocular retardation mouse caused by Chx10 homeobox null allele: impaired retinal progenitor proliferation and bipolar cell differentiation. Nat Genet. 12(April):376–384. doi:10.1038/ng0496-376.

Buss RR, Sun W, Oppenheim RW. 2006. Adaptive roles of programmed cell death during nervous system development. Annu Rev Neurosci. 29:1–35. doi:10.1146/annurev.neuro.29.051605.112800.

Carballo GB, Honorato JR, De Lopes GPF, Spohr TCLDSE. 2018. A highlight on Sonic hedgehog pathway. Cell Commun Signal. 16(1):1–15. doi:10.1186/s12964-018-0220-7.

Cayouette M, Barres BA, Raff M. 2003. Importance of Intrinsic Mechanisms in Cell Fate Decisions in the Developing Rat Retina. Neuron. 40(5):897–904. doi:10.1016/S0896-6273(03)00756-6.

Cellerino A, Carroll P, Thoenen H, Barde Y. 1997. Reduced Size of Retinal Ganglion Cell Axons and Hypomyelination in Mice Lacking Brain-Derived Neurotrophic Factor. Mol Cell Neurosci. 9:397–408. doi:10.1006/mcne.1997.0641.

Clark BS, Stein-O'Brien GL, Shiau F, Cannon GH, Davis-Marcisak E, Sherman T, Santiago CP, Hoang T V., Rajaii F, James-Esposito RE, et al. 2019. Single-Cell RNA-Seq Analysis of Retinal Development Identifies NFI Factors as Regulating Mitotic Exit and Late-Born Cell Specification. Neuron. 102(6):1111-1126.e5. doi:10.1016/j.neuron.2019.04.010.

Conradt B. 2009. Genetic control of programmed cell death during animal development. Annu Rev Genet. 43:493–523. doi:10.1146/annurev.genet.42.110807.091533.

Cui Q, Harvey AR. 1994. NT-4/5 reduces naturally occuring retinal ganglion cell death in neonatal rats. Regen Transplant. 5(15):1882–1884.

Cui Q, Harvey AR. 1995. At least two mechanisms are involved in the death of retinal ganglion cells following target ablation in neonatal rats. J Neurosci. 15(12):8143–8155. doi:10.1523/jneurosci.15-12-08143.1995.

Curcio M, Bradke F. 2018. Axon Regeneration in the Central Nervous System: Facing the Challenges from the Inside. Annu Rev Cell Dev Biol. 34:495–521. doi:10.1146/annurev-cellbio-100617-062508.

David S, Aguayo AJ. 1981. Axonal Elongation into Peripheral Nervous System "Bridges" after Central Nervous System Injury in Adult Rats. Science. 214(4523):931–933.

Deiner MS, Kennedy TE, Fazeli A, Serafini T, Tessier-Lavigne M, Sretavan DW. 1997. Netrin-1 and DCC mediate axon guidance locally at the optic disc: Loss of function leads to optic nerve hypoplasia. Neuron. 19(3):575–589. doi:10.1016/S0896-6273(00)80373-6.

de Melo J, Du G, Fonseca M, Gillespie LA, Turk WJ, Rubenstein JLR, Eisenstat DD. 2005. Dlx1 and Dlx2 function is necessary for terminal differentiation and survival of late-born retinal ganglion cells in the developing mouse retina. Development. 132(2):311–322. doi:10.1242/dev.01560.

Dräger UC, Olsen JF. 1980. Origins of crossed and uncrossed retinal projections in pigmented and albino mice. J Comp Neurol. 191(3):383–412. doi:10.1002/cne.901910306.

Dyer MA, Cepko CL. 2000. Control of Muller glial cell proliferation and activation following retinal injury. Nat Neurosci. 3(9):873–880. doi:10.1038/78774.

Elliott J, Jolicoeur C, Ramamurthy V, Cayouette M. 2008. Ikaros Confers Early Temporal Competence to Mouse Retinal Progenitor Cells. Neuron. 60(1):26–39. doi:10.1016/j.neuron.2008.08.008.

Ellis EM, Gauvain G, Sivyer B, Murphy GJ. 2016. Shared and distinct retinal input to the mouse superior colliculus and dorsal lateral geniculate nucleus. J Neurophysiol. 116(2):602–610. doi:10.1152/jn.00227.2016.

Erkman L, Mcevilly RJ, Luo L, Ryan AK, Hooshmand F, O'Connell SM, Keithley EM, Rapaport DH, Ryan AF, Rosenfeld MG. 1996. Role of transcription factors Brn-3.1 and Brn-3.2 in auditory and visual system development. Nature. 381(June):603–606.

Fabre PJ, Shimogori T, Charron F. 2010. Segregation of ipsilateral retinal ganglion cell axons at the optic chiasm requires the Shh receptor boc. J Neurosci. 30(1):266–275. doi:10.1523/JNEUROSCI.3778-09.2010.

Farah MH, Easter SS. 2005. Cell birth and death in the mouse retinal ganglion cell layer. J Comp Neurol. 489(1):120–134. doi:10.1002/cne.20615.

Fawcett JW. 1992. Intrinsic neuronal determinants of regeneration. Trends Neurosci. 15(1):5–8. doi:10.1016/0166-2236(92)90338-9.

Feng L, Xie ZH, Ding Q, Xie X, Libby RT, Gan L. 2010. MATH5 controls the acquisition of multiple retinal cell fates. Mol Brain. 3(1):1–16. doi:10.1186/1756-6606-3-36.

Gan L, Xiang M, Zhou L, Wagner DS, Klein WH, Nathans J. 1996. POU domain factor Brn-3b is required for the development of a large set of retinal ganglion cells. Proc Natl Acad Sci U S A. 93(9):3920–3925. doi:10.1073/pnas.93.9.3920.

Gan L, Wang SW, Huang Z, Klein WH. 1999. POU domain factor Brn-3b is essential for retinal ganglion cell differentiation and survival but not for initial cell fate specification. Dev Biol. 210(2):469–480. doi:10.1006/dbio.1999.9280.

Ghinia Tegla MG, Buenaventura DF, Kim DY, Thakurdin C, Gonzalez KC, Emerson MM. 2020. OTX2 represses sister cell fate choices in the developing retina to promote photoreceptor specification. Elife. 9:1–28. doi:10.7554/eLife.54279.

Gillespie LN. 2003. Regulation of axonal growth and guidance by the neurotrophin family of neurotrophic factors. Clin Exp Pharmacol Physiol. 30(10):724–733. doi:10.1046/j.1440-1681.2003.03909.x.

Goetz J, Jessen ZF, Jacobi A, Mani A, Cooler S, Greer D, Kadri S, Segal J, Shekhar K, Sanes J, et al. 2022. Unified Classification of Mouse Retinal Ganglion Cells Using Function, Morphology, and Gene Expression. Cell Rep. 40(111040):1–17. doi:10.2139/ssrn.3867730. Doi: 10.1016/j.celrep.2022.111040.

Gordon PJ, Yun S, Clark AM, Monuki ES, Murtaugh LC, Levine EM. 2013. Lhx2 balances progenitor maintenance with neurogenic output and promotes competence state progression in the developing retina. J Neurosci. 33(30):12197–12207. doi:10.1523/JNEUROSCI.1494-13.2013.

Hafler BP, Surzenko N, Beier KT, Punzo C, Trimarchi JM, Kong JH, Cepko CL. 2012. Transcription factor Olig2 defines subpopulations of retinal progenitor cells biased toward specific cell fates. Proc Natl Acad Sci U S A. 109(20):7882–7887. doi:10.1073/pnas.1203138109.

Harada C, Harada T, Quah HMA, Namekata K, Yoshida K, Ohno S, Tanaka K, Parada LF. 2005. Role of neurotrophin-4/5 in neural cell death during retinal development and ischemic retinal injury in vivo. Investig Ophthalmol Vis Sci. 46(2):669–673. doi:10.1167/iovs.04-0826.

Herrera E, Brown L, Aruga J, Rachel RA, Dolen G, Mikoshiba K, Brown S, Mason CA. 2003. Zic2 patterns binocular vision by specifying the uncrossed retinal projection. Cell. 114(5):545–557. doi:10.1016/S0092-8674(03)00684-6.

Herrera E, Erskine L, Morenilla-Palao C. 2019. Guidance of retinal axons in mammals. Semin Cell Dev Biol. 85:48–59. doi:10.1016/j.semcdb.2017.11.027. doi:10.1016/j.semcdb.2017.11.027.

Holt CE, Bertsch TW, Ellis HM, Harris WA. 1988. Cellular determination in the xenopus retina is independent of lineage and birth date. Neuron. 1(1):15–26. doi:10.1016/0896-6273(88)90205-X.

Hughes WF, McLoon SC. 1979. Ganglion cell death during normal retinal development in the chick: Comparisons with cell death induced by early target field destruction. Exp Neurol. 66:587–601. doi:10.1016/0014-4886(79)90204-8.

Jacobson M. 1968. Cessation of DNA synthesis in retinal ganglion cells correlated with the time of specification of their central connections. Dev Biol. 17(2):219–232. doi:10.1016/0012-1606(68)90062-6.

Javed A, Mattar P, Lu S, Kruczek K, Kloc M, Gonzalez-Cordero A, Bremner R, Ali RR, Cayouette M. 2020. Pou2f1 and Pou2f2 cooperate to control the timing of cone photoreceptor production in the developing mouse retina. Dev. 147(18). doi:10.1242/dev.188730.

Jiang Y, Ding Q, Xie X, Libby RT, Lefebvre V, Gan L. 2013. Transcription factors SOX4 and SOX11 function redundantly to regulate the development of mouse retinal ganglion cells. J Biol Chem. 288(25):18429–18438. doi:10.1074/jbc.M113.478503.

Karl MO, Hayes S, Nelson BR, Tan K, Buckingham B, Reh TA. 2008. Stimulation of neural regeneration in the mouse retina. Proc Natl Acad Sci U S A. 105(49):19508–19513. doi:10.1073/pnas.0807453105.

Kerschensteiner D. 2020. Mammalian Retina Development. In *The Senses: A Comprehensive Reference: Volume 1-7, Second Edition* 1:234-251. Elsevier. doi: 10.1016/B978-0-12-809324-5.24156-4.

Kerschensteiner D. 2022. Feature Detection by Retinal Ganglion Cells. Annu Rev Vis Sci. 8:135–169. doi:10.1146/annurev-vision-100419-112009.

Kiyama T, Long Y, Chen C-K, Whitaker CM, Shay A, Wu H, Badea TC, Mohsenin A, Parker-Thornburg J, Klein WH, et al. 2019. Essential Roles of Tbr1 in the Formation and Maintenance of the Orientation-Selective J-RGCs and a Group of OFF-Sustained RGCs in Mouse. Cell Rep. 27(3):900-915.e5. doi:10.1016/j.celrep.2019.03.077.

Kullander K, Klein R. 2002. Mechanisms and functions of Eph and ephrin signalling. Nat Rev Mol Cell Biol. 3(7):475–486. doi:10.1038/nrm856.

Kuwajima T, Yoshida Y, Takegahara N, Petros TJ, Kumanogoh A, Jessell TM, Sakurai T, Mason C. 2012. Optic Chiasm Presentation of Semaphorin6D in the Context of Plexin-A1 and Nr-CAM Promotes Retinal Axon Midline Crossing. Neuron. 74(4):676–690. doi:10.1016/j.neuron.2012.03.025.

Kuwajima T, Soares CA, Sitko AA, Lefebvre V, Mason C. 2017. SoxC Transcription Factors Promote Contralateral Retinal Ganglion Cell Differentiation and Axon Guidance in the Mouse Visual System. Neuron. 93(5):1110-1125.e5. doi:10.1016/j.neuron.2017.01.029.

La Vail MM, Rapaport DH, Rakic P. 1991. Cytogenesis in the monkey retina. J Comp Neurol. 309(1):86–114. doi:10.1002/cne.903090107.

Leamey CA, Merlin S, Lattouf P, Sawatari A, Zhou X, Demel N, Glendining KA, Oohashi T, Sur M, Fässler R. 2007. Ten_m3 regulates eye-specific patterning in the mammalian visual pathway and is required for binocular vision. PLoS Biol. 5(9):2077–2092. doi:10.1371/journal.pbio.0050241.

Leamey CA, Sawatari A. 2019. Teneurins: Mediators of complex neural circuit assembly in mammals. Front Neurosci. 13(JUN):1–8. doi:10.3389/fnins.2019.00580.

Lefebvre JL, Sanes JR, Kay JN. 2015. Development of Dendritic Form and Function. Annu Rev Cell Dev Biol. 31:741–777. doi:10.1146/annurev-cellbio-100913-013020.

Lipton SA. 1986. Blockade of electrical activity promotes the death of mammalian retinal ganglion cells in culture. Proc Natl Acad Sci U S A. 83(24):9774–9778. doi:10.1073/pnas.83.24.9774.

Liu J, Reggiani JDS, Laboulaye MA, Pandey S, Chen B, Rubenstein JLR, Krishnaswamy A, Sanes JR. 2018. Tbr1 instructs laminar patterning of retinal ganglion cell dendrites. Nat Neurosci. 21:659–670. doi:10.1038/s41593-018-0127-z.

Livesey F, Cepko C. 2001. Vertebrate neural cell-fate determination: Lessons from the retina. Nat Rev Neurosci. 2(February 2001):109–118. doi:10.1038/35053522.

Ma YT, Hsieh T, Forbes ME, Johnson JE, Frost DO. 1998. BDNF injected into the superior colliculus reduces developmental retinal ganglion cell death. J Neurosci. 18(6):2097–2107. doi:10.1523/jneurosci.18-06-02097.1998.

Majdan M, Lachance C, Gloster A, Aloyz R, Zeindler C, Bamji S, Bhakar A, Belliveau D, Fawcett J, Miller FD, et al. 1997. Transgenic mice expressing the intracellular domain of the p75 neurotrophin receptor undergo neuronal apoptosis. J Neurosci. 17(18):6988–6998. doi:10.1523/jneurosci.17-18-06988.1997.

Mao C-A, Kiyama T, Pan P, Furuta Y, Hadjantonakis A-K, Klein WH. 2008. Eomesodermin, a target gene of Pou4f2, is required for retinal ganglion cell and optic nerve development in the mouse. Development. 135(2):271–280. doi:10.1242/dev.009688.

Mao C-A, Li H, Zhang Z, Kiyama T, Panda S, Hattar S, Ribelayga CP, Mills SL, Wang SW. 2014. T-box Transcription Regulator Tbr2 Is Essential for the Formation and Maintenance of Opn4/Melanopsin-Expressing Intrinsically Photosensitive Retinal Ganglion Cells. J Neurosci. 34(39):13083–13095. doi:10.1523/JNEUROSCI.1027-14.2014.

Marler KJ, Suetterlin P, Dopplapudi A, Rubikaite A, Adnan J, Maiorano NA, Lowe AS, Thompson ID, Pathania M, Bordey A, et al. 2014. BDNF promotes axon branching of retinal ganglion cells via miRNA-132 and p250GAP. J Neurosci. 34(3):969–979. doi:10.1523/JNEUROSCI.1910-13.2014.

Marcos S, Nieto-Lopez F, Sandonìs A, Cardozo MJ, Di Marco F, Esteve P, Bovolenta P. 2015. Secreted frizzled related proteins modulate pathfinding and fasciculation of mouse retina ganglion cell axons by direct and indirect mechanisms. J Neurosci. 35(11):4729–4740. doi:10.1523/JNEUROSCI.3304-13.2015.

Marquardt T, Ashery-padan R, Andrejewski N, Scardigli R, Guillemot F, Gruss P. 2001. Pax6 is Required for the Multipotent State of Retinal Progenitor Cells. Cell. 105(1):43–55. doi:10.1016/S0092-8674(01)00295-1.

Martersteck EM, Hirokawa KE, Evarts M, Bernard A, Duan X, Li Y, Ng L, Oh SW, Ouellette B, Royall JJ, et al. 2017. Diverse Central Projection Patterns of Retinal Ganglion Cells. Cell Rep. 18(8):2058–2072. doi:10.1016/j.celrep.2017.01.075.

Martin P.R. 1986. The projection of different retinal ganglion cell classes to the dorsal lateral geniculate nucleus in the hooded rat. Exp Brain Res. 62(1986):77–88. doi:10.1007/BF00237404.

Mattar P, Ericson J, Blackshaw S, Cayouette M. 2015. A conserved regulatory logic controls temporal identity in mouse neural progenitors. Neuron. 85(3):497–504. doi:10.1016/j.neuron.2014.12.052.

Ming GL, Song H. 2005. Adult neurogenesis in the mammalian central nervous system. Annu Rev Neurosci. 28:223–250. doi:10.1146/annurev.neuro.28.051804.101459.

Morin LP, Studholme KM. 2014. Retinofugal projections in the mouse. J Comp Neurol. 522(16):3733–3753. doi:10.1002/cne.23635.

Mu X, Fu X, Beremand PD, Thomas TL, Klein WH. 2008. Gene-regulation logic in retinal ganglion cell development : Isl1 defines a critical branch distinct from but overlapping with Pou4f2 MT. 105(19).

Nishida A, Furukawa A, Koike C, Tano Y, Aizawa S, Matsuo I, Furukawa T. 2003. Otx2 homeobox gene controls retinal photoreceptor cell fate and pineal gland development. Nat Neurosci. 6(12):1255–1263. doi:10.1038/nn1155.

Nylen, Erik Lee. "Quantitative analysis of retinal function in early stages of retinal degeneration in the rd1 mouse." Master's thesis, University of Iowa, 2010.

Oppenheim RW. 1991. CELL DEATH DURING DEVELOPMENT OF THE NERVOUS SYSTEM. Annu Rev Neurosci. 14:453–501. doi:10.1146/annurev.neuro.14.1.453.

Osterhout JA, Josten N, Yamada J, Pan F, Wu S, Nguyen PL, Panagiotakos G, Inoue YU, Egusa SF, Volgyi B, et al. 2011. Cadherin-6 Mediates Axon-Target Matching in a Non-Image- Forming Visual Circuit. Neuron. 71(4):632–639. doi:10.1016/j.neuron.2011.07.006.

Osterhout JA, El-Danaf RN, Nguyen PL, Huberman AD. 2014. Birthdate and outgrowth timing predict cellular mechanisms of axon-target matching in the developing visual pathway. Cell Rep. 8(4):1006–1017. doi:10.1016/j.celrep.2014.06.063.

Pak W, Hindges R, Lim YS, Pfaff SL, O'Leary DDM. 2004. Magnitude of binocular vision controlled by islet-2 repression of a genetic program that specifies laterality of retinal axon pathfinding. Cell. 119(4):567–578. doi:10.1016/j.cell.2004.10.026.

Pan L, Deng M, Xie X, Gan L. 2008. ISL1 and BRN3B co-regulate the differentiation of murine retinal ganglion cells. Development. 135(11):1981–1990. doi:10.1242/dev.010751.

Peng YR, Tran NM, Krishnaswamy A, Kostadinov D, Martersteck EM, Sanes JR. 2017. Satb1 Regulates Contactin 5 to Pattern Dendrites of a Mammalian Retinal Ganglion Cell. Neuron. 95(4):869-883.e6. doi:10.1016/j.neuron.2017.07.019.

Peng J, Fabre PJ, Dolique T, Swikert SM, Kermasson L, Shimogori T, Charron F. 2018. Sonic Hedgehog Is a Remotely Produced Cue that Controls Axon Guidance Trans-axonally at a Midline Choice Point. Neuron. 97:326–340. doi:10.1016/j.neuron.2017.12.028.

Petridou E, Godinho L. 2022. Cellular and Molecular Determinants of Retinal Cell Fate. Annu Rev Vis Sci. 8:79–99. doi:10.1146/annurev-vision-100820-103154.

Petros TJ, Shrestha BR, Mason C. 2009. Specificity and sufficiency of EphB1 in driving the ipsilateral retinal projection. J Neurosci. 29(11):3463–3474. doi:10.1523/JNEUROSCI.5655-08.2009.

Plas DT, Lopez JE, Crair MC. 2005. Pretarget sorting of retinocollicular axons in the mouse. J Comp Neurol. 491(4):305–319. doi:10.1002/cne.20694.

Prada C, Puga J, Perez-Mendez L, Lopez R, Ramirez G. 1991. Spatial and temporal patterns of neurogenesis in the chick retina. Eur J Neurosci. 3(11):1187. doi:10.1111/j.1460-9568.1991.tb00053.x.

Purves D, Snider WD, Voyvodic JT. 1988. Trophic regulation of nerve cell morphology and innervation in the autonomic nervous system. Nature. 336(6195):123–128. doi:10.1038/336123a0.

Ramón y Cajal, S. 1928. Degeneration and regeneration of the nervous system.

Rapaport DH, Patheal SL, Harris WA. 2001. Cellular competence plays a role in photoreceptor differentiation in the developing Xenopus retina. J Neurobiol. 49(2):129–141. doi:10.1002/neu.1070.

Reh TA, Kijavin IJ. 1989. Age of differentiation determines rat retinal germinal cell phenotype: Induction of differentiation by dissociation. J Neurosci. 9(12):4179–4189. doi:10.1523/jneurosci.09-12-04179.1989.

Rheaume BA, Jereen A, Bolisetty M, Sajid MS, Yang Y, Renna K, Sun L, Robson P, Trakhtenberg EF. 2018. Single cell transcriptome profiling of retinal ganglion cells identifies cellular subtypes. Nat Commun. 9(2759):1–17. doi:10.1038/s41467-018-05134-3.

Sanes JR, Masland RH. 2015. The Types of Retinal Ganglion Cells: Current Status and Implications for Neuronal Classification. Annu Rev Neurosci. 38(1):221–246. doi:10.1146/annurev-neuro-071714-034120.

Santos-França PL, David LA, Kassem F, Meng XQ, Cayouette M. 2022. Time to see: How temporal identity factors specify the developing mammalian retina. Semin Cell Dev Biol.(March). doi:10.1016/j.semcdb.2022.06.003.

Schmitt AM, Shi J, Wolf AM, Lu CC, King LA, Zou Y. 2006. Wnt-Ryk signalling mediates medial-lateral retinotectal topographic mapping. Nature. 439(7072):31–37. doi:10.1038/nature04334.

Schwab ME, Thoenen H. 1985. Dissociated neurons regenerate into sciatic but not optic nerve explants in culture irrespective of neurotrophic factors. J Neurosci. 5(9):2415–2423. doi:10.1523/jneurosci.05-09-02415.1985.

Shekhar K, Whitney IE, Butrus S, Peng YR, Sanes JR. 2022. Diversification of multipotential postmitotic mouse retinal ganglion cell precursors into discrete types. Elife. 11. doi:10.7554/ELIFE.73809.

Strom RC, Williams RW. 1998. Cell production and cell death in the generation of variation in neuron number. J Neurosci. 18(23):9948–9953. doi:10.1523/jneurosci.18-23-09948.1998.

Sun LO, Brady CM, Cahill H, Al-Khindi T, Sakuta H, Dhande OS, Noda M, Huberman AD, Nathans J, Kolodkin AL. 2015. Functional Assembly of Accessory Optic System Circuitry Critical for Compensatory Eye Movements. Neuron. 86(4):971–984. doi:10.1016/j.neuron.2015.03.064.

Sweeney NT, Tierney H, Feldheim DA. 2014. Tbr2 Is Required to Generate a Neural Circuit Mediating the Pupillary Light Reflex. J Neurosci. 34(16):5447–5453. doi:10.1523/JNEUROSCI.0035-14.2014.

Sweeney NT, James KN, Nistorica A, Lorig-Roach RM, Feldheim DA. 2017. Expression of transcription factors divides retinal ganglion cells into distinct classes. J Comp Neurol.(December 2016):1–11. doi:10.1002/cne.24172.

Taranova O V., Magness ST, Fagan BM, Wu Y, Surzenko N, Hutton SR, Pevny LH. 2006. SOX2 is a dose-dependent regulator of retinal neural progenitor competence. Genes Dev. 20(9):1187–1202. doi:10.1101/gad.1407906.

Thomas, L. (1992). The Fragile Species. (New York: Macmillan), p. 18.

Tran NM, Shekhar K, Whitney IE, Jacobi A, Benhar I, Hong G, Yan W, Adiconis X, Arnold ME, Lee JM, et al. 2019. Single-cell profiles of retinal neurons differing in resilience to injury reveal neuroprotective genes. Neuron. 104:1–17. doi:10.1016/j.neuron.2019.11.006.

Triplett JW, Wei W, Gonzalez C, Sweeney NT, Huberman AD, Feller MB, Feldheim DA. 2014. Dendritic and axonal targeting patterns of a genetically-specified class of retinal ganglion cells that participate in image-forming circuits. Neural Dev.:1–13.

Turner DL, Cepko CL. 1987. A common progenitor for neurons and glia persists in rat retina late in development. Nature. 328:131–136.

Turner DL, Snyder EY, Cepko CL. 1990. Lineage-independent determination of cell type in the embryonic mouse retina. Neuron. 4(6):833–845. doi:10.1016/0896-6273(90)90136-4.

Waid DK, McLoon SC. 1998. Ganglion cells influence the fate of dividing retinal cells in culture. Development. 125(6):1059–1066. doi:10.1242/dev.125.6.1059.

Wang SW, Kim BS, Ding K, Wang H, Sun D, Johnson RL, Klein WH, Gan L. 2001. Requirement for math5 in the development of retinal ganglion cells. Genes Dev. 15(1):24–29. doi:10.1101/gad.855301.

Wang Y, Dakubo GD, Thurig S, Mazerolle CJ, Wallace VA. 2005. Retinal ganglion cell-derived sonic hedgehog locally controls proliferation and the timing of RGC development in the embryonic mouse retina. Development. 132(22):5103–5113. doi:10.1242/dev.02096.

Wang Q, Marcucci F, Cerullo I, Mason C. 2016. Ipsilateral and contralateral retinal ganglion cells express distinct genes during decussation at the optic chiasm. eNeuro. 3(6). doi:10.1523/ENEURO.0169-16.2016.

Wässle H, Riemann HJ. 1978. The Mosaic of Nerve Cells in the Mammalian. Proc R Soc London - Biol Sci. 200(1141):441–461. doi:10.1098/rspb.1978.0026.

Williams SE, Mann F, Erskine L, Sakurai T, Wei S, Rossi DJ, Gale NW, Holt CE, Mason CA, Henkemeyer M. 2003. Ephrin-B2 and EphB1 mediate retinal axon divergence at the optic chiasm. Neuron. 39(6):919–935. doi:10.1016/j.neuron.2003.08.017.

Williams SE, Grumet M, Colman DR, Henkemeyer M, Mason CA, Sakurai T. 2006. A Role for Nr-CAM in the Patterning of Binocular Visual Pathways. Neuron. 50(4):535–547. doi:10.1016/j.neuron.2006.03.037.

Williams PR, Benowitz LI, Goldberg JL, He Z. 2020. Axon Regeneration in the Mammalian Optic Nerve. Annu Rev Vis Sci. 6:195–213. doi:10.1146/annurev-vision-022720-094953.

Wu F, Kaczynski TJ, Sethuramanujam S, Li R, Jain V, Slaughter M, Mu X. 2015. Two transcription factors, Pou4f2 and Isl1, are sufficient to specify the retinal ganglion cell fate. Proc Natl Acad Sci. 112(13):E1559–E1568. doi:10.1073/pnas.1421535112.

Yang Z, Ding K, Pan L, Deng M, Gan L. 2003. Math5 determines the competence state of retinal ganglion cell progenitors. Dev Biol. 264(1):240–254. doi:10.1016/j.ydbio.2003.08.005.

Young RW. 1983. The life history of retinal cells. Trans Am Ophthalmol Soc. 81:193–228.

Young RW. 1984. Cell death during differentiation of the retina in the mouse. J Comp Neurol. 229(3):362–373. doi:10.1002/cne.902290307.

Young RW. 1985. Cell differentiation in the retina of the mouse. Anat Rec. 212(2):199–205. doi:10.1002/ar.1092120215.

Young TR, Bourke M, Zhou X, Oohashi T, Sawatari A, Fässler R, Leamey CA. 2013. Ten-m2 is required for the generation of binocular visual circuits. J Neurosci. 33(30):12490–12509. doi:10.1523/JNEUROSCI.4708-12.2013.

Zhang Q, Zagozewski J, Cheng S, Dixit R, Zhang S, De Melo J, Mu X, Klein WH, Brown NL, Wigle JT, et al. 2017. Regulation of Brn3b by DLX1 and DLX2 is required for retinal ganglion cell differentiation in the vertebrate retina. Dev. 144(9):1698–1711. doi:10.1242/dev.142042.

Chapter 2: Adult Expression of Tbr2 is required for the maintenance but not survival of intrinsically photosensitive retinal ganglion cells

Chapter 2 is a modified version of the following publication:

Abed S, Reilly A, Arnold SJ, Feldheim DA. 2022. Adult Expression of Tbr2 Is Required for the Maintenance but Not Survival of Intrinsically Photosensitive Retinal Ganglion Cells. Front Cell Neurosci. 16:1–13. doi:10.3389/fncel.2022.826590.

2.1 Abstract

Retinal ganglion cells expressing the photopigment melanopsin are intrinsically photosensitive (ipRGCs). ipRGCs regulate subconscious non-image-forming behaviors such as circadian rhythms, pupil dilation, and light-mediated mood. Previously, we and others showed that the transcription factor Tbr2 (EOMES) is required during retinal development for the formation of ipRGCs. Tbr2 is also expressed in the adult retina leading to the hypothesis that it plays a role in adult ipRGC function. To test this, I removed Tbr2 in adult mice. I found that this results in the loss of melanopsin expression in ipRGCs but does not lead to cell death or morphological changes to their dendritic or axonal termination patterns. Additionally, I found ectopic expression of Tbr2 in conventional RGCs does not induce melanopsin expression but can increase melanopsin expression in existing ipRGCs. An interesting feature of ipRGCs is their superior survival relative to conventional RGCs after an optic nerve injury. I found that loss of Tbr2 decreases the survival rate of ipRGCs after optic nerve damage suggesting that Tbr2 plays a role in ipRGC survival after injury. Lastly, I show that the GABAergic amacrine cell marker Meis2, is expressed in the majority of Tbr2-expressing displaced amacrine cells as well as in a subset of Tbr2-expressing RGCs. These findings demonstrate that Tbr2 is necessary but not sufficient for melanopsin expression, that Tbr2 is involved in ipRGC survival after optic nerve injury, and identify a marker for Tbr2-expressing displaced amacrine cells.

2.2 Introduction

The retina comprises six neuronal cell types, each with distinct roles in visual scene detection and processing. Among these are retinal ganglion cells (RGCs) which send axons to > 50 retinorecipient brain regions (Martersteck et al., 2017), and amacrine cells (ACs) which modulate RGC activity. RGCs and ACs can be further divided into > 30 and > 40 subtypes, respectively, based on molecular, morphological, and physiological features (MacNeil and Masland, 1998; Lin and Masland, 2006; Sanes and Masland, 2015; Baden et al., 2016; Bae et al., 2018; Rheaume et al., 2018; Yan et al., 2020). The processes of generating and maintaining this diversity largely remain elusive, but transcription factor codes have been shown to be important for neuronal subtype specification and maintenance (Guillemot, 2007; Deneris and Hobert, 2014; Peng et al., 2017; Sajgo et al., 2017; Lyu et al., 2021).

Neuron types are defined in part by the expression of the genes that contribute to their identity and function, including those that encode sensory receptors, signaling molecules, ion channels, and structural features such as dendritic arborization (Deneris and Hobert, 2014). Our lab and others have shown that the t-box transcription factor, Tbr2 (also known as EOMES), is expressed in a subset of RGCs early in development that will become ipRGCs (defined by expression of melanopsin, and axonal targeting patterns; Mao et al., 2014; Sweeney et al., 2014). Tbr2 is also expressed in a subset of displaced ACs. Removal of Tbr2 from RGCs during development leads to a loss of ipRGCs (Mao et al., 2014; Sweeney et al., 2014). Tbr2 expression is maintained in the adult and is expressed in all ipRGC subtypes (Tran et al., 2019; Chen et al., 2021).

ipRGCs are intrinsically photosensitive because they express the photopigment melanopsin which allows them to detect light and thus execute several light-induced behaviors (Provencio et al., 2000, 2002a; Berson et al., 2002; Hattar et al., 2002), including: Circadian photoentrainment, pupillary light reflex, mood regulation, and learning; ipRGCs also play a role in some aspects of image-forming vision including contrast detection (Panda et al., 2002; Ruby et al., 2002; Güler et al., 2008; Hatori et al., 2008; Legates et al., 2012; Schmidt et al., 2014; Sonoda et al., 2018; Stabio et al., 2018). ipRGCs integrate rod, cone, and melanopsin signals before transmitting this information to many subcortical areas of the brain. Loss of ipRGCs in blinding diseases in humans results in sleep disorders, depression, anxiety, defects in post-illumination pupil response, and loss of light-induced suppression of melatonin secretion (Pérez-Rico et al., 2010; Feigl et al., 2011; Agorastos et al., 2013; Wang et al., 2013; Gracitelli et al., 2016). In mice, loss of ipRGCs results in defects in circadian photoentrainment, the pupillary light reflex, light-suppression of locomotor activity, mood, and learning (Güler et al., 2008; Hatori et al., 2008; Legates et al., 2012).

It has been well-documented that ipRGCs survive after injuries to the optic nerve, however, the reason for their survival is not well understood (Robinson and Madison, 2004; Li et al., 2008; Pérez De Sevilla Müller et al., 2014; Duan et al., 2015). Single-cell RNA-sequencing of RGCs after optic nerve crush shows that Tbr2 is enriched in the RGCs that survive (Tran et al., 2019), suggesting a role for Tbr2 in RGC survival after injury.

Here, I set out to determine the role that Tbr2 plays in ipRGC maintenance and in ipRGC survival after injury. I employed a tamoxifen-inducible Cre recombinase system to specifically remove Tbr2 during adulthood in cells that endogenously express Tbr2 (Pimeisl et al., 2013). I find that Tbr2 loss does not alter the dendritic stratification, brain innervation, or survival of ipRGCs. However, I do find that Tbr2-deficient RGCs lose melanopsin expression, but that ectopic expression of Tbr2 in non-Tbr2^{+} RGCs is not sufficient to induce melanopsin expression. Additionally, I demonstrate that removal of Tbr2 leads to reduced survival of ipRGCs in an optic nerve injury model. Finally, I discover that almost all Tbr2^{+} displaced amacrine cells express Meis2 adding to the molecular definition of this subtype.

2.3 Results

2.3.1 Tbr2 is required for maintaining melanopsin expression in intrinsically photosensitive retinal ganglion cells

To test the hypothesis that Tbr2 is required in adulthood for ipRGC survival, I removed *Tbr2* from adult Tbr2-expressing RGCs using *Tbr2$^{CreER/flox}$;tdT* mice. These mice have a tamoxifen-inducible Cre recombinase inserted into exon 1 of the *Tbr2* locus (*Tbr2^{CreER}*; Pimeisl et al., 2013), a *Tbr2* floxed allele (*Tbr2^{flox}*; Zhu et al., 2010), and a Rosa26-tdTomato reporter (*tdT*; Madisen et al., 2010). Tamoxifen administration to *Tbr2$^{CreER/flox}$;tdT* mice results in coincident fluorescent labeling and Tbr2 removal in CreER-expressing cells (**Fig. 2.1A**). We administered tamoxifen to adult *Tbr2$^{CreER/+}$;tdT* (hereafter "control") *and Tbr2$^{CreER/flox}$;tdT* (hereafter "*Tbr2^{KO}*") animals and asked if loss of *Tbr2* results in Tbr2-expressing RGC death, as happens

when *Tbr2* is deleted during development, and if not, whether Tbr2 is required for specifying their axonal projections or dendrite stratification patterns. First I verified that Tbr2^{CreER} labels endogenous Tbr2-expressing RGCs by immunostaining retinas derived from control mice with antibodies directed against Tbr2 and RBPMS (a pan-RGC marker; Rodriguez et al., 2014) and determining the percent overlap of these markers with Tomato fluorescence (**Fig. 2.1B**). I find that all Tomato-labeled cells are also labeled with an anti-Tbr2 antibody, illustrating that Tbr2^{CreER} recapitulates endogenous Tbr2 expression (**Fig. 2.1B**). I also find that 63% ± 3 (393 cells, n = 3 mice) of Tomato-expressing cells do not express RBPMS, corroborating the recent finding that these cells are displaced amacrine cells (ACs; Chen et al., 2021, see below). The majority of Tomato-expressing cells in the ganglion cell layer (GCL) have dendrites that laminate in the innermost ON sublamina of the inner plexiform layer (IPL) and sparsely in the outermost OFF sublamina (**Fig. 2.1D** and **Fig. S2.1**), consistent with displaced AC and ipRGC lamination patterns (Provencio et al., 2002b; Viney et al., 2007; Schmidt and Kofuji, 2009; Ecker et al., 2010; Quattrochi et al., 2018; Chen et al., 2021).

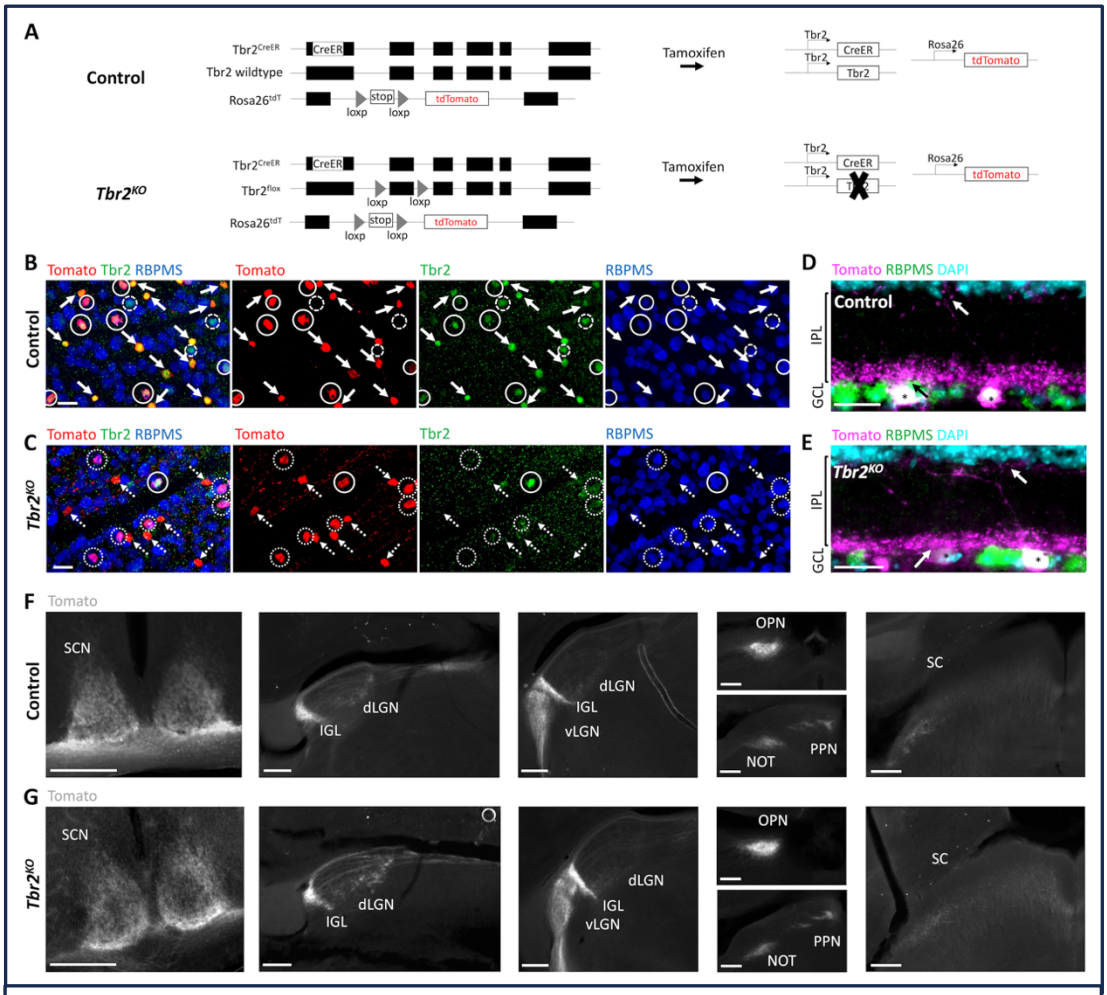

Figure 2.1 Characterization of Tbr2^{CreER} expression visualized by tdTomato reporter in wildtype and *Tbr2^{KO}* retinas and brains

(A) Schematic of genetic strategy used to label and remove Tbr2 from Tbr2^{+} cells in adulthood. Black boxes are exons, thin lines are non-coding regions. **(B, C)** Flatmount view, GCL side up, of a retina derived from a *Tbr2$^{CreER/+}$;tdT* (control, **B**) or *Tbr2$^{CreER/flox}$;tdT* (*Tbr2^{KO}*, **C**) P60 mouse immunostained to reveal expression of Tomato (red), Tbr2 (green), RBPMS (blue) with the first image being a merge of all markers; white circles represent Tbr2^{+} Tomato-labeled RGCs, solid arrows point to Tbr2^{+} Tomato-labeled amacrine cells (lack RBPMS expression), dashed circles indicate Tbr2^{+} RGCs that do not express Tomato, dotted circles indicate Tomato-labeled RGCs that do not express Tbr2, and dashed arrows point to Tomato-labeled amacrine cells that do not express Tbr2; scale bar=25 µm. While 98% of wildtype Tomato^{+} RGCs express Tbr2 **(B)**, only 15% express Tbr2 in the mutant **(C)**. **(D, E)** Section of a control **(D)** and *Tbr2^{KO}* **(E)** mouse retina immunostained to reveal expression of Tomato (magenta), RBPMS (green),

DAPI (cyan); scale bar=25 μm. There is no difference in localization of Tomato$^+$ dendrites between these mice (arrows indicate dendrites of Tomato$^+$ RGCs (asterisks) in the innermost and outermost lamina of the IPL). **(F, G)** Comparison of the axonal trajectories of Tomato-labeled RGCs in control **(F)** and *Tbr2*^{KO} **(G)** mice. Coronal sections reveal that Tomato$^+$ RGCs innervate the SCN, dLGN, IGL, vLGN, OPN, PPN, and deep SC in controls **(F)** and maintain this innervation in *Tbr2*^{KO} mice **(G)**. Scale bars=250 μm. GCL, ganglion cell layer; IPL, inner plexiform layer; INL, inner nuclear layer; SCN, suprachiasmatic nucleus; dLGN, dorsal lateral geniculate nucleus; IGL, intergeniculate leaflet; vLGN, ventral lateral geniculate nucleus; OPN, olivary pretectal nucleus; PPN, posterior pretectal nucleus; SC, superior colliculus.

Because the Tomato labels the axons of RGCs, the location of Tbr2-expressing axon projects in the brain can be determined. I find that Tomato-expressing RGCs project to all brain regions known to be innervated by ipRGCs including the SCN, external vLGN, IGL, OPN, PPN, as well as sparsely to the dLGN and deep SC (**Fig. 2.1F**).

Next I aimed to determine if loss of *Tbr2* in adulthood affects the survival or health of Tbr2$^+$ RGCs by administering tamoxifen to *Tbr2*^{KO} mice and analyzing (as above) the retina and brain targets 33–36 days later. I find that Cre activation results in the loss of expression of Tbr2 in most Tomato-expressing RGCs (85% ± 3, 162/189 Tomato$^+$ RGCs, n = 3 mice; **Fig. 2.1C**). However, removing Tbr2 does not affect the overall number of Tomato-expressing RGCs compared to controls (112 ± 22 cells/mm^2 in *Tbr2*^{KO} mice, 200 Tomato$^+$ RGCs counted vs. 122.7 ± 3 cells/mm^2 in control mice, 219 Tomato$^+$ RGCs counted, n = 3 mice for each genotype, P = 0.9998; **Fig. 2.1B**, **2.1C**, **2.2C**). Analysis of retina sections (n = 3 mice) shows that Tbr2-deficient RGC and AC dendrites continue to laminate within the innermost ON

and sparsely in the outermost OFF sublaminae of the IPL (**Fig. 2.1E** and **Fig. S2.1**). I also find that Tomato-labeled RGC axons in mutant mice maintain projections to their brain targets and innervate them to a similar extent as in control mice (**Fig. 2.1G**). Taken together these results demonstrate that *Tbr2* is not required for the maintenance of dendrite localization, axon projections, or RGC survival.

Melanopsin expression is a key feature of ipRGCs therefore I next asked whether Tbr2 is required for this aspect of ipRGC identity. I stained control and $Tbr2^{KO}$ retinas with an anti-melanopsin antibody (**Fig. 2.2A-B**) and found that there is a 75% reduction in melanopsin-expressing Tomato-labeled cells in $Tbr2^{KO}$ retinas relative to control retinas (42/200 $Tomato^{+}$ RGCs vs. 171/219 $Tomato^{+}$ RGCs; **Fig. 2.2C**) derived from littermates. However, as previously mentioned, there is no difference in the number of Tomato-expressing RGCs in the mutant retinas. Because there is some variation in the proportion of Cre-activated cells in each mouse, I also looked at the percentage of Tomato-labeled cells belonging to cell populations of interest (**Fig. 2.2D**). I found a significant reduction in the percentage of Tomato-labeled cells that also express melanopsin (8% ± 1 vs. 29% ± 3, $P < 0.001$, 505 $Tomato^{+}$ cells and 612 $Tomato^{+}$ cells scored per genotype, respectively) and a significant increase in the percentage of Tomato-labeled cells that are non-melanopsin-expressing RGCs (33% ± 4 vs. 8% ± 1, $P < 0.001$) in $Tbr2^{KO}$ mice relative to control mice (**Fig. 2.4D**). Together, these data illustrate that while melanopsin expression is lost in Tbr2-mutant RGCs, their survival is unaffected. This result conflicts with two recent studies that reported a decrease in survival of melanopsin and/or Tbr2-

expressing RGCs after conditional removal of *Tbr2* using different Cre systems. One study showed a ~50% reduction in the number of ipRGCs ~40 days after conditional Tbr2 removal (Bray et al., 2019) and the other found a near complete loss of Tbr2-expressing cells 38 days after conditional Tbr2 removal (Chen et al., 2021). I worried that one difference in these studies compared to ours is the time after Cre activation (~40 vs. ~30 days, respectively). To address this discrepancy, I performed a separate experiment in which I waited 45–50 days before analysis. I found that the number of Tomato-expressing RGCs in $Tbr2^{KO}$ mice remained similar to controls (101 ± 15 cells/mm^2, 219 Tomato$^+$ RGCs counted vs. 117 ± 11 cells/mm^2, 255 Tomato$^+$ RGCs counted, respectively, $n = 3$ for each genotype, $P = 0.9995$; **Fig. 2.5B**). However, there appears to be a trending, but not statistically significant, decrease of Tomato-expressing amacrine cells (117 ± 22 cells/mm^2, 254 Tomato$^+$ACs counted in $Tbr2^{KO}$ mice and 199 ± 45 cells/mm^2, 432 Tomato$^+$ ACs counted in control mice, $n = 3$ mice for each genotype, $P = 0.39$; **Fig. 2.5B**).

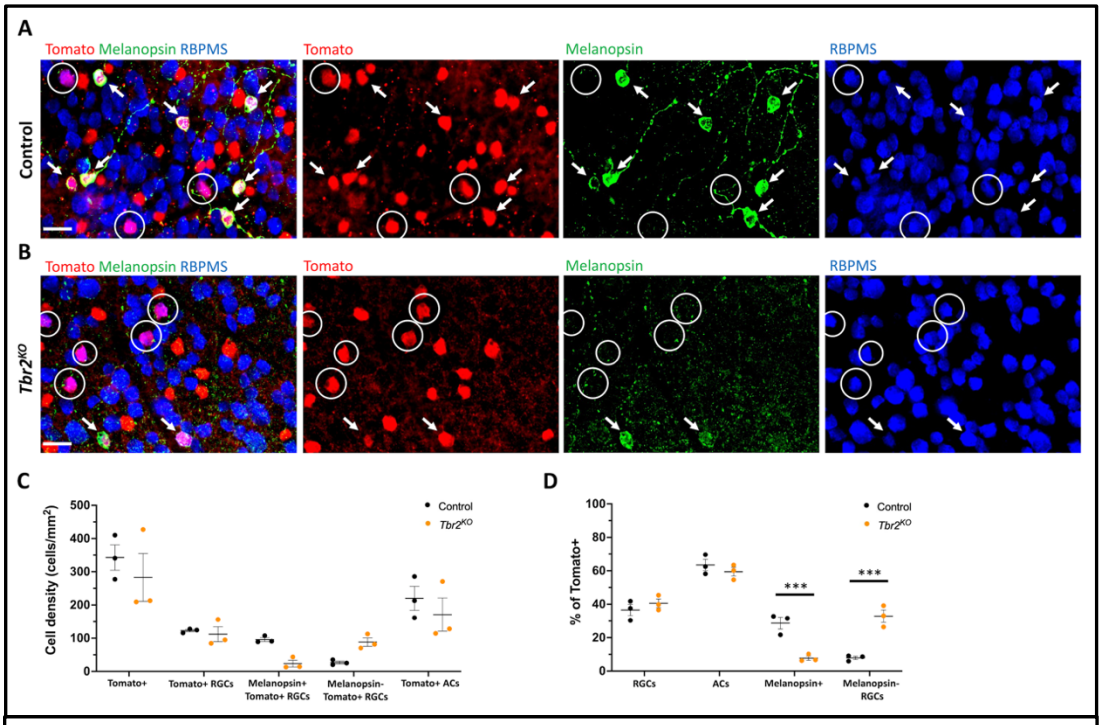

Figure 2.2 Loss of Tbr2 in adulthood results in loss of melanopsin expression but not cell death of Tomato$^+$ RGCs.

(A) Flatmounted control (*Tbr2$^{CreER/+}$;tdT*) retina (GCL side up) immunostained to reveal expression of Tomato (red), melanopsin (green), and RBPMS (blue); circled cells are Tomato$^+$ RGCs that do not express melanopsin, arrows point to melanopsin$^+$Tomato$^+$ RGCs, scale bar= 25 µm. **(B)** Flatmounted *Tbr2^{KO}* (*Tbr2$^{CreER/flox}$;tdT*) retina immunostained to reveal expression of Tomato (red), melanopsin (green), and RBPMS (blue); circled cells are Tomato$^+$ RGCs that do not express melanopsin, arrows point to melanopsin$^+$Tomato$^+$ RGCs. Tomato$^+$ cells lose melanopsin expression. **(C)** Quantification of cell densities (cells/mm^2) of different cell populations in control and *Tbr2^{KO}* mice (n=3 mice in each group; each dot represents the sum of 4 fields of view (FOVs) for 1 retina; mean ± SEM displayed; two-way ANOVA with Sidak's multiple comparisons test; no significant differences). **(D)** Quantification of the percentages of Tomato$^+$ cells that belong to cell populations of interest in control and *Tbr2^{KO}* mice (n=3 mice in each group; each dot represents the percentage for 4 summed FOVs of 1 retina; mean ± SEM displayed; two-way ANOVA with Sidak's multiple comparisons test; *** P<0.001).

2.3.2 Tbr2 Is Not Sufficient for Melanopsin Expression

To test whether ectopic expression of Tbr2 can induce expression of melanopsin, I intravitreally injected Tbr2-GFP-AAV2 or GFP-AAV2 into the eyes of wildtype adult mice and examined expression of markers 4 weeks later (**Fig. 2.3A**). First, to determine if infection of RGCs with Tbr2-GFP-AAV2 results in production of Tbr2 protein, I performed intravitreal virus injection with AAV during adulthood (~P40), waited 2 weeks, then dissected retinas and examined Tbr2 expression. I found that all Tbr2-GFP-AAV2-infected cells also express Tbr2, while 17% of cells infected with GFP-AAV2 express Tbr2 (**Fig 2.3B**). Interestingly, this is higher than the percent of Tbr2-expressing RGCs in wildtype retina (11.3% ± 0.3, 596 $Tbr2^+$ RGCs/5,279 total RGCs, n = 3 mice, uncrushed eyes from **Fig. 2.4B**; consistent with Chen et al., 2021), suggesting that Tbr2-expressing RGCs are preferentially infected with the virus. I also found that there is increased density of melanopsin-expressing RGCs in Tbr2-GFP-AAV2-infected retinas relative to GFP-AAV2-infected retinas 4 weeks after AAV injection (173 ± 6 cells/mm^2, 308 melanopsin cells counted vs. 133 ± 5 cells/mm^2, 237 melanopsin cells counted, n = 3 mice, P = 0.00855; **Fig. 2.3C**). However, many Tbr2-GFP-AAV2-infected RGCs do not express melanopsin (89%, 662 cells, **Fig. S2.2**) leading to the hypothesis that this increase in ipRGC density is the result of over-expressing Tbr2 in cells that already express Tbr2, but do not express melanopsin at levels sufficient to be detected by melanopsin antibody. To determine whether expression of Tbr2 can induce melanopsin expression in non-Tbr2-expressing RGCs, I injected Tbr2-GFP-AAV2 and GFP-AAV2 into the eyes of $Isl1^{Cre/+};Tbr2^{flox/flox}$ mice.

Isl1-Cre removes *Tbr2* during development and leads to cell death, thus these mice lack > 99% of ipRGCs as assayed by melanopsin expression (**Fig. S2.3**) and loss of axon projections to non-image-forming brain targets. In these mice, I do not observe an increase in melanopsin expression in the Tbr2-GFP-AAV2-infected retinas (**Fig. 2.3D**), indicating that Tbr2 is not sufficient for melanopsin expression in non-Tbr2^{+} RGCs (13.5 ± 0.96 cells per Tbr2-GFP-AAV2-infected retina vs. 12 ± 0.82 cells per GFP-AAV2-infected retina, n=4 mice, P= 0.2782). To determine whether melanopsin expression is only induced in endogenous Tbr2 cells, I performed the same experiment in control (*Tbr2$^{CreER/+}$;tdT)* and *Tbr2^{KO}* (*Tbr2$^{CreER/flox}$;tdT)* mice after tamoxifen induction to label endogenous Tbr2 cells with tdTomato. I found a significant increase in the percentage of Tbr2-expressing RGCs that also express melanopsin in the Tbr2-GFP-AAV2-infected retinas relative to retinas infected with control virus (**Fig. 2.3E**) (80% ± 2 vs. 70% ± 1, n = 4 mice, P = 0.0156, 259 Tbr2-GFP-AAV2-infected Tomato^{+}RGCs scored and 301 GFP-AAV2-infected Tomato^{+} RGCs scored), but there is not a significant increase when Tbr2 is absent (22% ± 3 vs. 17% ± 4, n = 3 mice, P = 0.2651, 231 Tbr2-GFP-AAV2-infected Tomato^{+} RGCs scored and 172 GFP-AAV2-infected Tomato^{+} RGCs scored; **Fig. 2.3E**). These data show that Tbr2 can increase melanopsin expression in a subset of Tbr2-expressing RGCs but cannot if Tbr2 is deleted.

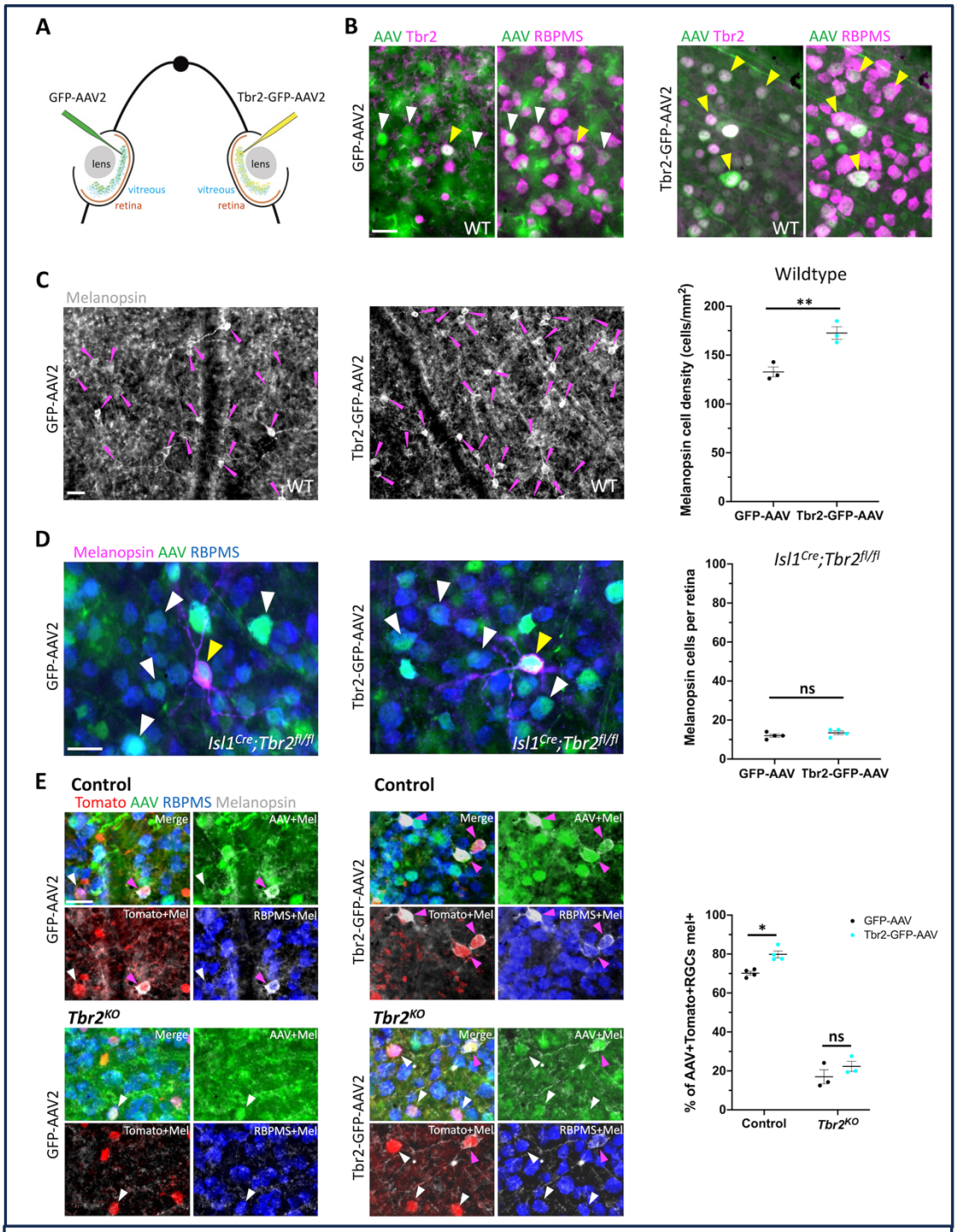

Figure 2.3 Ectopic expression of Tbr2 does not induce melanopsin expression in non-Tbr2 RGCs

(A) Experimental overview of intravitreal AAV2 injection. One eye of an adult

mouse (~P40) was injected with a control virus, GFP-AAV2, while the contralateral eye was injected with a Tbr2-expressing virus, Tbr2-GFP-AAV2. **(B)** Flatmounted retinas (GCL side up) of eyes injected with GFP-AAV2 (left) or Tbr2-GFP-AAV2 (right) are immunostained with the antibody indicated: Tbr2 (magenta), GFP (green), and RBPMS (magenta); the left images for each virus condition are showing overlap of GFP and Tbr2 expression while the right images are showing overlap of GFP and RBPMS expression; white arrowheads indicate example virus-infected RGCs that do not express Tbr2 and yellow arrowheads indicate example virus-infected RGCs that express Tbr2; scale bar=25 μm. In the Tbr2-GFP-AAV2-infected retina (right), all virus-infected RGCs express Tbr2. **(C)** Flatmounted retinas of a wildtype mouse infected with GFP-AAV2 (left) and Tbr2-GFP-AAV2 (middle) and immunostained to reveal expression of melanopsin (grayscale); magenta arrowheads point to melanopsin$^+$ cells, scale bar=25 μm. Right panel is showing the quantification of melanopsin$^+$ cells in these retinas (n=3 mice for each group; each dot represents the sum of 4 FOVs per retina; mean ± SEM displayed; Student's t-test; ** P<0.01). There is a significant increase in melanopsin$^+$ cells in the Tbr2-GFP-AAV2-infected retina. **(D)** Flatmounted retinas of an *Isl1^{Cre};Tbr2$^{flox/flox}$* mouse infected with GFP-AAV2 (left) and Tbr2-GFP-AAV2 (middle) immunostained to reveal expression of melanopsin (magenta), GFP (green), RBPMS (blue); white arrowheads point to example melanopsin-negative RGCs infected with virus, yellow arrowheads point to rare melanopsin$^+$ cells, scale bar=25 μm. Right panel is showing the quantification of melanopsin$^+$ cells (n=4 mice in each group; each dot represents the total number of melanopsin$^+$ cells in 1 retina; mean ± SEM displayed; Student's t-test; ns=P>0.05). There is no change in melanopsin expression in Tbr2-GFP-AAV2-infected retinas in *Isl1^{Cre};Tbr2$^{flox/flox}$* mice. **(E)** Flatmounted retinas of control (*Tbr2$^{CreER/+}$;tdT*, left) and *Tbr2^{KO}* (*Tbr2$^{CreER/flox}$;tdT*, right) mice immunostained to reveal tomato (red), GFP (green), RBPMS (blue), and melanopsin (gray) expression in GFP-AAV2-infected (left) and Tbr2-GFP-AAV2-infected (middle) retinas. The first image of each is a merge of all color channels, others are showing melanopsin in combination with the other markers indicated. Magenta arrowheads point to virus-infected Tomato$^+$ RGCs that express melanopsin and white arrowheads point to virus-infected Tomato$^+$ RGCs that do not express melanopsin. Scale bar=25 μm. Bottom, quantification of the percentage of virus-infected Tomato$^+$ RGCs that express melanopsin in control and *Tbr2^{KO}* mice infected with GFP-AAV2 and Tbr2-GFP-AAV2 (n=4 mice for each group, each dot represents the percentage for the sum of 7 or more FOVs in one retina; mean ± SEM displayed; two-way ANOVA with Sidak's multiple comparisons, * P<0.05, ns=P>0.05). There is increased melanopsin expression in Tbr2-GFP-AAV2-infected Tomato$^+$ RGCs.

2.3.3 Tbr2 Expression Influences Intrinsically Photosensitive Retinal Ganglion Cell Survival After Injury

IpRGCs preferentially survive after optic nerve injury relative to RGCs that are not intrinsically photosensitive (Robinson and Madison, 2004; Li et al., 2008; Pérez De Sevilla Müller et al., 2014; Duan et al., 2015), yet the reason for this is poorly understood. Because Tbr2 is enriched in surviving RGCs (Tran et al., 2019), we hypothesized that Tbr2 could be required for RGC survival after optic nerve crush (ONC). First I wanted to determine whether all Tbr2-expressing RGCs survive ONC or if only the melanopsin-expressing subset of Tbr2-expressing RGCs is spared. To test this, I performed ONC on one eye of an adult (~P60) mouse, waited 2 weeks, then examined both retinas for expression of RGC markers. In the uncrushed eye, 11.3% ± 0.3 (n = 3 mice, 596 cells) of RBPMS-labeled cells express Tbr2 and 30.9% ± 2.1 (186 cells) of Tbr2-expressing RGCs express melanopsin (the melanopsin-negative Tbr2-expressing RGCs are likely M4-M6 ipRGCs that express low levels of melanopsin; Ecker et al., 2010; Quattrochi et al., 2018). In the ONC retinas, I find that 13% ± 1 (670 cells; normalized to control "uncrushed" eye) of RGCs survive (**Fig. 2.4A, 2.4B**). I also found that 22% ± 2 (134 cells) of total Tbr2-expressing RGCs survive. The majority of these surviving cells express melanopsin (71% ± 1; 95 cells), suggesting that the melanopsin-expressing Tbr2-expressing RGCs preferentially survive optic nerve injury (**Fig. 2.4B**). When separating Tbr2-expressing RGCs into those that express melanopsin and those that do not, I found that 52% ± 4 (95 cells, $P <$ 0.001, significantly greater than survival of all RGCs: 13% ± 1) and 10% ± 1 (39 cells)

survive, respectively (Fig. 2.4B). There is no change in the survival of Tbr2-expressing amacrine cells (Fig. 2.4B) indicating that they are unaffected by ONC, consistent with previous reports regarding amacrine cell survival after optic nerve injury (Nadal-Nicolás et al., 2015).

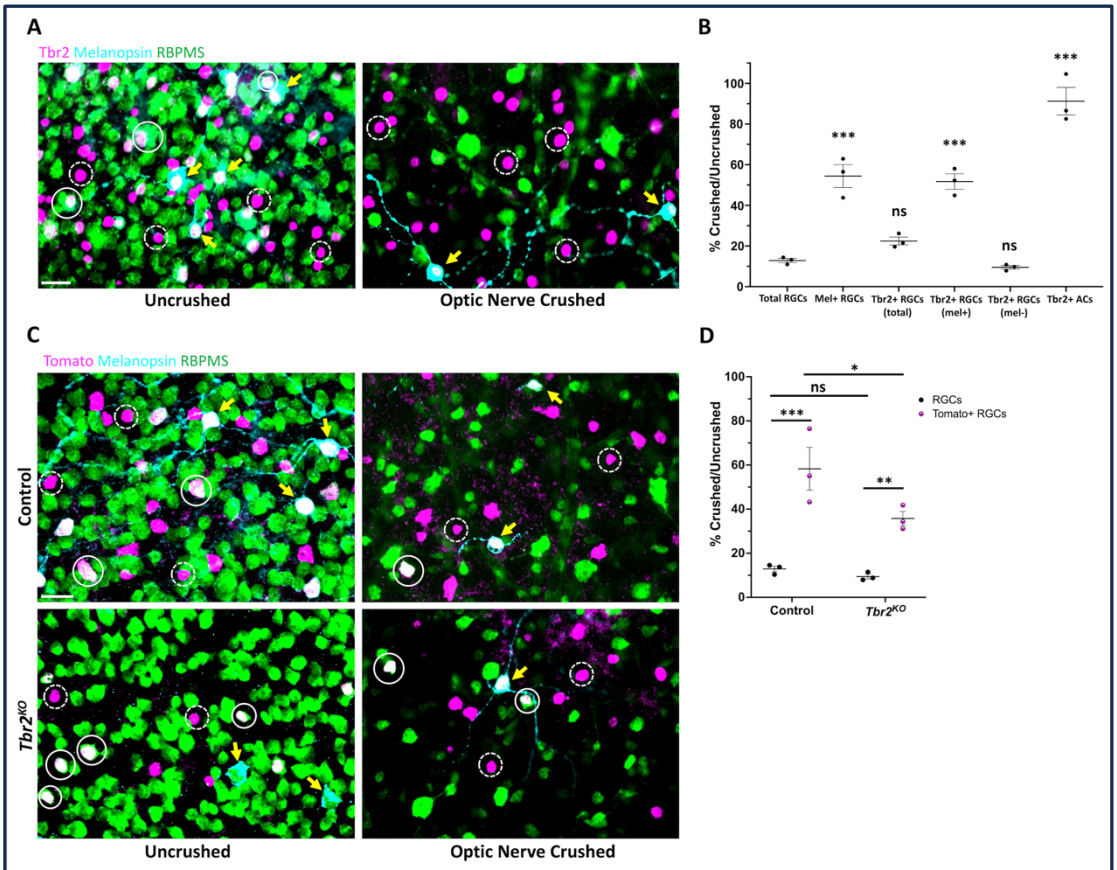

Figure 2.4 Tbr2-expressing RGCs preferentially survive optic nerve injury and Tbr2 influences their survival

(A) Flatmounted retinas of an uncrushed control eye (left) and optic nerve crushed eye (right) immunostained to reveal expression of Tbr2 (magenta), melanopsin (cyan), and RBPMS (green); solid white circles represent Tbr2$^+$ RGCs that do not express melanopsin, yellow arrows point to melanopsin$^+$Tbr2$^+$ RGCs, dashed white circles indicate Tbr2$^+$ amacrine cells, scale bar=25 µm. **(B)** Quantification of percent survival of cell populations of interest in ONC eyes normalized to uncrushed control eyes (n=3 mice, each dot represents the percentage for one mouse-4 FOVs/retina; mean ± SEM displayed; one-way ANOVA with Dunnett's multiple comparisons,

comparing each group to RGCs; *** P<0.001, ns=P>0.05). A significantly greater percentage of melanopsin^{+}Tbr2^{+} RGCs survive ONC compared to other RGCs. **(C)** Left, flatmounted retinas of uncrushed control (*Tbr2$^{CreER/+}$;tdT,* top) and *Tbr2^{KO}* (*Tbr2$^{CreER/flox}$,* bottom) eyes. Right, flatmounted retinas of optic nerve crushed control (top) and *Tbr2^{KO}* (bottom) eyes immunostained to reveal expression of Tomato (magenta), melanopsin (cyan), and RBPMS (green). Scale bar=25 μm. **(D)** Quantification of percent survival of Tomato^{+} RGCs (purple, pattern) and all other RGCs (black, solid) in ONC eyes normalized to uncrushed control eyes in control and *Tbr2^{KO}* mice (n=3 mice for each group, each dot represents the percentage for one mouse-4 FOVs/retina; mean ± SEM displayed; two-way ANOVA with Sidak's multiple comparisons,*** P<0.001,** P<0.01 * P<0.05, ns P>0.05). Tomato^{+} RGCs have increased survival relative to other RGCs in both control and *Tbr2^{KO}* mice but show decreased survival in *Tbr2^{KO}* mice.

To test if Tbr2 expression is required for the preferential survival of Tbr2-expressing RGCs, I performed ONC in control (*Tbr2$^{CreER/+}$;tdT*) and *Tbr2^{KO}* (*Tbr2$^{CreER/flox}$;tdT*) mice (**Fig. 2.4C, 2.4D**). I found that in control mice, 58% ± 10 (100 cells crushed, 183 cells uncrushed) of Tomato-expressing RGCs survive nerve crush while only 13% ± 1 (711 cells crushed, 6,058 cells uncrushed) of non-Tomato-expressing RGCs survive ($P <$ 0.001; **Fig. 2.4C, 2.4D**). However, in *Tbr2^{KO}* mice only 35% ± 3 (70 cells crushed, 199 cells uncrushed) of Tomato-expressing RGCs survive (P = 0.0153, compared to survival in control mice) while 9% ± 1 (508 cells crushed, 5,544 cells uncrushed) of non-Tomato-expressing RGCs survive ($P <$ 0.01; **Fig. 2.4C, 2.4D**) suggesting that Tbr2 influences, but is not essential for, ipRGC survival after injury.

2.3.4 Tbr2^{+} Cells in the GCL Include Displaced Amacrine Cells That Express the GABAergic Amacrine Cell Marker, Meis2

As noted earlier, I found that 63% of Tbr2-expressing cells in the GCL of the adult retina do not express the RGC marker RBPMS, suggesting that these are displaced amacrine cells. It has been previously reported that some Tbr2-expressing cells also express the pan-amacrine cell marker syntaxin-1 (Mao et al., 2008), and more recently that over half of the Tbr2-expressing cells in the GCL are displaced amacrine cells labeled in the *slc32aiCre;Ai9* mouse strain (Chen et al., 2021). Most displaced amacrine cells are GABAergic (Pérez De Sevilla Müller et al., 2007). However, we previously looked at the degree of GABA and Tbr2 co-expression in P8 retinas and found that only 3% of Tbr2 cells in the GCL express GABA (Sweeney et al., 2014). Recently, Meis2, a GABAergic amacrine cell marker (Bumsted-O'Brien et al., 2007), was found to be expressed in Tbr2^{+} cells in the inner nuclear layer (INL) of mouse retina (Yan et al., 2020), therefore I revisited this question. To determine whether Meis2 is also expressed in displaced Tbr2-expressing amacrine cells, I treated retinas from adult tamoxifen-induced *Tbr2$^{CreER/+}$;tdT* mice (45–50 days after tamoxifen administration) with an anti-Meis2 antibody and found that Meis2 is expressed in 93% ± 2 (405 cells) of Tbr2-expressing cells that do not express RBPMS in the GCL (**Fig. 2.5A, 2.5B**). Meis2 is also expressed in a subset of Tbr2-expressing RGCs (18% ± 11, 48 cells). I then asked whether Tbr2 is required for Meis2 expression or maintenance of Meis2-expressing cells. In adult *Tbr2^{KO}* mice, I found that Meis2 expression was unchanged; the percentage of Tbr2-expressing cells that also express

Meis2 is not significantly different in *Tbr2*^{KO} mice relative to control mice (67% ± 4 vs. 65% ± 3, $P = 0.9978$, 473 Tomato^{+} cells scored and 687 Tomato^{+} cells scored, respectively; **Fig. 2.5C**). Additionally, there is no difference in the percentage of Tomato-labeled cells that are Meis2-expressing ACs (52% ± 2 in *Tbr2*^{KO} mice and 57% ± 4 in control mice, $P = 0.8399$) or Meis2-expressing RGCs (15% ± 5 in Tbr2^{KO}mice and 8% ± 2 in control mice, $P = 0.6008$). However, there does appear to be a trend toward a reduction in the number of Tomato^{+} amacrine cells in the mutant mice (Fig. 2.5B, 2.5C). I immunostained wildtype retinas with anti-Meis2 antibody and the anti-GABA antibody that was used in our previous study (Sweeney et al., 2014) to determine whether Meis2 cells express GABA (**Fig. S2.4**). I found that hardly any cells in the GCL are labeled by the anti-GABA antibody (**Fig. S2.4C**), contrary to previous findings using a different anti-GABA antibody (Pérez De Sevilla Müller et al., 2007). Additionally, many Meis2-expressing cells in the INL are not labeled by the anti-GABA antibody while it has been shown that the majority of Meis2-expressing cells in the INL express GAD65/67 (Bumsted-O'Brien et al., 2007), the GABA synthesizing enzymes. We suspect that this particular anti-GABA antibody does not reliably identify GABAergic cells with our immunostaining technique and thus our previous conclusion that Tbr2 cells do not express GABA was misconceived.

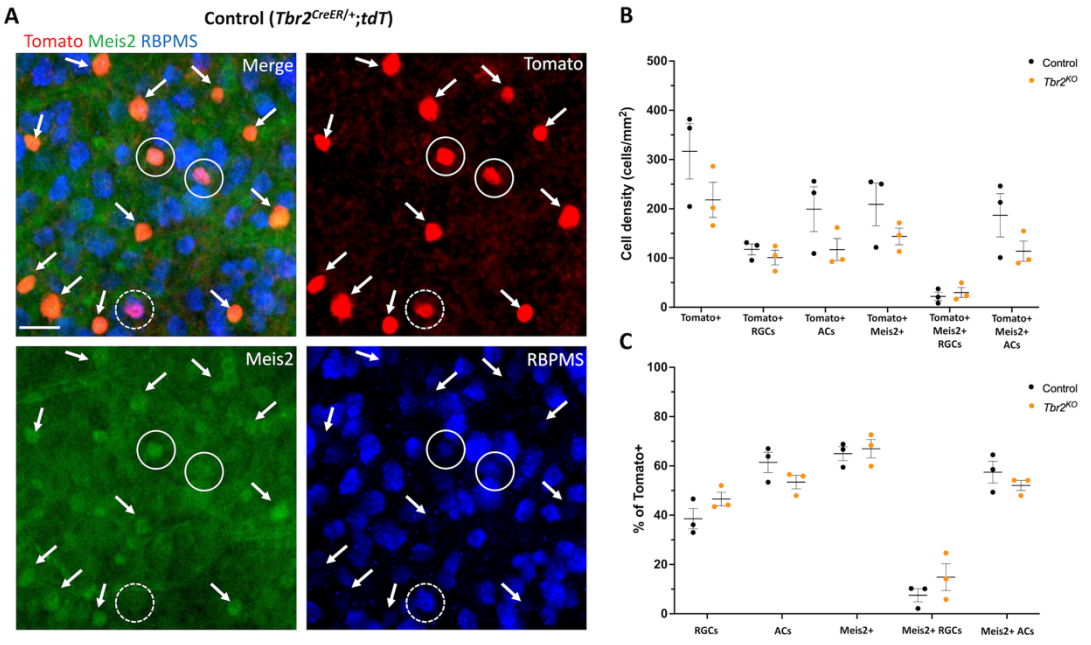

Figure 2.5 Meis2 is expressed in the majority of Tbr2-expressing displaced amacrine cells and in a subset of Tbr2-expressing RGCs

(A) Flatmounted retina of a control (*Tbr2*$^{CreER/+}$*;tdT)* mouse immunostained to reveal expression of tomato (red), Meis2 (green), and RBPMS (blue). First image is a merge of all color channels, others are showing each channel independently; arrows point to Tomato^{+} ACs expressing Meis2; closed white circles represent Tomato^{+} RGCs expressing Meis2; dashed white circles indicate Tomato^{+} RGCs that do not express Meis2. All Tomato^{+} ACs in this image express Meis2. **(B)** Quantification of the density (cells/mm^2) of cell populations of interest in control and *Tbr2*^{KO} mice (n=3 mice in each group, each dot represents the sum of 4 FOVs per retina, mean ± SEM displayed; two-way ANOVA with Sidak's multiple comparisons test; no significant differences). There is a trend towards a decrease in the density of labeled amacrine cells. **(C)** Quantification of the percentage of Tomato^{+} cells that belong to cell populations of interest in control and *Tbr2*^{KO} mice (n=3 mice in each group; each dot represents the percentage for 4 summed FOVs of 1 retina; mean ± SEM displayed; two-way ANOVA with Sidak's multiple comparisons test; no significant differences).

2.4 Discussion

Here I use a tamoxifen-inducible Cre line to examine the role of Tbr2 in the adult mouse retina. Previous work from our lab and others has shown that *Tbr2* is

required for the development of ipRGCs (Mao et al., 2014; Sweeney et al., 2014), but its role in the adult retina has only recently been explored (Bray et al., 2019; Chen et al., 2021). In the present study, I show that Tbr2 is required for the maintenance of melanopsin expression in ipRGCs but is dispensable for their survival. Additionally, I found that Tbr2 induces melanopsin expression in endogenous Tbr2 RGCs but is unable to do so in conventional RGCs nor can it restore melanopsin expression in Tbr2-mutant RGCs. Furthermore, I show that Tbr2-expressing ipRGCs survive after optic nerve injury and that this resilience is diminished in Tbr2-mutant RGCs. Lastly, I identified a marker for Tbr2-expressing displaced amacrine cells that also labels a subset of Tbr2-expressing RGCs.

2.4.1 Tbr2 Is Not Required for the Survival of Mature Intrinsically Photosensitive Retinal Ganglion Cells

Our results showing that conditional deletion of Tbr2 in the adult does not affect RGC survival is contrary to what others have reported using different methods. Bray et al. (2019) concluded that Tbr2 is required for the maintenance of ipRGC viability. They used Opn4^{CreER} to remove a conditional Tbr2 allele while labeling the mutant cells with a tdTomato fluorescent reporter (Bray et al., 2019). They reported that ~40 days after tamoxifen administration there was a ~50% reduction in the number tdTomato-expressing cells compared to controls, while I found no significant differences (**Fig. 2.2, 2.5**). One possible explanation for the difference between this result and ours comes from the different methods to remove adult Tbr2 expression. Because Opn4 expression is dependent upon Tbr2 expression (**Fig. 2.2**), the removal of Tbr2 in adult

RGCs should result in a loss of melanopsin expression and thus Opn4^{CreER} expression. This would lead to a decrease of tdTomato-labeled RGCs because once Tbr2 expression is removed no new cells can become activated. A second recent study by Chen et al. (2021) removed Tbr2 via intravitreal injection of AAV-Cre in *Tbr2*$^{TauGFP–IRESCreER2/fx}$ mice. They found that 12 days after injection, Tbr2 expression was lost as assayed by Tbr2 antibody staining, but the cells survived (labeled by GFP via *Tbr2*$^{TauGFP–IRESCreER2}$; Chen et al., 2021). However, 38 days after injection, there were few GFP-expressing RGCs in Tbr2-deleted regions. In this model, GFP expression relies on the expression of Tbr2. One hypothesis for their observations is that Tbr2 regulates its own gene expression and once Tbr2 is removed it can no longer activate GFP expression. Consistent with this, Chip-seq experiments show that Tbr2 binds its own locus in E14.5 mouse cortex and has been identified as a direct activator of *Tbr2* (Sessa et al., 2017; Elsen et al., 2018; Hevner, 2019).

2.4.2 Tbr2 Regulates Adult Melanopsin Expression

While removal of Tbr2 in adult mice leads to the loss of melanopsin expression (**Fig. 2.2**), ectopic expression of Tbr2 only induces melanopsin expression in Tbr2-expressing RGCs. When Tbr2 was ectopically expressed in the retinas of wildtype mice, I observed a modest increase (30% ± 8) in the number of melanopsin-expressing cells (**Fig. 2.3C**). However, when I did the same experiment in ipRGC-deficient mice (*Isl1*^{Cre}*;Tbr2*$^{flox/flox}$), I did not detect an increase of melanopsin expressing RGCs (**Fig. 2.3D**). This result could be explained if only the endogenously Tbr2-expressing RGCs can change their melanopsin expression upon Tbr2 addition. Consistent with this,

ectopic expression of Tbr2 in *Tbr2$^{CreER/+}$;tdT* mice but not in *Tbr2$^{CreER/fl}$;tdT* mice resulted in increased melanopsin expression in Tomato-labeled RGCs (**Fig. 2.3E**). Lower levels of expression of Tbr2 could be one reason why M4-M6 ipRGC types express less melanopsin than M1-M3 ipRGC types (Ecker et al., 2010; Quattrochi et al., 2018).

2.4.3 Tbr2 Mutant Retinal Ganglion Cells Have Reduced Survival After Injury

Although ipRGCs preferentially survive after optic nerve crush, the reason for their survival is unknown. In this study I found that Tbr2 mutant RGCs (which lack melanopsin expression) do not survive as well as their wildtype counterparts after nerve crush. This result is consistent with what was reported by Bray et al. (2019) in which they reported a 30% reduction in Tomato-expressing cell survival after optic nerve crush in Tbr2 mutants (*Opn4$^{CreER/+}$;Tbr2$^{flox/flox}$;tdT*) relative to wildtype (*Opn4$^{CreER/+}$;Tbr2$^{+/+}$;tdT)*. They further showed that lack of melanopsin expression alone does not account for the survival difference leading to the hypothesis that Tbr2 regulates non-melanopsin genes that are involved in ipRGC survival after injury, such as PACAP (Seki et al., 2008; Ye et al., 2019), but this remains to be determined.

2.4.4 Meis2 Labels the Majority of Tbr2$^+$ Displaced ACs and a Subset of Tbr2$^+$ RGCs

It has been previously shown that all Tbr2-expressing cells in the inner nuclear layer of the retina also express Meis2 (Yan et al., 2020) but the expression of Meis2 in cells within the GCL has not yet been explored. Here we show that Meis2 is expressed in the majority of Tbr2-expressing displaced amacrine cells and in a subset of Tbr2-

expressing RGCs. Using the Broad Institute's Single Cell Portal to explore the single cell sequencing dataset acquired in the aforementioned study (Yan et al., 2020), I found that Tbr2 is expressed in 6 out of 63 uniquely identified clusters of amacrine cells out of 63 total clusters identified (clusters # 44, 48, 54, 57, 59, 63). Of these 6 clusters, all express Gad1 and Gad2 (GABA synthesis enzymes) and all but 1 cluster (#57) express Meis2. This non-Meis2-expressing cluster accounts for the 7% of displaced Tbr2-expressing ACs that were not labeled by the Meis2 antibody in this study. Using the same tool to explore RGC RNA-sequencing datasets (Tran et al., 2019), I found that Tbr2 is expressed in 8 clusters (clusters # 7, 8, 22, 29, 31, 33, 40, 43) which include all of those that express melanopsin (7-low, 8-low, 22, 31, 33, 40, 43). Of the clusters expressing Tbr2, #s 29 and 40 express Meis2. Cluster 29 corresponds to the only cluster of Tbr2-expressing RGCs that does not express melanopsin and is a "novel" cluster, indicating that no known RGC subtypes correspond to this cluster. It would be interesting to determine whether this group is the newly identified Tbr2-expressing Pou4f1/Brn3a OFF RGC subtype (Chen et al., 2021). Cluster 40 corresponds to M1 cells which also express Gad2 according to this dataset. These Tbr2-expressing Meis2-expressing M1 cells are likely the recently identified GABAergic subset of ipRGCs (Sonoda et al., 2020).

In conclusion, these findings demonstrate several important roles of the transcription factor Tbr2 in the mature retina: its requirement for melanopsin expression in ipRGCs, and therefore for the maintenance of ipRGC identity; its ability

to activate melanopsin expression in endogenous Tbr2 cells; and its involvement in ipRGC survival after optic nerve injury.

2.6 Materials and Methods

2.6.1 Mice

The *Tbr2*^{CreER} (*Eomes*^{CreER}) mouse line used in this study was previously described (Pimeisl et al., 2013) (Fig. 2.1). To induce expression of Tbr2^{CreER}, tamoxifen (Sigma t5648-1G), diluted to 25 mg/mL in corn oil (Sigma c8267), was administered intraperitoneally at a dose of 100 mg/kg of body weight for 3 consecutive days to adult mice. PCR genotyping was performed using the forward primer 5′-GAGGGAGGAAGGGGACATTA-3′ and the reverse primers 5′ CAGGTTCTTGCGAACCTCAT-3′ (to detect Cre) and 5′-AGACTGCCCGGAAACTTCTT-3′ (wildtype allele).

The Tbr2 floxed mouse line (Zhu et al., 2010) was acquired from The Jackson Laboratory (stock no. 017293). PCR genotyping was performed using primers 5′-AGATGGAAATTTGGGAATGAA-3′ and 5′-GGCTACTACGGCCTGAAAC-3′.

The Isl1^{Cre} mouse line (Srinivas et al., 2001) was acquired from Dr. Eric Ullien (UCSF, Department of Ophthalmology). PCR genotyping was performed using primers 5′-ACCAGAGACGGAAATCCATCG-3′ and 5′-TGCCACGACCAAGTGACA GCAATG-3′.

The Rosa26-loxp-stop-loxp-tdTomato (Madisen et al., 2010) mouse line was acquired from The Jackson Laboratory (stock no. 007905). PCR genotyping was performed using primers 5′AAGGGAGCTGCAGTGGAGTA-3′ and 5′CCGAAAATCTGTGGGAAGTC-3′ to detect the wildtype allele and primers 5′-

CTGTTCCTGTACGGCATGG-3′ and 5′-GGCATTAAAGCAGCGTATCC-3′ to detect the Tomato allele.

C57Bl/6 “wildtype” mice were acquired from The Jackson Laboratory. Genotyping was performed using genomic DNA extracted from tail clippings using standard techniques.

Both female and male mice were used in this study and no significant differences were observed between them. For each experiment, 3 or more adult mice (P40-P100) were used (number of mice used for each experiment is indicated in the figure legends).

All experimental procedures were performed in accordance with protocols approved by the Institutional Animal Care and Use Committee at the University of California, Santa Cruz.

2.6.2 Immunohistochemistry and Tissue Processing

Eyes and brains were harvested from mice after intracardial perfusion with phosphate buffered saline (PBS; pH 7.4) followed by perfusion with 4% paraformaldehyde (PFA). For retina wholemount staining, retinas were dissected out of the eye; for retina sections, a hole was made in the cornea prior to fixation. Retinas and eyes were fixed in 4% PFA for 1 h while brains were fixed overnight. Retinas were then transferred to PBS while eyes and brains were transferred to 30% sucrose in PBS. For retina sections, eyes were frozen in Tissue Plus™ O.C.T. compound (Fisher HealthCare) and 20 μm thick sections were obtained via cryostat (Leica cm 3050s) and collected onto SuperFrost Plus slides (Fisher Scientific). For brain tissue, 100 μm thick

sections were obtained via a freezing sliding microtome (ThermoFisher microm hm430). For wholemount retinas, retinas were incubated in blocking solution (5% donkey serum, 0.25% TritonX-100 in PBS) for 3 h at room temperature (RT), incubated in primary antibody for 2–3 days at 4°C, washed 3 times (2 h each wash) with 0.1% PBST (PBS with TritonX-100) at RT, incubated in secondary antibody overnight at 4°C, washed 3 times (2 h each wash) with PBS at RT. Immunostained retinas were mounted retinal ganglion cell layer (GCL) side up onto SuperFrost Plus slides where relieving cuts were made. Fluoromount-g tissue mounting medium (SouthernBiotech) was applied prior to coverslipping. For retina sections, slides were incubated in blocking solution for 1 h, incubated in primary antibody overnight at 4°C, washed 3 times (15 min each wash) in PBS at RT, incubated in secondary antibody for 1 h at RT, incubated in DAPI for 10 min, washed 3 times (15 min each wash) in PBS at RT, and lastly covered with fluoromount-g (SouthernBiotech) and coverslipped.

Primary antibodies were diluted in blocking solution at the following concentrations: Chick anti-GFP (1:1,000; Aves Labs GFP-1020), chick anti-Tbr2 (1:500 flatmount, 1:1,000 sections; Millipore AB15894), rabbit anti-Tbr2 (1:500; Abcam AB183991), rabbit anti-melanopsin (1:1,000; Advanced Targeting Systems AB-N39), goat anti-tdTomato (1:500 flatmount, 1:750 sections; Acris/Sicgen AB8181-200), guinea pig anti-RBPMS (1:250; PhosphoSolutions 1832-RBPMS), mouse anti-meis2 (1:100; DSHB 1A11), rabbit anti-GABA (1:1,000; Sigma A2052).

All secondary antibodies used were diluted 1:1,000 in blocking solution; they are as follows: AlexaFluor647 donkey anti-guinea pig (Jackson ImmunoResearch

AB_2340476 #706-605-148), AlexaFluor594 donkey anti-rabbit (Life Technologies A21207), AlexaFluor555 donkey anti-rabbit (Invitrogen A31572), AlexaFluor555 donkey anti-goat (Invitrogen A21432), AlexaFluor488 donkey anti-mouse (Life Technologies A21202), AlexaFluor488 donkey anti-chick (Jackson ImmunoResearch AB_2340375 #703-545-155), AlexaFluor568 donkey anti-Rabbit (Invitrogen A10042).

2.6.3 Intravitreal Virus Injection

Mice were anesthetized with isoflurane. This procedure was performed under a dissecting microscope. A hole was created at the corneal-scleral junction with a 26 gauge needle. The vitreous humor was gently massaged out with a cotton swab in order to minimize back-pressure upon injection of virus. A pulled glass pipette preloaded with virus was inserted into the hole and a Picospritzer III (Parker) was used to administer ~1 µl of virus. One eye in each animal was infected with Tbr2-GFP-AAV2 (Vector Biolabs) while the other was infected with GFP-AAV2 (Vector Biolabs). Retinas were harvested 2 weeks or > 4 weeks after virus injection.

2.6.4 Optic Nerve Crush

Mice were anesthetized using isoflurane. A ketamine/xylazine cocktail was administered intraperitoneally at a concentration of 100 mg/kg ketamine and 10 mg/kg xylazine. This procedure was performed under a dissecting microscope. Ointment containing atropine sulfate (Bausch and Lomb, NDC 24208-825-55) was applied to both eyes to prevent drying and minimize pain. An incision was made in the sclera using spring scissors (Vannas 3 mm, FST). Subsequently, layers of the eye were gently

peeled back using fine forceps (Dumont #55, FST) until the optic nerve was exposed. The optic nerve was crushed ~2 mm from the posterior pole for 5 s using fine forceps. After the procedure, buprenorphine (0.1 mg/kg of body weight) was administered intraperitoneally and Terramycin ophthalmic ointment (Zoetis) was applied to the experimental eye. Both retinas were harvested 2 weeks after the procedure.

2.6.5 Data Acquisition

Fluorescent images were obtained with an Olympus BX51 microscope equipped with a Qimaging Retiga EXi Fast 1394 camera or a Zeiss LSM880 confocal microscope. All images presented here were taken with the Olympus microscope.

2.6.6 Data Analysis and Statistics

Lamination depth of Tomato$^+$ AC and RGC dendrites was determined using the IPLaminator plugin (Li et al., 2016) in FIJI. The 20x objective of the Olympus microscope was used to obtain images of retina sections. One or more regions (4000 μm^2 or greater) from four or more retina sections were analyzed per mouse. Both the "percentile values" (percentile distance across ROI based on measurement of ChAT bands in wildtype mice) and "n Equal boundaries" (ROI divided into 20 equal layers) methods were used to calculate inner plexiform layer (IPL) boundaries.

For cell density analyses, cells were manually counted in FIJI using the multi-point tool. For **Figures 2.2, 2.3C, 2.4** four fields of view (446.15 μm × 333.33 μm) were imaged with the 20x objective of the Olympus microscope. One image was taken per retina quadrant at approximately the same distance from the center of the retina (between ~1.5 and 3.5 mm from center). For **Figure 2.3D**, the entire retina was

analyzed as there are very few melanopsin cells in the *Isl1*^{Cre}*;Tbr2*$^{flox/flox}$ mice. For **Figure 2.3E**, seven or more fields of view (446.15 μm × 333.33 μm) were imaged. For **Figures 2.5B, 2.5C,** four fields of view (425.1 × 425.1 μm) were imaged with the 20x objective of the Zeiss confocal microscope.

Statistical analyses and graph generation were performed using GraphPad's Prism 9 software. Statistical tests used and number of animals used are indicated in the figure legends. In experiments where multiple cell populations were compared in more than one genotype (*Tbr2*$^{CreER/+}$*;tdT* vs. *Tbr2*$^{CreER/flox}$*;tdT*), two-way ANOVA was performed with Sidak's multiple comparisons *post-hoc* test. In experiments where multiple cell populations were compared in a single genotype, one-way ANOVA was performed. Student's *t*-test was performed for comparisons between two groups.

2.5 Supplementary Figures

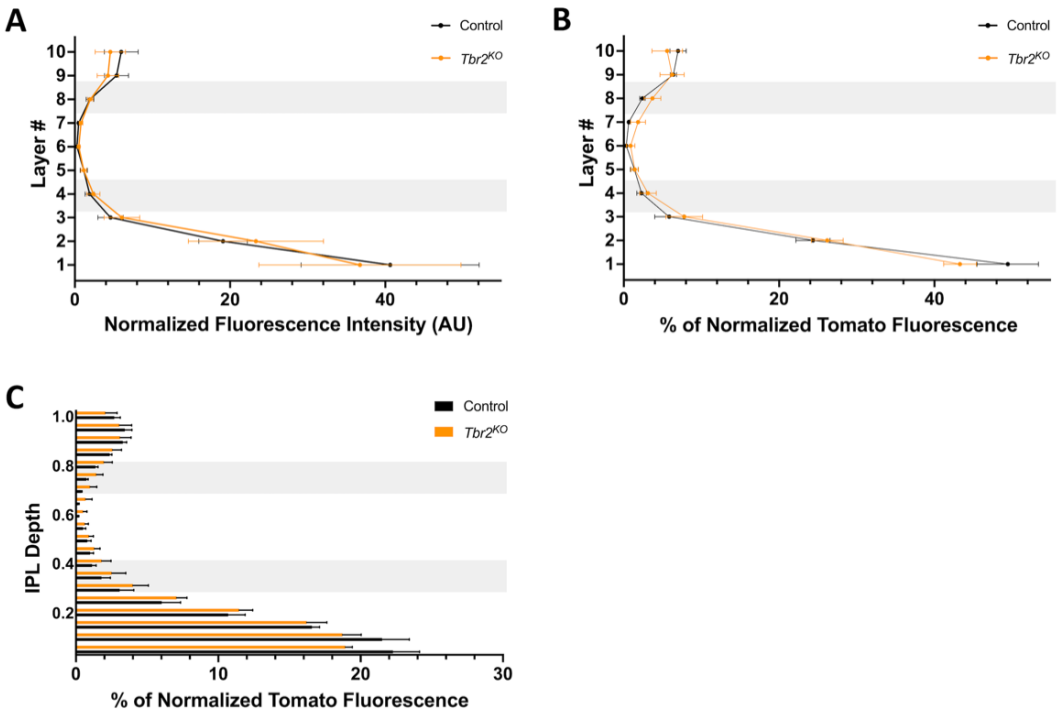

Figure S2.1 Tbr2 is not required for Tomato$^+$ AC and RGC dendritic lamination

(A) Normalized fluorescence intensities (AU) plotted for each layer in control (*Tbr2*$^{CreER/+}$*;tdT*, n=3 mice) and *Tbr2*^{KO} (*Tbr2*$^{CreER/flox}$*;tdT*, n=3 mice) retina sections using "percentile values" in IPLaminator to determine layer boundaries. Grey bars indicate approximate location of ChAT bands. Mean±SEM displayed. There are no significant differences between control and *Tbr2*^{KO} mice in fluorescence intensity/layer (Student's t-tests for each layer, P>0.05 for all). **(B)** Normalized fluorescence intensity distribution across the 10 layers shows no significant differences between control and *Tbr2*^{KO} mice (Student's t-tests for each layer, P>0.05 for all). Grey bars indicate approximate location of ChAT bands. Mean±SEM displayed. **(C)** Normalized fluorescence intensity distribution plot using "n Equal boundaries" to divide the IPL into 20 equal sections shows no significant differences between control and *Tbr2*^{KO} mice (Student's t-tests for each section, P>0.05 for all). IPL depth is plotted on the Y-axis with 0 being its border with the GCL and 1 being its border with the INL. Grey bars indicate approximate location of ChAT bands. Mean±SEM displayed. Tomato$^+$ dendrites laminate within the same layers of the IPL in control and *Tbr2*^{KO} mice (innermost ON and outermost OFF sublaminae).

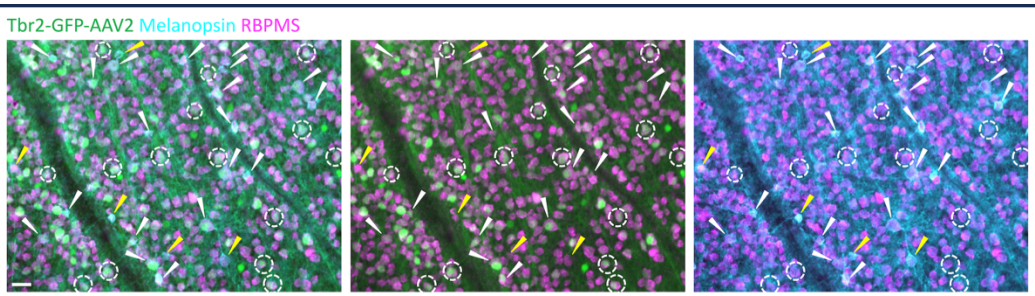

Figure S2.3 Many RGCs are infected with Tbr2-GFP-AAV2 but do not express melanopsin

Flatmounted wildtype retina infected with Tbr2-GFP-AAV2 (green) immunostained to reveal expression of RBPMS (magenta), Melanopsin (cyan), and GFP. First panel is a merge of all markers, the middle panel is showing Tbr2-GFP-AAV2 and RBPMS, and the right panel is showing melanopsin and RBPMS. White arrowheads point to melanopsin^{+} cells expressing Tbr2-GFP while yellow arrowheads point to melanopsin^{+} cells that are not infected with the virus. Dashed circles indicate RGCs that are infected with the virus but do not express melanopsin. Scale bar=25 µm.

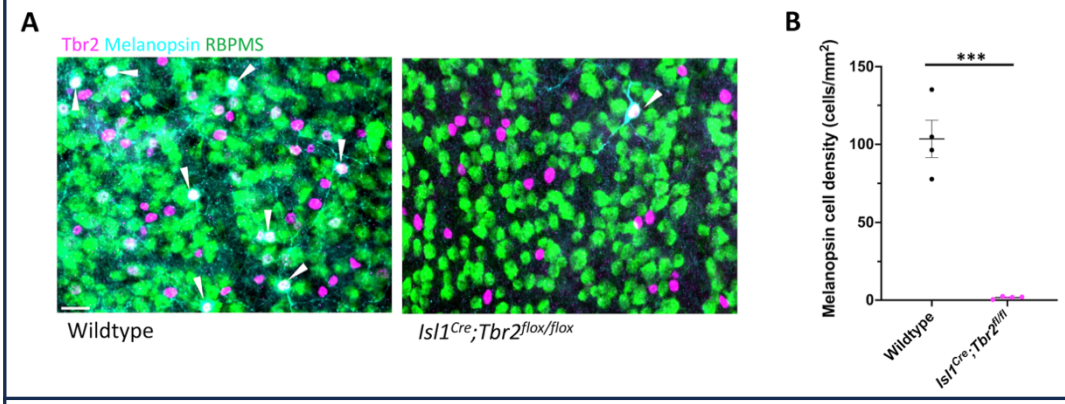

Figure S2. 2 *Isl1^{Cre};Tbr2$^{flox/flox}$* mice lack ipRGCs

A) Flatmounted retinas of a wildtype (left) and *Isl1^{Cre}; Tbr2$^{flox/flox}$* (right) mouse immunostained to reveal expression of Tbr2 (magenta), Melanopsin (cyan), and RBPMS (green). White arrowheads point to melanopsin^{+} cells. *Isl1^{Cre}; Tbr2$^{flox/flox}$* mice have significantly fewer melanopsin^{+} cells. Scale bar=25 µm. **(B)** Quantification of melanopsin-expressing cell density in wildtype and *Isl1^{Cre};Tbr2$^{flox/flox}$* mice. *Isl1^{Cre}; Tbr2$^{flox/flox}$* mice have significantly reduced melanopsin-expressing cells (2±0.44 cells/mm^2 in *Isl1^{Cre};Tbr2$^{flox/flox}$* mice vs. 104±12 cells/mm^2 in wildtype mice, n=4 mice, Student's t-test, ***=P<0.001). Mean±SEM displayed.

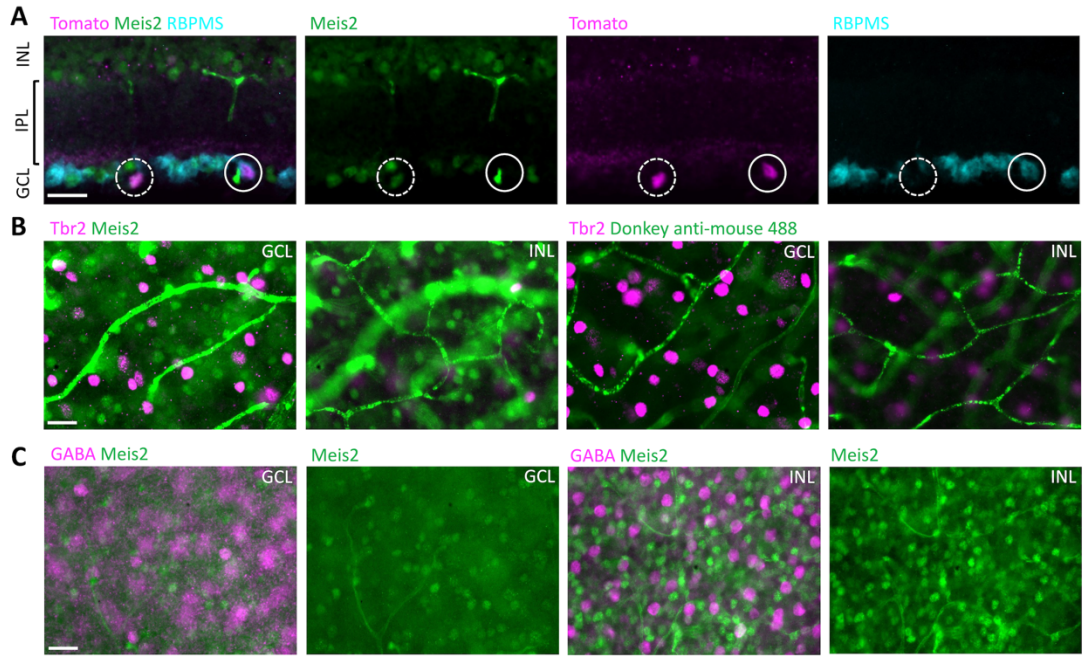

Figure S2.4 Meis2 labels many cells in the INL and GCL

(A) Retina section of a *Tbr2*$^{CreER/+}$*;tdT* mouse expressing tdTomato (magenta) and immunostained with Meis2 (green) and RBPMS (cyan) antibodies; dashed white circles indicate a Meis2^{+}Tomato^{+} amacrine cell and solid white circles indicate a Tomato^{+} RGC that does not express Meis2. Many cells in the INL express Meis2. **(B)** Flatmounted retina regions of an adult wildtype mouse stained with Tbr2 (magenta) and Meis2 (green) antibodies (left two panels) showing the GCL (left) and INL (right); right two panels are a control showing the GCL (left) and INL (right) stained with the same antibodies as the left two images but without the mouse anti-Meis2 primary antibody (green=Donkey anti-mouse 488 secondary antibody). **(C)** Flatmounted retina regions (left two panels=GCL, right two panels=INL) of an adult wildtype mouse stained with GABA (magenta) and Meis2 (green) antibodies. Many Meis2-expressing cells in both the GCL and INL are not labeled by the GABA antibody. Scale bars= 25 µm.

2.7 Bibliography

Agorastos, A., Skevas, C., Matthaei, M., Otte, C., Klemm, M., Richard, G., & Huber, C. G. (2013). Depression, Anxiety, and Disturbed Sleep in Glaucoma. *The Journal of Neuropsychiatry and Clinical Neurosciences*, *25*(3), 205–213.

Altimus, C. M., Güler, A. D., Villa, K. L., McNeill, D. S., LeGates, T. A., & Hattar, S. (2008). Rods-cones and melanopsin detect light and dark to modulate sleep independent of image formation. *Proceedings of the National Academy of Sciences*, *105*(50), 19998–20003. doi: 10.1073/pnas.0808312105

Baden, T., Berens, P., Franke, K., Román Rosón, M., Bethge, M., & Euler, T. (2016). The functional diversity of retinal ganglion cells in the mouse. *Nature*, *529*(7586), 345–350. doi: 10.1038/nature16468

Bae, J. A., Mu, S., Kim, J. S., Turner, N. L., Tartavull, I., Kemnitz, N., Jordan, C. S., Norton, A. D., Silversmith, W. M., Prentki, R., Sorek, M., David, C., Jones, D. L., Bland, D., Sterling, A. L. R., Park, J., Briggman, K. L., & Seung, H. S. (2018). Digital Museum of Retinal Ganglion Cells with Dense Anatomy and Physiology. *Cell*, *173*(5), 1293-1306.e19. doi: 10.1016/j.cell.2018.04.040

Berson, D. M., Dunn, F. A., & Takao, M. (2002). Phototransduction by retinal ganglion cells that set the circadian clock. *Science*, *295*(5557), 1070–1073. doi: 10.1126/science.1067262

Bray, E. R., Yungher, B. J., Levay, K., Ribeiro, M., Dvoryanchikov, G., Ayupe, A. C., Thakor, K., Marks, V., Randolph, M., Danzi, M. C., Schmidt, T. M., Chaudhari, N., Lemmon, V. P., Hattar, S., & Park, K. K. (2019). Thrombospondin-1 Mediates Axon Regeneration in Retinal Ganglion Cells. *Neuron*, *103*, 1–16. doi: 10.1016/j.neuron.2019.05.044

Chen, C., Kiyama, T., Weber, N., Whitaker, C. M., Pan, P., Badea, T. C., Massey, S. C., & Mao, C. (2021). Characterization of Tbr2-expressing retinal ganglion cells. *The Journal of Comparative Neurology*, 1–20. doi: 10.1002/cne.25208

Deneris, E. S., & Hobert, O. (2014). Maintenance of postmitotic neuronal cell identity. *Nature Neuroscience*, *17*(7), 899–907. doi: 10.1038/nn.3731

Duan, X., Qiao, M., Bei, F., Kim, I. J., He, Z., & Sanes, J. R. (2015). Subtype-Specific regeneration of retinal ganglion cells following axotomy: Effects of osteopontin and mtor signaling. *Neuron*, *85*(6), 1244–1256. doi: 10.1016/j.neuron.2015.02.017

Ecker, J. L., Dumitrescu, O. N., Wong, K. Y., Alam, N. M., Chen, S. K., LeGates, T., Renna, J. M., Prusky, G. T., Berson, D. M., & Hattar, S. (2010). Melanopsin-expressing retinal ganglion-cell photoreceptors: Cellular diversity and role in pattern vision. *Neuron*, *67*(1), 49–60. doi: 10.1016/j.neuron.2010.05.023

Elsen, G. E., Bedogni, F., Hodge, R. D., Bammler, T. K., MacDonald, J. W., Lindtner, S., Rubenstein, J. L. R., & Hevner, R. F. (2018). The epigenetic factor landscape of developing neocortex is regulated by transcription factors Pax6→ Tbr2→ Tbr1. *Frontiers in Neuroscience*, *12*(571). doi: 10.3389/fnins.2018.00571

Feigl, B., Mattes, D., Thomas, R., & Zele, A. J. (2011). Intrinsically photosensitive (melanopsin) retinal ganglion cell function in glaucoma. *Investigative Ophthalmology and Visual Science*, *52*(7), 4362–4367. doi: 10.1167/iovs.10-7069

Gracitelli, C. P. B., Duque-Chica, G. L., Moura, A. L. de A., Roizenblatt, M., Nagy, B. V., de Melo, G. R., Borba, P. D., Teixeira, S. H., Tufik, S., Ventura, D. F., & Paranhos, A. (2016). Relationship between Daytime Sleepiness and Intrinsically Photosensitive Retinal Ganglion Cells in Glaucomatous Disease. *Journal of Ophthalmology*, *2016*, 1–9. doi: 10.1155/2016/5317371

Guillemot, F. (2007). Spatial and temporal specification of neural fates by transcription factor codes. *Development*, *134*(21), 3771–3780. doi: 10.1242/dev.006379

Güler, A. D., Ecker, J. L., Lall, G. S., Haq, S., Altimus, C. M., Liao, H. W., Barnard, A. R., Cahill, H., Badea, T. C., Zhao, H., Hankins, M. W., Berson, D. M., Lucas, R. J., Yau, K. W., & Hattar, S. (2008). Melanopsin cells are the principal conduits for rod-cone input to non-image-forming vision. *Nature*, *453*(7191), 102–105. doi: 10.1038/nature06829

Hatori, M., Le, H., Vollmers, C., Keding, S. R., Tanaka, N., Schmedt, C., Jegla, T., & Panda, S. (2008). Inducible ablation of melanopsin-expressing retinal ganglion cells reveals their central role in non-image forming visual responses. *PLoS ONE*, *3*(6), 1–10. doi: 10.1371/journal.pone.0002451

Hattar, S., Liao, H. W., Takao, M., Berson, D. M., Yau, K. W., Heller, H. C., & O'Hara, B. F. (2002). Melanopsin-Containing Retinal Ganglion Cells: Architecture, Projections, and Intrinsic Photosensitivity. *Science*, *295*(5557), 1065–1070. doi: 10.1126/science.1069609

Hevner, R. F. (2019). Intermediate progenitors and Tbr2 in cortical development. *Journal of Anatomy*, *235*(3), 616–625. doi: 10.1111/joa.12939

Legates, T. A., Altimus, C. M., Wang, H., Lee, H. K., Yang, S., Zhao, H., Kirkwood, A., Weber, E. T., & Hattar, S. (2012). Aberrant light directly impairs mood and learning through melanopsin-expressing neurons. *Nature*, *491*(7425), 594–598. doi: 10.1038/nature11673

Li, S., Woodfin, M., Long, S. S., & Fuerst, P. G. (2016). IPLaminator: An ImageJ plugin for automated binning and quantification of retinal lamination. *BMC Bioinformatics*, *17*(1), 1–9. doi: 10.1186/s12859-016-0876-1

Li, S.-Y., Yau, S.-Y., Chen, B.-Y., Tay, D. K., Lee, V. W. H., Pu, M.-L., Chan, H. H. L., & So, K.-F. (2008). Enhanced Survival of Melanopsin-expressing Retinal Ganglion Cells After Injury is Associated with the PI3 K / Akt Pathway. *Cell Mol Neurobiol*, *28*, 1095–1107. doi: 10.1007/s10571-008-9286-x

Lin, B., & Masland, R. H. (2006). Populations of Wide-Field Amacrine Cells in the Mouse Retina. *The Journal of Comparative Neurology*, *499*, 797–809. doi: 10.1002/cne.21126

Lin, X. M., Liao, X. P., Chen, H., Chang, X. C., Chen, X. S., & Chern, Y. (2019). Degeneration of ipRGCs in Mouse Models of Huntington's Disease Disrupts Non-Image-Forming Behaviors Before Motor Impairment. *The Journal of Neuroscience*, *39*(8), 1505–1524. doi: 10.1523/JNEUROSCI.0571-18.2018

Lyu, P., Hoang, T., Santiago, C. P., Thomas, E. D., Timms, A. E., Appel, H., Gimmen, M., Le, N., Jiang, L., Kim, D. W., Chen, S., Espinoza, D., Telger, A. E., Weir, K., Clark, B. S., Cherry, T. J., Qian, J., & Blackshaw, S. (2021). Gene Regulatory Networks Controlling Temporal Patterning, Neurogenesis, and Cell Fate Specification in the Mammalian Retina. *SSRN Electronic Journal*, *37*(7), 109994. doi: 10.2139/ssrn.3921283

Macneil, M. A., & Masland, R. H. (1998). Extreme Diversity among Amacrine Cells: Implications for Function. *Neuron*, *20*, 971–982.

Madisen, L., Zwingman, T. A., Sunkin, S. M., Oh, S. W., Zariwala, H. A., Gu, H., Ng, L. L., Palmiter, R. D., Hawrylycz, M. J., Jones, A. R., Lein, E. S., & Zeng, H. (2010). A robust and high-throughput Cre Reporting and characterization system for the whole mouse brain. *Nat Neurosci*, *13*(1), 133–140. doi: 10.1038/nn.2467

Mao, C.-A., Li, H., Zhang, Z., Kiyama, T., Panda, S., Hattar, S., Ribelayga, C. P., Mills, S. L., & Wang, S. W. (2014). T-box Transcription Regulator Tbr2 Is Essential for the Formation and Maintenance of Opn4/Melanopsin-Expressing Intrinsically Photosensitive Retinal Ganglion Cells. *Journal of Neuroscience*, *34*(39), 13083–13095. doi: 10.1523/JNEUROSCI.1027-14.2014

Mao, C.-A., Kiyama, T., Pan, P., Furuta, Y., Hadjantonakis, A.-K., & Klein, W. H. (2008). Eomesodermin, a target gene of Pou4f2, is required for retinal ganglion cell and optic nerve development in the mouse. *Development*, *135*(2), 271–280. doi: 10.1080/1536710X.2013.870512.Behavioral

Martersteck, E. M., Hirokawa, K. E., Evarts, M., Bernard, A., Duan, X., Li, Y., Ng, L., Oh, S. W., Ouellette, B., Royall, J. J., Stoecklin, M., Wang, Q., Zeng, H., Sanes, J. R., & Harris, J. A. (2017). Diverse Central Projection Patterns of Retinal Ganglion Cells. *Cell Reports*, *18*(8), 2058–2072. doi: 10.1016/j.celrep.2017.01.075

Nadal-Nicolás, F. M., Sobrado-Calvo, P., Jimenez-Lopez, M., Vidal-Sanz, M., & Agudo-Barriuso, M. (2015). Long-Term Effect of Optic Nerve Axotomy on the Retinal Ganglion Cell Layer. *Investigative Ophthalmology & Visual Science*, *56*, 6095–6112. doi: 10.1167/iovs.15-17195

Panda, S., Sato, T. K., Castrucci, A. M., Rollag, M. D., DeGrip, W. J., Hogenesch, J. B., Provencio, I., & Kay, S. A. (2002). Melanopsin (Opn4) requirement for normal light-induced circadian phase shifting. *Science*, *298*(5601), 2213–2216. doi: 10.1126/science.1076848

Peng, Y. R., Tran, N. M., Krishnaswamy, A., Kostadinov, D., Martersteck, E. M., & Sanes, J. R. (2017). Satb1 Regulates Contactin 5 to Pattern Dendrites of a Mammalian Retinal Ganglion Cell. *Neuron*, *95*(4), 869-883.e6. doi: 10.1016/j.neuron.2017.07.019

Pérez De Sevilla Müller, L., Sargoy, A., Rodriguez, A. R., & Brecha, N. C. (2014). Melanopsin Ganglion Cells Are the Most Resistant Retinal Ganglion Cell Type to Axonal Injury in the Rat Retina. *PLoS ONE*, *9*(3), 1–7. doi: 10.1371/journal.pone.0093274

Pérez De Sevilla Müller, L., Shelley, J., & Weiler, R. (2007). Displaced Amacrine Cells of the Mouse. *The Journal of Comparative Neurology*, *505*, 177–189. doi: 10.1002/cne

Pérez-Rico, C., de la Villa, P., Arribas-Gómez, I., & Blanco, R. (2010). Evaluation of functional integrity of the retinohypothalamic tract in advanced glaucoma using multifocal electroretinography and light-induced melatonin suppression. *Experimental Eye Research*, *91*, 578–583. doi: 10.1016/j.exer.2010.07.012

Pimeisl, I. M., Tanriver, Y., Daza, R. A., Vauti, F., Hevner, R. F., Arnold, H. H., & Arnold, S. J. (2013). Generation and characterization of a tamoxifen-inducible EomesCreER mouse line. *Genesis*, *51*(10), 725–733. doi: 10.1002/dvg.22417

Provencio, I., Rodriguez, I. R., Jiang, G., Hayes, W. P., Moreira, E. F., & Rollag, M. D. (2000). A novel human opsin in the inner retina. *Journal of Neuroscience*, *20*(2), 600–605. doi: 10.1523/jneurosci.20-02-00600.2000

Provencio, I., Cooper, H. M., Foster, R. G., Comp, J., Lucas, R. J., Res, B. B., Panda, S., Sato, T. K., Castrucci, A. M., Rollag, M. D., Degrip, W. J., Hogenesch, J. B., Provencio, I., & Kay, S. A. (2002a). Melanopsin (Opn4) Requirement for Normal Light-Induced Circadian Phase Shifting. *Science*, *298*, 2213–2217.

Provencio, I., Rollag, M. D., & Castrucci, A. M. (2002b). Photoreceptive net in the mammalian retina. *Nature*, *415*, 493–494. doi: 10.1038/415493a

Quattrochi, L. E., Stabio, M. E., Kim, I., Ilardi, M. C., Michelle Fogerson, P., Leyrer, M. L., & Berson, D. M. (2018). The M6 cell: A small-field bistratified photosensitive retinal ganglion cell. *Journal of Comparative Neurology*, *527*, 297–311. doi: 10.1002/cne.24556

Rheaume, B. A., Jereen, A., Bolisetty, M., Sajid, M. S., Yang, Y., Renna, K., Sun, L., Robson, P., & Trakhtenberg, E. F. (2018). Single cell transcriptome profiling of retinal ganglion cells identifies cellular subtypes. *Nature Communications*, *9*(2759), 1–17. doi: 10.1038/s41467-018-05134-3

Robinson, G. A., & Madison, R. D. (2004). Axotomized mouse retinal ganglion cells containing melanopsin show enhanced survival , but not enhanced axon regrowth into a peripheral nerve graft. *Vision Research*, *44*, 2667–2674. doi: 10.1016/j.visres.2004.06.010

Rodriguez, A. R., Perez De Sevilla Muller, L., & Brecha, N. C. (2014). The RNA Binding Protein RBPMS is a Selective Marker of Ganglion Cells in the Mammalian Retina. *The Journal of Comparative Neurology*, *522*, 1411–1443. doi: 10.1002/cne.23521

Rosenthal, N. E., Sack, D. A., Gillin, C., Lewy, A. J., Goodwin, F. K., Davenport, Y., Mueller, P. S., Newsome, D. A., & Wehr, T. A. (1984). Seasonal Affective Disorder. *Archives of General Psychiatry*, *41*, 72–80. doi: 10.1080/15398285.2013.780576

Ruby, N. F., Brennan, T. J., Xie, X., Cao, V., Franken, P., Heller, H. C., & O'Hara, B. F. (2002). Role of melanopsin in circadian responses to light. *Science*, *298*(5601), 2211–2213. doi: 10.1126/science.1076701

Sanes, J. R., & Masland, R. H. (2015). The Types of Retinal Ganglion Cells: Current Status and Implications for Neuronal Classification. *Annual Review of Neuroscience*, *38*(1), 221–246. doi: 10.1146/annurev-neuro-071714-034120

Sajgo, S., Ghinia, M. G., Brooks, M., Kretschmer, F., Chuang, K., Hiriyanna, S., Wu, Z., Popescu, O., & Badea, T. C. (2017). Molecular codes for cell type specification in Brn3 retinal ganglion cells. *Proceedings of the National Academy of Sciences*, *114*(20), E3974–E3983. doi: 10.1073/pnas.1618551114

Schmidt, T. M., & Kofuji, P. (2009). Functional and morphological differences among intrinsically photosensitive retinal ganglion cells. *Journal of Neuroscience*, *29*(2), 476–482. doi: 10.1523/JNEUROSCI.4117-08.2009

Schmidt, T. M., Alam, N. M., Chen, S., Kofuji, P., Li, W., Prusky, G. T., & Hattar, S. (2014). A role for melanopsin in alpha retinal ganglion cells and contrast detection. *Neuron*, *82*(4), 781–788. doi: 10.1016/j.neuron.2014.03.022.A

Seki, T., Itoh, H., Nakamachi, T., & Shioda, S. (2008). Suppression of ganglion cell death by PACAP following optic nerve transection in the rat. *Journal of Molecular Neuroscience*, *36*(1–3), 57–60. doi:10.1007/s12031-008-9091-5

Sessa, A., Ciabatti, E., Drechsel, D., Massimino, L., Colasante, G., Giannelli, S., Satoh, T., Akira, S., Guillemot, F., & Broccoli, V. (2017). The Tbr2 Molecular Network Controls Cortical Neuronal Differentiation Through Complementary Genetic and Epigenetic Pathways. *Cerebral Cortex*, *27*(6), 3378–3396. doi: 10.1093/cercor/bhw270

Sonoda, T., Lee, S., Birnbaumer, L., & Schmidt, T. M. (2018). Melanopsin phototransduction is repurposed by ipRGC subtypes to shape the function of distinct visual circuits - preprint. *Neuron*, *99*, 1–14. doi: 10.1016/j.neuron.2018.06.032

Sonoda, T., Li, J. Y., Hayes, N. W., Chan, J. C., Okabe, Y., Belin, S., Nawabi, H., & Schmidt, T. M. (2020). A noncanonical inhibitory circuit dampens behavioral sensitivity to light. *Science*, *368*, 527–531.

Srinivas, S., Watanabe, T., Lin, C. S., William, C. M., Tanabe, Y., Jessell, T. M., & Costantini, F. (2001). Cre reporter strains produced by targeted insertion of EYFP and ECFP into the ROSA26 locus. *BMC Developmental Biology*, *1*, 1–8. doi: 10.1186/1471-213X-1-4

Sweeney, N. T., Tierney, H., & Feldheim, D. A. (2014). Tbr2 Is Required to Generate a Neural Circuit Mediating the Pupillary Light Reflex. *Journal of Neuroscience*, *34*(16), 5447–5453. doi: 10.1523/JNEUROSCI.0035-14.2014

Tran, N. M., Shekhar, K., Whitney, I. E., Jacobi, A., Benhar, I., Hong, G., Yan, W., Adiconis, X., Arnold, M. E., Lee, J. M., Levin, J. Z., Lin, D., Wang, C., Lieber, C. M., Regev, A., He, Z., & Sanes, J. R. (2019). Single-cell profiles of retinal

neurons differing in resilience to injury reveal neuroprotective genes. *Neuron*, *104*, 1–17. doi: 10.1016/j.neuron.2019.11.006

Viney, T. J., Balint, K., Hillier, D., Siegert, S., Boldogkoi, Z., Enquist, L. W., Meister, M., Cepko, C. L., & Roska, B. (2007). Local Retinal Circuits of Melanopsin-Containing Ganglion Cells Identified by Transsynaptic Viral Tracing. *Current Biology*, *17*(11), 981–988. doi: 10.1016/j.cub.2007.04.058

Wang, H., Zhang, Y., Ding, J., & Wang, N. (2013). Changes in the Circadian Rhythm in Patients with Primary Glaucoma. *PLoS ONE*, *8*(4), 1–7. doi: 10.1371/journal.pone.0062841

Yan, W., Laboulaye, M. A., Tran, N. M., Whitney, I. E., Benhar, I., & Sanes, J. R. (2020). Mouse Retinal Cell Atlas: Molecular Identification of Over Sixty Amacrine Cell Types. *The Journal of Neuroscience*, *40*(27), 5177–5195. doi: 10.1523/jneurosci.0471-20.2020

Ye, D., Yang, Y., Lu, X., Xu, Y., Shi, Y., Chen, H., & Huang, J. (2019). Spatiotemporal Expression Changes of PACAP and Its Receptors in Retinal Ganglion Cells After Optic Nerve Crush. *Journal of Molecular Neuroscience*, *68*(3), 465–474. doi: 10.1007/s12031-018-1203-2

Zhu, Y., Ju, S., Chen, E., Dai, S., Li, C., Morel, P., Liu, L., Zhang, X., & Lu, B. (2010). T-bet and Eomesodermin Are Required for T Cell-Mediated Antitumor Immune Responses. *The Journal of Immunology*, *185*, 3174–3183. doi: 10.4049/jimmunol.1000749

Chapter 3: Isl2 is required in RPCs and RGCs for the survival of Isl2^{+} RGC subtypes but not for eye-specific axon-pathfinding

3.1 Abstract

Retinal ganglion cells (RGCs) exhibit remarkable diversity owing to their expression of various transcription factors. Many transcription factors are expressed in unique RGC populations, but their roles within these populations remain unknown. The transcription factor Isl2 is expressed in ~30-40% of contralateral-projecting RGCs and is one such factor. Previous work by others found increased ipsilateral innervation of the thalamus in *Isl2*$^{-/-}$ mice, implicating Isl2 in promoting a contralateral RGC axon trajectory. Because these mice suffer early neonatal lethality, the role of Isl2 in RGC specification could not be fully explored. To study this, I generated *Isl2* conditional knockout mice using two different retina-specific Cre lines. Contrary to the findings in *Isl2*$^{-/-}$ mice, *Isl2* conditional knockout does not lead to increased ipsilateral projections. Instead, I observed a significant reduction in the size of the dorsal lateral geniculate nucleus (dLGN) of the thalamus and a mild reduction in the size of the ipsilateral projection to the dLGN. I also found that *Isl2* conditional knockouts display a loss of RGCs and a specific loss of expression of proteins that are normally expressed in Isl2-RGC subtypes (Foxp2, Zic1, Tusc5) but not of those expressed in non-Isl2-RGC subtypes (melanopsin). Lastly, I found that there is increased expression of the apoptotic protein cleaved-caspase3 in the ganglion cell layer of *Isl2* conditional knockout retinas during development. These findings combined suggest that *Isl2* is required for the development and survival of Isl2-RGC subtypes.

3.2 Introduction

Retinal ganglion cells (RGCs) are the sole output neurons of the retina and are thus responsible for communicating visual information to the brain. There have been over 40 RGC subtypes identified in mice, each differing in its molecular, morphological, and functional properties (Sanes and Masland 2015; Baden et al., 2016; Bae et al., 2018; Rheaume et al., 2018; Tran et al., 2019; Goetz et al., 2022). How each subtype acquires its unique identity is not well understood and is an active area of research. Different transcription factors encode unique neuronal characteristics that contribute to an RGC's identity, each type being regulated by a combination of transcription factors (Lyu and Mu 2021).

In some cases, single transcription factors have been shown to be required for the generation of an RGC subtype, and in others, multiple subtypes. We and others previously demonstrated that the T-box transcription factor Tbr2 is required for the generation of a class of RGCs that are intrinsically photosensitive (ipRGCs; Mao et al., 2008; Sweeney et al., 2014; Mao et al., 2014). The ipRGC class comprises 6 subtypes (Aranda and Schmidt 2021), all of which depend on Tbr2 expression. Other T-box transcription factors, Tbr1 and Tbx5, are required for the formation of separate RGC subtypes (Kiyama et al., 2019; Al-Khindi et al., 2022). Tbr1 is necessary for the development of orientation-selective J-RGCs and a group of OFF-sustained RGCs (Kiyama et al., 2019) while Tbx5 is required for the formation of upward-preferring ON-DSGCs (Al-Khindi et al., 2022). Some transcription factors, like the special AT-rich sequence binding protein 1 (Satb1), are dispensable for the formation of RGC

subtypes but not for their appropriate development; when Satb1 is knocked out during retina development, the ON arbor of ooDSGCs does not form (Peng et al., 2017).

We have previously shown that the majority (>90%) of RGCs express one of the transcription factors Tbr2, Satb1/2, or Islet2 (Isl2) (Sweeney et al., 2017). They are expressed in a non-overlapping fashion in developing RGCs as well as in mature RGCs, leading to the hypothesis that each is responsible for regulating the fate of distinct RGC types. While Tbr2 and Satb1 have been shown to be required for the formation of ipRGCs and for the normal development of ooDSGCs, respectively (Mao et al., 2008; Sweeney et al., 2014; Mao et al., 2014; Peng et al., 2017), the role of Isl2 in RGC specification is unknown.

Isl2 (also known as insulin related protein 2) is a lim-homeodomain transcription factor that is required for visceral motor neuron differentiation (Thaler et al., 2004). It has recently been identified as a regulator of angiogenesis (Qi et al., 2020) and as a putative tumor suppressor (Ozturk et al., 2022). It is expressed in the neural retina during development and is expressed in several subtypes of postmitotic RGCs in adult mice (Pak et al., 2004; Triplett et al., 2014; Tran et al., 2019). We have previously characterized the properties of $Isl2^+$ RGCs using a BAC transgenic Isl2-GFP mouse line (Triplett et al., 2014). $Isl2^+$ RGCs project solely to image-forming regions of the brain, the dLGN and SC, and strictly contralaterally (Triplett et al., 2014; Pak et al., 2004). Their dendrites laminate primarily in S3 of the IPL in a monostratified fashion (Triplett et al., 2014). Isl2-GFP^+ RGCs include $SMI32^+$ ON-alpha RGCs and exclude DSGCs (Triplett et al., 2014; Sweeney et al., 2017). Work from others has implicated

Isl2 in suppressing an ipsilateral RGC axon trajectory (Pak et al., 2004). In Isl2 null mice (*Isl2*$^{-/-}$), there is increased ipsilateral innervation of the lateral geniculate nucleus (LGN) of the thalamus at P0. Additionally, these mice have increased expression of Zic2 in the ventral temporal crescent (VTC) of the retina. Zic2 is a transcription factor that specifies an ipsilateral axon trajectory (Herrera et al., 2003) and the VTC is the region in which ipsilateral-projecting RGCs reside (Dräger 1985). The role of Isl2 in RGC specification was not fully explored because *Isl2*$^{-/-}$ mice die shortly after birth at P0 (Thaler et al., 2004).

To study the role of Isl2 in RGC development, I generated Isl2 conditional knockout mice using two different Cre lines that act to remove Isl2 at different stages during retinal development: in RPCs and in early postmitotic RGCs. I found that Isl2 loss in RPCs (*Chx10*^{Cre}*;Isl2*$^{flox/flox}$) or RGCs (*Isl1*^{Cre}*;Isl2*$^{flox/flox}$) does not result in increased ipsilateral innervation of the dLGN at P0 or in adulthood, in contrast to what was observed in *Isl2*$^{-/-}$ mice at P0 (Pak et al., 2004). Isl2 conditional knockout (*Isl2*^{CKO}) results in a significant but modest reduction in total RGC density, as well as a significant loss of expression of Isl2^{+} RGC markers (Zic1, Foxp2, and Tusc5) but not of markers of non-Isl2^{+}-RGC subclasses (melanopsin). This coupled with the finding that there is increased expression of cleaved-caspase3 in the GCL of early postnatal *Isl2*^{CKO} mice suggests that Isl2 is required for the survival of subsets of Isl2^{+} RGC subclasses.

3.3 Results

3.3.1 Isl2 conditional knockout using retina-specific Cre lines leads to loss of Isl2 expression in the GCL of the retina

To study the role of Isl2 in RGC development, I first developed an $Isl2^{flox}$ mouse line that would allow for conditional knockout (CKO) of Isl2 in the presence of Cre recombinase. The $Isl2^{flox}$ mouse was designed such that the exons encoding the homeodomain and C-terminus of Isl2 (exons 4-6) are flanked by loxP sites (**Fig. 3.1A**). I used Islet1-Cre ($Isl1^{Cre}$) or Chx10-Cre ($Chx10^{Cre}$) mice to generate Isl2 CKO ($Isl2^{CKO}$) mice: $Isl1^{Cre};Isl2^{flox/flox}$ and $Chx10^{Cre};Isl2^{flox/flox}$. Within the retina, Isl1 is expressed in newly postmitotic RGCs prior to subtype specification, as well as in the majority of mature RGC subtypes (Rachel et al., 2002; Elshatory et al., 2007). According to single-cell RNA sequencing data, Isl1 is expressed in ~36 of the 45 identified RGC clusters, including all but 2 of the ~15 $Isl2^{+}$ RGC subtypes (Tran et al., 2019). Chx10 is expressed in retinal progenitor cells but not in RGCs (Liu et al., 1994; Burmeister et al., 1996; Rowan and Cepko 2004). $Chx10^{Cre}$ displays mosaic expression, thus it is not expressed in all RPCs (Rowan and Cepko 2004).

Due to the lack of antibodies that specifically detect Isl2 in the retina, I confirmed *Isl2* CKO via RT-PCR of RNA isolated from adult $Isl1^{Cre};Isl2^{flox/flox}$ and $Chx10^{Cre};Isl2^{flox/flox}$ retinas (**Fig. 3.1B**). Both $Isl2^{CKO}$ lines show significantly reduced retinal *Isl2* expression, with a 73% decrease in $Isl1^{Cre};Isl2^{flox/flox}$ retinas ($p<0.001$, two-tailed t-test) and a 93% decrease in $Chx10^{Cre};Isl2^{flox/flox}$ retinas ($p=0.001$, two-tailed t- test) relative to their littermate controls. To further characterize the loss of *Isl2* in

Isl2^{CKO} mice, I performed fluorescent in-situ hybridization (RNAscope) on retina sections using probes directed against exons 4-6 of *Isl2* mRNA (**Fig. 3.1C-D**). In wildtype mice, the majority of cells in the GCL express *Isl2* at P0 (**Fig. 3.1C**), this pattern becomes more refined at P5 (**Fig. 3.1D**), and expression is maintained in the adult (**Fig. 3.1C', 3.1D'**). In *Isl2*^{CKO} retinas, there is a significant loss of *Isl2*-expressing cells in the GCL at P0, P5, and in adulthood (**Fig. 3.1C',D'**) with a 76% loss of *Isl2*-expressing cells in the GCL of adult *Isl1*^{Cre}*;Isl2*$^{flox/flox}$ mice (6±1% vs. 25±3% in littermate controls) and a 61% loss in *Chx10*^{Cre}*;Isl2*$^{flox/flox}$ mice (10±1% vs. 25±1% in littermate controls). Neither Cre completely removes *Isl2* from RGCs, likely due to the nature of their expression. *Isl1* is not expressed in all *Isl2*-expressing RGCs—it is absent from 2 of ~15 Isl2-expressing transcriptomically distinct subsets (Tran et al., 2019) and *Chx10*^{Cre} displays mosaic expression (Rowan and Cepko 2004; Damiani et al., 2008). Taken together, these data show that conditional knockout of *Isl2* using *Isl1*^{Cre} (**Fig. 3.1C'**) or *Chx10*^{Cre} (**Fig. 3.1D'**) results in a significant but incomplete loss of *Isl2* mRNA in the GCL of the retina.

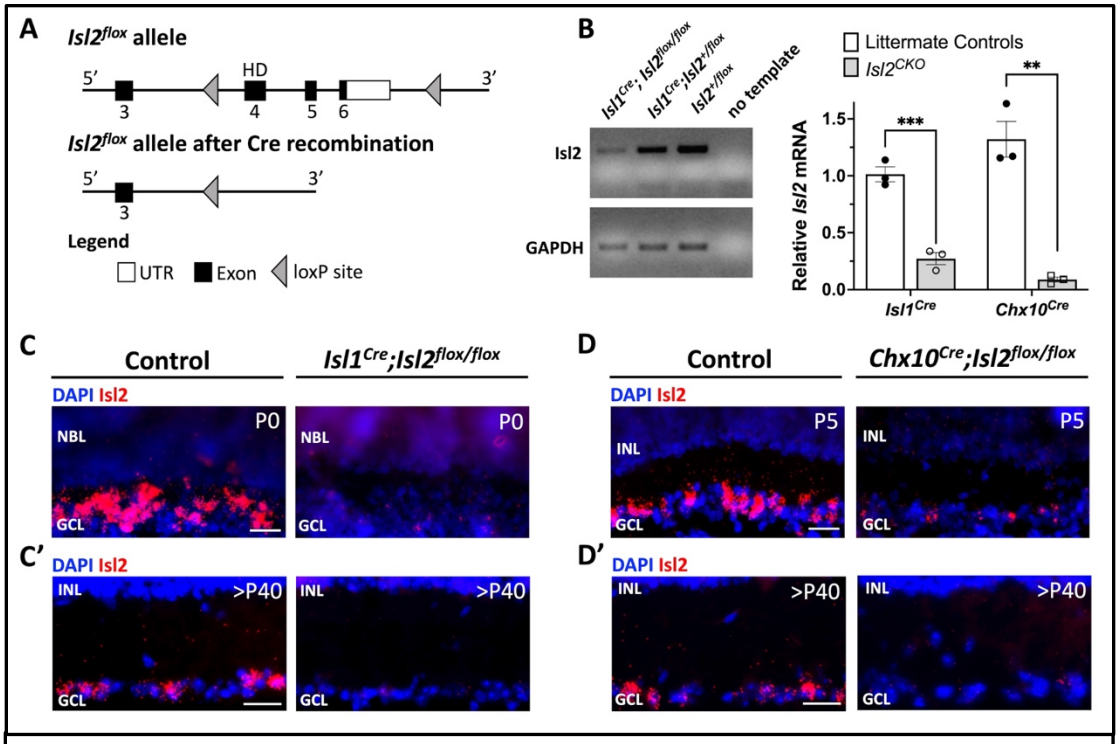

Figure 3.1 Generation and validation of *Isl2* conditional knockout mice

(A) Schematic of genetic strategy used to generate *Isl2*^{flox} mice; HD=homeodomain, UTR=untranslated region. **(B)** RT-PCR of RNA isolated from retinas shows significantly reduced Isl2 expression in both Isl2$^{CKO\text{-}Isl1}$ and Isl2$^{CKO\text{-}Chx10}$. Left, representative image of RT-PCR products ran on an agarose gel. Bands correspond to Isl2 (top) or GAPDH (bottom) which was used for normalization. Isl2$^{CKO\text{-}Isl1}$ retinas show reduced Isl2 expression. Right, graph showing relative Isl2 expression based on quantification of RT-PCR bands (n=3 each, two-tailed t-tests, ***p<0.001, ** p<0.01). **(C,C')** Fluorescent in situ hybridization of Isl2 mRNA in P0 (top) and adult (bottom) retina sections in control (left) and *Isl1*^{Cre}*;Isl2*$^{flox/flox}$ (right) mice. **(D,D')** Fluorescent in situ hybridization of Isl2 mRNA in P5 (top) and adult (bottom) retina sections in control (left) and *Chx10*^{Cre}*;Isl2*$^{flox/flox}$ (right) mice. There is a loss of Isl2 mRNA in the GCL at P0 **(C)** and P5 **(D)** in *Isl2*^{CKO} retinas, as well as a significant reduction in Isl2 mRNA in the GCL during adulthood **(C', D')**.

3.3.2 Loss of retinal Isl2 does not affect eye-specific retinogeniculate projections

Next, I wanted to determine whether the increased ipsilateral innervation of the thalamus observed by Pak et al. (2004) in newborn *Isl2*$^{-/-}$ mice persists into adulthood

(*Isl2*$^{-/-}$ mice die shortly after birth). To assess this, I performed bilateral intravitreal CTB injections in adult *Isl1*^{Cre};*Isl2*$^{flox/flox}$ mice and sacrificed the mice three days later (**Fig. 3.2**). To analyze the extent of the dLGN innervated by ipsilateral RGCs, I obtained serial coronal sections and quantified the ipsilateral and contralateral inputs into the dLGN using fluorescence microscopy (see methods). This analysis revealed that ipsilateral RGCs innervate 25.4% (± 3.1) of the dLGN in controls and 23.2% (± 3.6) in *Isl1*^{Cre};*Isl2*$^{flox/flox}$ mice (**Fig. 3.2D**) and therefore there is no significant difference in the proportion of the dLGN innervated by ipsilateral RGCs (p=0.673, two-tailed t-test). However, the size of the dLGN is significantly smaller in *Isl1*^{Cre};*Isl2*$^{flox/flox}$ mice (wt: 0.276 ± 0.009 mm^2, *Isl1*^{Cre};*Isl2*$^{flox/flox}$: 0.240 ± 0.010 mm^2, p<0.05, 2-way ANOVA); the ipsilateral projection is also smaller, but not significantly (wt: 0.071 ± 0.010 mm^2, *Isl1*^{Cre};*Isl2*$^{flox/flox}$: 0.056 ± 0.007 mm^2, p=0.462) (**Fig. 3.2F-G**). This may reflect a loss of RGC inputs due to increased RGC death (see below).

This result prompted me to determine whether the increased ipsilateral innervation into the dLGN observed in *Isl2*$^{-/-}$ mice at P0 (Pak et al., 2004) also occurs in *Isl2*^{CKO} mice at this stage. I performed bilateral intravitreal CTB injections at P0 in *Isl1*^{Cre};*Isl2*$^{flox/flox}$ mice and sacrificed them one day later (**Fig. 3.3**). In this case, I also did not find a significant difference in ipsilateral innervation of the dLGN in *Isl1*^{Cre};*Isl2*$^{flox/flox}$ mice relative to controls (**Fig. 3.3B-E**) (*Isl1*^{Cre};*Isl2*$^{flox/flox}$: 0.69 ± 0.055 vs. control: 0.70 ± 0.028, p=0.9015, two-tailed t-test). There is a reduction in the size of the dLGN (**Fig. 3.3F**) and of the area occupied by ipsilateral fibers (**Fig. 3.3G**), but neither reduction is statistically significant (dLGN area: wt: 0.144 ± 0.007

mm^2, vs. *Isl1^{Cre};Isl2$^{flox/flox}$*: 0.125 ± 0.004 mm^2, p=0.173, 2-way ANOVA, Šídák's multiple comparisons test; ipsilateral area: wt: 0.102 ± 0.009 mm^2, vs. *Isl1^{Cre};Isl2$^{flox/flox}$*: 0.086 ± 0.006 mm^2, p=0.279). The SC, another retinal recipient target, is also normally innervated by RGC axons at this age (**Fig. S3.1A**). However, there is a greater amount of axon defasciculation in the optic tract at P0 (**Fig. S3.1B,B'**). Taken together, these data suggest that *Isl2* is not required in the retina for normal eye-specific retinogeniculate or retinocollicular innervation.

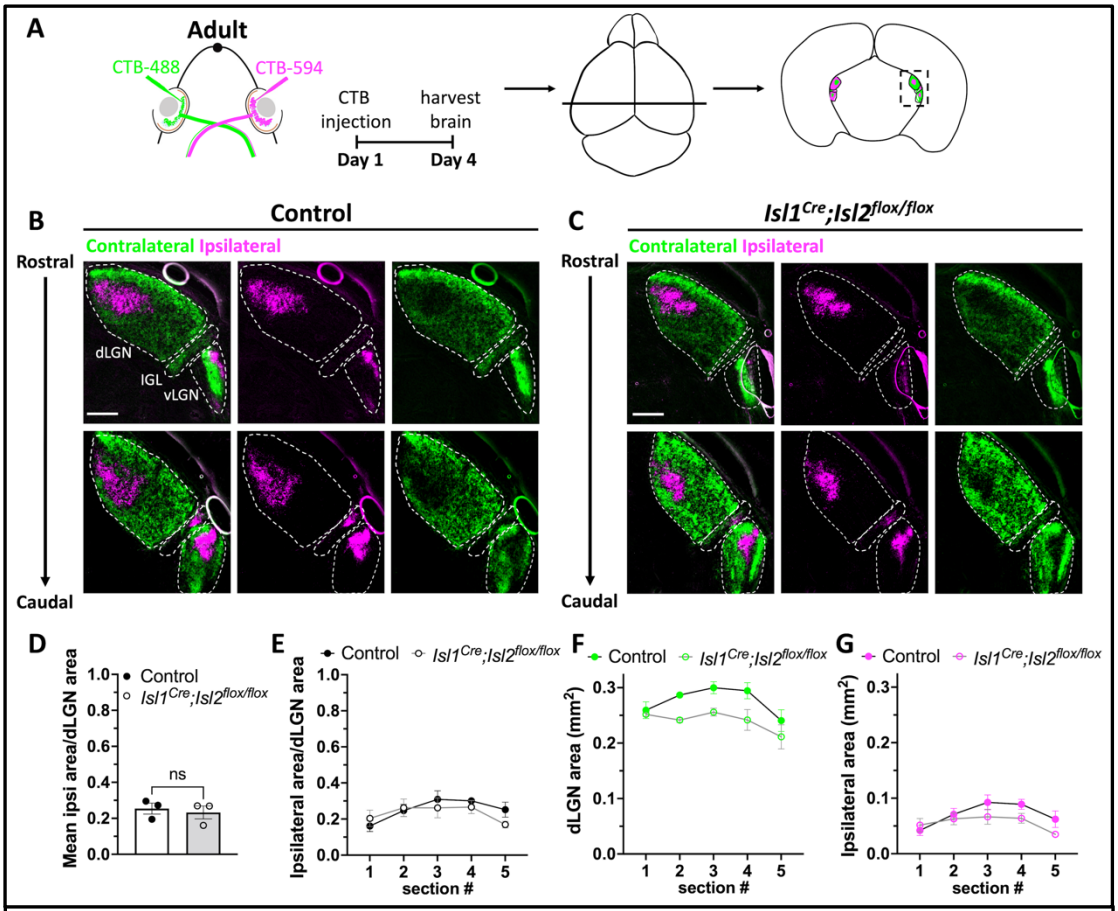

Figure 3.2 Eye-specific retinogeniculate projections are unaffected in adult *Isl1^{Cre};Isl2$^{flox/flox}$* mice

A) Schematic of experimental design. One eye of an adult mouse was intravitreally injected with CTB-488 while the contralateral eye was injected with CTB-594. Mice were sacrificed 3 days after CTB injection and their brains were sectioned coronally. (**B-C)** Coronal sections of control mouse brain **(B)** and $Isl1^{Cre};Isl2^{flox/flox}$ mouse brain **(C)** where contralateral fibers are labeled green and ipsilateral fibers are magenta, scale bar=200µm. (**D-G)** Quantification of the ipsilateral and contralateral projections in control and $Isl1^{Cre};Isl2^{flox/flox}$ mice, where **(D)** displays the mean proportion of the dLGN occupied by ipsilateral RGC axons across 5 sections and shows no significant difference (n=3, ns= not significant as $p>0.05$, two-tailed t-test). (**E-G)** display values for each of the 5 sections sequentially from rostral to caudal. There is also no difference in the extent of the dLGN innervated by ipsilateral fibers when comparing each section individually **(E)** (n=3, $p>0.05$ for each section, 2-way ANOVA, Šídák's multiple comparisons test). **F** and **G** show the mean area of the contralateral projections and of the ipsilateral projections, respectively, for each section. 2-way ANOVA reveals a significant main effect of genotype ($P<0.001$) and of section number ($P<0.05$) on the size of the dLGN, but no interaction between the two ($P=0.505$); Šídák's multiple comparisons test does not find any significant differences in dLGN size in any of the sections **(F)** (n=3, $P>0.05$ for each section). There is also a significant main effect of genotype ($P<0.05$) and of section number ($P<0.05$) on ipsilateral area, but no interaction ($P=0.0396$, 2-way ANOVA). Šídák's multiple comparisons test does not find a significant difference in ipsilateral area in any of the sections (n=3, $P>0.05$ for each section). does not reveal a significant change in any of the 5 sections (n=3, $p>0.05$ for each section, 2-way ANOVA, Šídák's multiple comparisons test). When combining data across the 5 sections in each mouse, there is a significant reduction in the size of the dLGN in $Isl1^{Cre};Isl2^{flox/flox}$ mice relative to controls but not in the size of the ipsilateral projection (n=3, 2-way ANOVA, genotype main effect: $p<0.05$, brain area main effect: $p<0.0001$, Šídák's multiple comparisons test, dLGN area: $p<0.05$, ipsilateral area: $p=0.462$).

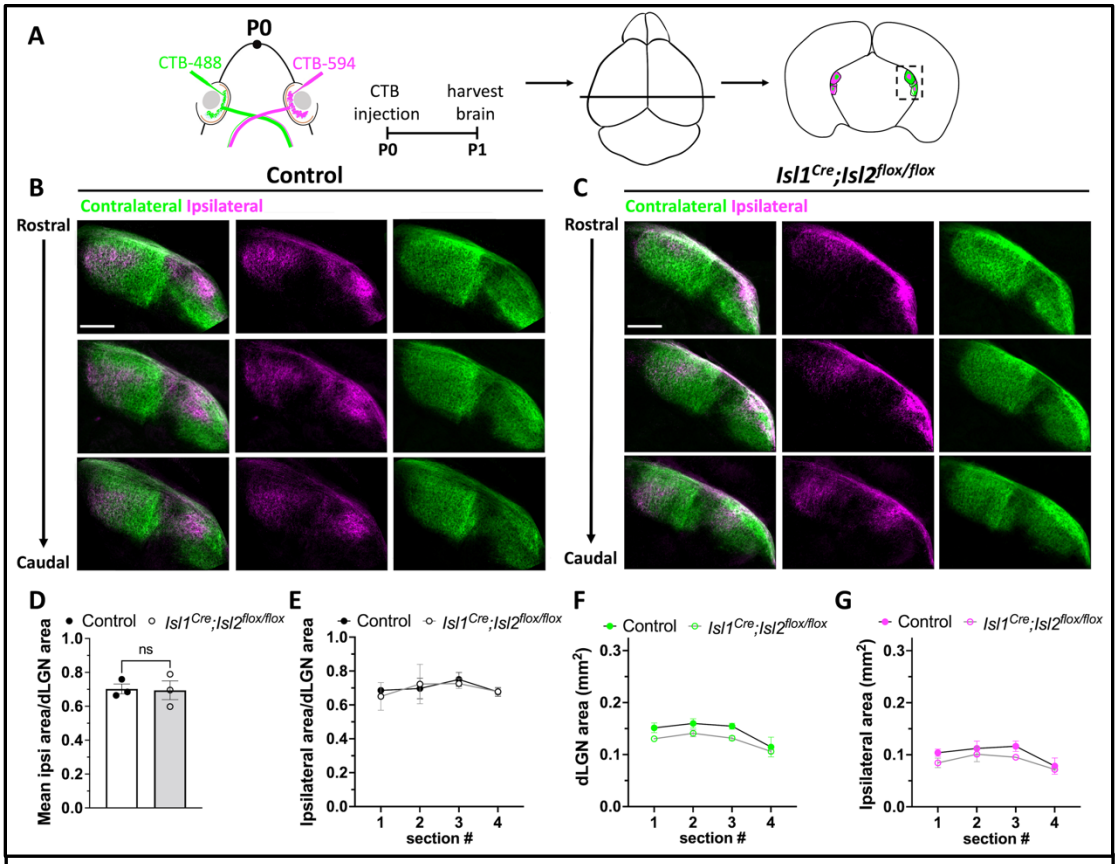

Figure 3.3 Eye-specific retinogeniculate projections are unaffected in P0 *Isl1^{Cre};Isl2$^{flox/flox}$* mice

(A) Schematic of experimental design. Each eye was intravitreally injected with CTB at P0, one eye with CTB-488 and the contralateral eye with CTB-594. Mice were sacrificed 24 hours after injection and coronal sections were obtained. (**B, C**) Coronal sections of control mouse brain **(B)** and *Isl1^{Cre};Isl2$^{flox/flox}$* mouse brain **(C)** showing contralateral (green) and ipsilateral (magenta) innervation of the dLGN from rostral (top) to caudal (bottom); contralateral=green, ipsilateral=magenta, scale bar=200µm. **(D-G)** Quantification of the ipsilateral and contralateral projections in P0 control and *Isl1^{Cre};Isl2$^{flox/flox}$* mice (n=3 each genotype) where **(D)** is the average across 4 sections and (**E-G**) display values for each of the 4 sections sequentially from rostral to caudal. (**D**) and (**E**) display the ratio of the dLGN occupied by ipsilateral RGC axons; there is no difference in the extent of the dLGN innervated by ipsilateral fibers when comparing the averages across 5 sections (**D**, $p>0.05$, two-tailed t-test) or when comparing the innervation in individual sections (**E**, $p>0.05$ for each section, 2-way ANOVA, Šídák's multiple comparisons test). **(F)** and **(G)** show the area of the contralateral projections and of the ipsilateral projections, respectively. Both show an insignificant decrease in size in the mutants relative to controls in sections 1-3. 2-way ANOVA reveals a main effect of genotype ($p<0.05$)

and section number ($p<0.01$) on the size of the dLGN, but no interaction or differences in individual sections ($p>0.05$ for each section, Šídák's multiple comparisons test). Section number has a main effect on the size of the ipsilateral projection (2-way ANOVA, $p<0.05$) but genotype does not ($p>0.05$), with no individual differences (Šídák's multiple comparisons test, $p>0.05$ for each section).

3.3.3 Isl2 is required for the development of Isl2$^+$ RGC subtypes

To determine whether Isl2 plays a role in RGC subtype specification, I assessed the expression of proteins that are known to be expressed in Isl2$^+$ RGCs. I performed a literature search for potential Isl2-RGC markers and identified Foxp2, Zic1, and Tusc5 as candidate genes that may be regulated by Isl2 (Rousso et al., 2016; Rheaume et al., 2018; Tran et al., 2019; Goetz et al., 2022). To determine if loss of Isl2 leads to decreased expression of these markers, I treated adult *Isl1^{Cre};Isl2$^{flox/flox}$* and *Chx10^{Cre};Isl2$^{flox/flox}$* retinas with antibodies directed against these proteins together with the pan-RGC marker, RBPMS (Rodriguez et al., 2014) (**Fig. 3.4A, 3.4F, 3.4K, 3.4L**). I then determined the proportion of RGCs that express each protein (**Fig. 3.4C, E, H, J, N**), their abundance (cells/mm^2) (**Fig. 3.4B, D, G, I**), as well as the abundance (cells/mm^2) of all RGCs in control and *Isl2^{CKO}* retinas (**Fig. 3.5B**). I found that significantly fewer cells express each of these markers in both *Isl2^{CKO}* Cre lines (**Fig. 3.4B-I, 3.4N**). Specifically, there is a 48% (*Isl1^{Cre};Isl2$^{flox/flox}$*: 266.9±15.6 cells/mm^2 vs. wt: 517.4 ± 21.7 cells/mm^2, $p<0.001$, two-tailed t-test) and 44% (*Chx10^{Cre};Isl2$^{flox/flox}$*: 268.7 ± 24.9 vs. 483.4 ± 19.8 cells/mm^2, $p<0.001$, two-tailed t-test) reduction in Foxp2$^+$ RGCs and a 58% (*Isl1^{Cre};Isl2$^{flox/flox}$*: 75.7 ± 11.9 cells/mm^2 vs. wt: 180.4 ± 5.9 cells/mm^2, $p=0.0014$, two-tailed t-test) and 27% reduction in Zic1$^+$ RGCs (*Chx10^{Cre};Isl2$^{flox/flox}$*: 151.3 ± 4.2 vs. 206.8 ± 4.4 cells/mm^2, $p<0.001$, two-tailed

t-test) in *Isl1*^{Cre};*Isl2*$^{flox/flox}$ and *Chx10*^{Cre};*Isl2*$^{flox/flox}$ retinas relative to their littermate controls, respectively. Foxp2 RGCs make up ~17% of all RGCs in wildtype retinas (*Isl1*^{Cre};*Isl2*$^{flox/flox}$ littermate controls: 16.9% ± 0.4; *Chx10*^{Cre};*Isl2*$^{flox/flox}$ littermate controls: 14.1% ± 0.2) and only ~10% of all RGCs in *Isl2*^{CKO} retinas (**Fig. 3.4C**) (*Isl1*^{Cre};*Isl2*$^{flox/flox}$: 10.2% ± 0.6, p=0.0008, two-tailed t-test; *Chx10*^{Cre};*Isl2*$^{flox/flox}$: 9.1% ± 0.8, p<0.01, two-tailed t-test). Zic1 RGCs make up ~6% of all RGCs in wildtype retinas (*Isl1*^{Cre};*Isl2*$^{flox/flox}$ littermate controls: 5.4% ± 0.3; *Chx10*^{Cre};*Isl2*$^{flox/flox}$ littermate controls: 6.0% ± 0.1) and only 2.7% ± 0.3 in *Isl1*^{Cre};*Isl2*$^{flox/flox}$ (p=0.0035, two-tailed t-test) (**Fig. 3.4F, H**); there is no change in the percentage of RGCs that are Zic1^{+} in *Chx10*^{Cre};*Isl2*$^{flox/flox}$ (5.5% ± 0.4, p>0.05, two-tailed t-test) retinas relative to controls (**Fig. 3.4J**). In control retina sections, 32.8% ± 1.5 of RGCs express Tusc5 while 28% ± 0.9 of RGCs are Tusc5^{+} in *Isl1*^{Cre};*Isl2*$^{flox/flox}$ sections (**Fig. 3.4L, N**) (>950 RGCs scored per genotype, p=0.052, two-tailed t-test). Tusc5 is a transmembrane protein and thus dendrites that express Tusc5 are labeled (**Fig. 3.4K-L**), which allows for visualization of the lamination pattern of Tusc5-expressing cells. To determine whether loss of *Isl2* affects dendritic lamination of Tusc5^{+} cells, which include Isl2^{+} RGC subtypes, I sectioned adult *Isl1*^{CKO} eyes and labeled the sections with antibodies directed against Tusc5 and choline acetyltransferase (ChAT), a marker of starburst amacrine cells (SACs) (**Fig. 3.4L**). SAC dendrites form 2 discrete "ChAT bands" that allow for the distinction between IPL sublaminae, with one band residing in S2 and the other in S4. Tusc5^{+} dendrites laminate within S2-S4 of the IPL, with the densest labeling occuring in between the ChAT bands (S3) (**Fig. 3.4L-M**), consistent with the

lamination of Isl2-GFP^{+} dendrites (Triplett et al., 2014). In *Isl1^{Cre};Isl2$^{flox/flox}$* mice, there is a significant reduction in Tusc5^{+} dendrite labeling in the sublaminae that lie between the ChAT bands and those that costratify with them, but not in S1, the OFF layer above the OFF-ChAT band (**Fig. 3.4L-M**). These results together show that in the absence of Isl2, the expression of Isl2^{+} RGC markers is significantly diminished.

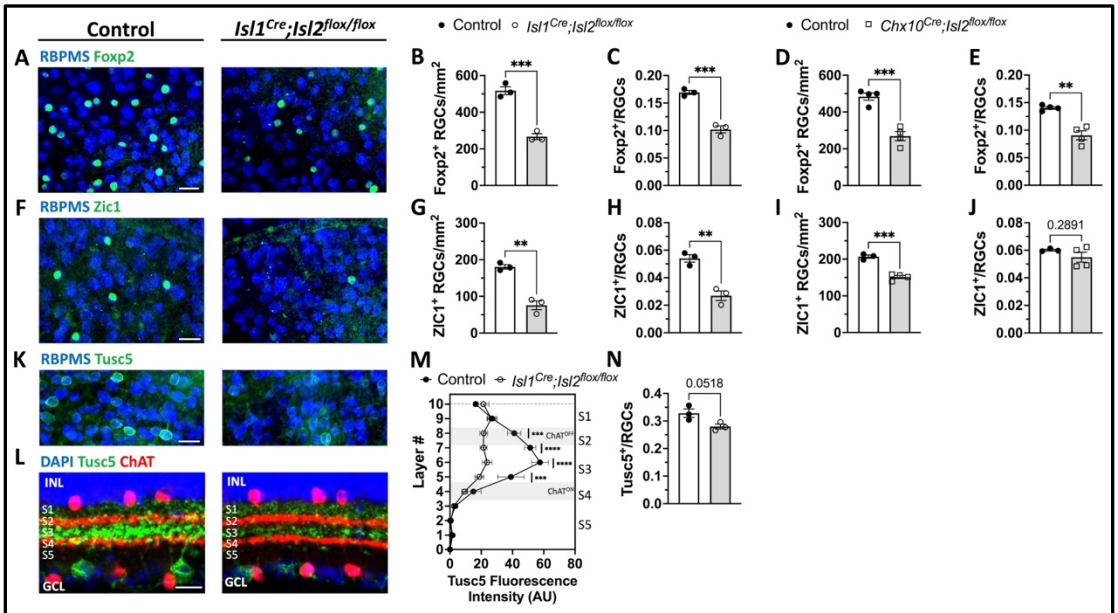

Figure 3.4 Isl2 is required for the expression of Isl2-RGC subtype markers Foxp2, Zic1, and Tusc5

(A, F, K) Flatmounted adult retinas, ganglion cell layer up, from control (left) and *Isl1^{Cre};Isl2$^{flox/flox}$* (right) mice. Retinas were treated with antibodies directed against RBPMS (blue) and Foxp2 **(A)**, Zic1 **(D)**, or Tusc5 **(G)** in green. Scale bars= 25µm. **(B, G, D, I)** Graphs showing the densities (marker+RBPMS/mm^2) of proteins indicated on Y-axes in controls and mutants; there are significantly fewer Foxp2^{+} (**B, D**) and Zic1^{+} (**G, I**) RGCs in *Isl2^{CKO}* retinas. **(C, E, H, J, N)** Graphs displaying the ratio of RGCs expressing the proteins indicated on Y-axes in controls and mutants; the proportion of RGCs expressing Foxp2 **(C, E)** is significantly reduced in *Isl2^{CKO}* retinas. The proportion of RGCs expressing Zic1 **(H, J)** is significantly reduced in *Isl1^{Cre};Isl2$^{flox/flox}$* (**H**) retinas but not in *Chx10^{Cre};Isl2$^{flox/flox}$* (**J**). There is a reduction in RGCs that express Tusc5 in *Isl1^{Cre};Isl2$^{flox/flox}$* retina sections but not statistically significant **(N)**. To generate graph **(N)**, Tusc5 expression was assessed in adult retina sections **(L)** as the dense dendritic labeling in retinal flatmounts **(K)** made quantification difficult. **(L)** Retina cross-sections from control (left) and

Isl1^{Cre}*;Isl2*$^{flox/flox}$ (right) mice were treated with DAPI (blue) and with antibodies directed against ChAT (red), Tusc5 (green), and RBPMS (not shown here).
(**M)** Tusc5^{+} RGC IPL lamination depth was quantified in control (closed circles) and mutant (open circles) retina sections and plotted here. ChAT^{+} dendrite lamination depth was also quantified and the intensity peaks (ChAT bands) are represented by the light grey bars. Layer 8 corresponds to the OFF ChAT band (~S2) and Layer 4 corresponds to the ON ChAT band (~S4). There is a significant reduction in Tusc5^{+} RGC dendrites laminating in between and costratifying with the 2 ChAT bands in mutant retinas. (**B-E, G-J, M-N)** White bars and black circles= littermate controls, grey bars= *Isl2*^{CKO}, open circles= *Isl1*^{Cre}*;Isl2*$^{flox/flox}$, open squares= *Chx10*^{Cre}*;Isl2*$^{flox/flox}$. Each circle or square represents 1 animal (n ≥ 3 for all groups); ns= not significant, *p<0.05, **p<0.01, ***p<0.001, ****p<0.0001; all graphs display mean ± SEM; two-tailed t-test for all graphs except (**M**) where 2-way ANOVA was performed followed by Šídák's multiple comparisons test.

The loss of these subtype markers could mean that, upon loss of Isl2, RGCs once fated to become an Isl2^{+} subtype now belong to other RGC classes and/or that Isl2^{+} RGC subtypes undergo cell death in the absence of Isl2. If the cells are switching fates, I hypothesize that this would lead to an increase in the number of non-Isl2 RGC classes. To test this hypothesis, I treated retinas and retina sections with an antibody directed against melanopsin, a marker of ipRGCs that is not expressed in Isl2^{+} RGCs, and found no significant change in its expression in *Chx10*^{Cre}*;Isl2*$^{flox/flox}$ compared to littermate controls (melanopsin^{+}: *Chx10*^{Cre}*;Isl2*$^{flox/flox}$: 111.8 ± 7.1 cells/mm^2 vs. control: 110.6 ± 5.0 cells/mm^2, p=0.902 , student's t-test) (**Fig. 3.5A-B**). However, there is a significant reduction in total RGC density in both conditional knockout lines with a loss of 13% in *Isl1*^{Cre}*;Isl2*$^{flox/flox}$ (2622 ± 76 cells/mm^2 vs. wt: 3027 ± 67 cells/mm^2, p<0.01, two-tailed t-test) and a loss of 15% in *Chx10*^{Cre}*;Isl2*$^{flox/flox}$ (2744 ± 107 cells/mm^2 vs. wt: 3223 ± 205 cells/mm^2, p<0.05, 2-way ANOVA, Šídák's multiple comparisons test). Given that there is decreased expression of Isl2-subtype markers

(**Fig. 3.4**), no change in expression of non-Isl2 RGC markers (**Fig. 3.5A-D**), and a loss of RGCs in *Isl2*^{CKO} retinas (**Fig. 3.5B**), I hypothesize that Isl2^{+} RGCs are selectively dying in *Isl2*^{CKO} mice. To test this hypothesis, I labeled early postnatal *Isl2*^{CKO} retinas with an antibody directed towards cleaved-caspase3, a marker of apoptosis (Srinivasan et al., 1998) (**Fig. 3.5G**). I found that there is increased expression of cleaved-caspase3 in the GCL of both *Isl1*^{Cre}*;Isl2*$^{flox/flox}$ (31 ± 4.3 cells/section vs. 17 ± 0.68 cells/section in controls, p<0.05, two-tailed t-test) and *Chx10*^{Cre}*;Isl2*$^{flox/flox}$ (71 ± 5.5 cells/section vs. 46 ± 3.5 cells/section in controls, p<0.05, two-tailed t-test) retinas at P0 (**Fig. 3.5A-B**). These data suggest that *Isl2* is important for the survival of Isl2^{+} RGC subtypes.

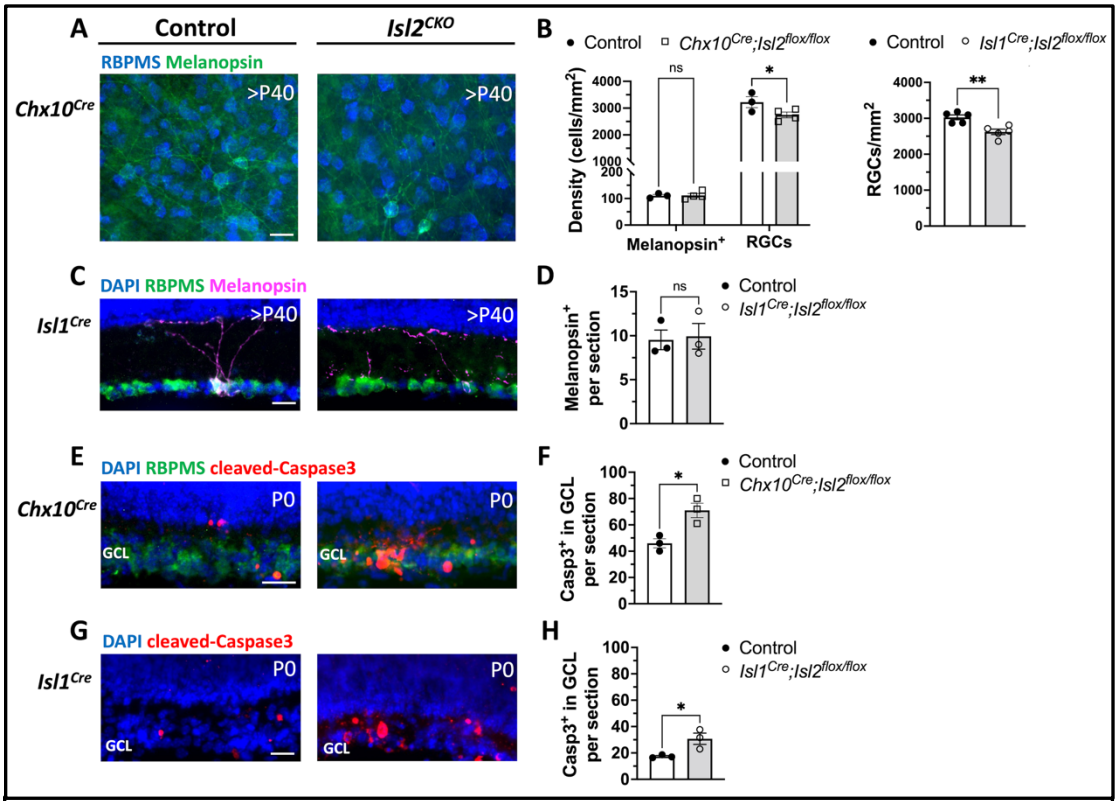

Figure 3.5 There are fewer RGCs in the adult accompanied by increased apoptosis at P0, but markers of non-Isl2 RGCs are unaffected in *Isl2*^{CKO}

(A) Flatmounted retinas, GCL up, from control (left) and *Chx10*^{Cre}*;Isl2*$^{flox/flox}$

(right) mice. Retinas were treated with antibodies directed against RBPMS (blue) and melanopsin (green); Scale bars= 25µm. **(B)** Quantification of melanopsin^{+} and RBPMS^{+} density (marker/mm^{2}) in *Chx10^{Cre};Isl2$^{flox/flox}$* (left) and of RBPMS^{+} density in *Isl1^{Cre};Isl2$^{flox/flox}$* (right) retinas reveals a significant reduction in RGC density in both *Isl2^{CKO}* models but no change in melanopsin^{+} density in *Chx10^{Cre};Isl2$^{flox/flox}$* retinas (left) relative to controls. **(C)** Images of retina sections from *Isl1^{Cre};Isl2$^{flox/flox}$* (right) and control (left) mice treated with DAPI and antibodies directed against RBPMS (green) and melanopsin (magenta) reveal no change in the proportion of RGCs that express melanopsin **(D)**. **(E, G)** Retina sections from P0 control (left) and *Isl2^{CKO}* (right) mice treated with DAPI and antibodies directed against RBPMS (green) and cleaved-caspase3 (red) (**E**) or just cleaved-caspase3 (red) (**G**) reveal a significant increase in apoptotic cells in the GCL of both *Chx10^{Cre};Isl2$^{flox/flox}$* (**E, F**) and *Isl1^{Cre};Isl2$^{flox/flox}$* (**G, H**). **(B, D, F, H)** White bars and black circles= littermate controls, grey bars= *Isl2^{CKO}*, open circles= *Isl1^{Cre};Isl2$^{flox/flox}$*, open squares= *Chx10^{Cre};Isl2$^{flox/flox}$*. Each circle or square represents 1 animal ($n \geq 3$ for all groups); ns= not significant ($p>0.05$), *$p<0.05$, **$p<0.01$; all graphs display mean ± SEM; two-tailed t-test for all analyses except for (**B, left**) where 2-way ANOVA was performed followed by Šídák's multiple comparisons test.

3.4 Discussion

Here I generated *Isl2* conditional knockout mice to investigate the role of *Isl2* in RGC specification. I found that eye-specific retinogeniculate projections are unaffected in *Isl2* conditional knockout mice in contrast to previous studies in *Isl2$^{-/-}$* mice where increased ipsilateral innervation of the LGN was observed. I do however show that Isl2 plays a role in the differentiation and survival of RGC classes that it is expressed in. *Isl2* conditional knockout retinas display reduced RGC numbers, reduced expression of proteins normally expressed in Isl2^{+} RGCs, no change in the expression of non-Isl2-RGC markers, and increased apoptosis in the early postnatal GCL. These findings illustrate that Isl2 is required in developing RGCs for their survival but not for eye-specific axon projections.

Isl2 is not required in RGCs for eye-specific axon-pathfinding

Pak et al. (2004) found that *Isl2*$^{-/-}$ mice have significantly greater ipsilateral retinogeniculate projections than their wildtype counterparts. Because these mice are subject to early postnatal lethality (Thaler et al., 2004), this phenotype was only assessed at P0, an age at which eye-specific segregation has not yet occurred (~P5; Godement et al., 1984; Ballesteros et al., 2005). The generation of *Isl2*^{CKO} mice in the present study allowed me to ask whether this phenotype persists in the adult visual system or whether it is corrected during circuit maturation. I found that developmental removal of Isl2 from the retina does not cause increased ipsilateral innervation of the dLGN in adults (**Fig. 3.2**). To determine if this is due to a correction of aberrant projections or a difference in phenotype between *Isl2*$^{-/-}$ and *Isl2*^{CKO} mice, I assessed retinogeniculate projections of early postnatal *Isl1*^{Cre}*;Isl2*$^{flox/flox}$ mice and also found no difference in ipsilateral innervation compared to littermate controls (**Fig. 3.3**). The phenotypic difference observed in our study relative to that of Pak et al. (2004) could be a function of the difference in knockout strategy. *Isl2*$^{-/-}$ mice may display a greater defect due to global loss of Isl2, whereas in our study, Isl2 knockout is restricted to Isl1^{Cre} or Chx10^{Cre}-expressing cells. Additionally, I found that both of these *Isl2*^{CKO} Cre lines exhibited incomplete knockout of Isl2 (**Fig. 3.1**); 5-10% of DAPI^{+} nuclei in the GCL express 4 or more *Isl2* transcripts as detected by RNAscope probes (5% in *Isl1*^{Cre}*;Isl2*$^{flox/flox}$, 10% in *Chx10*^{Cre}*;Isl2*$^{flox/flox}$). Another hypothesis that could explain the phenotypic discrepancy between studies is that it is due to varying times of sacrifice after CTB injection (8 hours post-injection vs. 24 hours post-injection in the present

study). We found that *Isl1*^{Cre};*Isl2*$^{flox/flox}$ mice have reduced brain size relative to their littermate controls. Previous work analyzing the rate of CTB transport in mice and other rodents estimates the rate of anterograde transport to be as slow as 10mm/day (Mikkelsen 1992). It is possible that the tracer reaches the brain quicker in the mutants owing to a shorter distance between the eye and the brain, and that 8 hours is not sufficient for the tracer to label the full extent of control RGC axons. This could explain why the images of control LGN sections in Pak et al.'s study appear to have minimal ipsilateral projections to the dLGN at P0, an age at which it has been well-established that the majority of the dLGN is covered by ipsilateral fibers (Godement et al., 1984; Ballesteros et al., 2005). However, the contralateral projection in the control appears normal by eye, weakening this hypothesis. Lastly, our method of analysis may not be as sensitive as the analyses performed in the *Isl2*$^{-/-}$ study. In the latter, the total pixel intensity above background within the entirety of the LGN (dLGN, IGL, vLGN) and the proportion of those pixels 2-5X above background thresholds were measured. Here I measured the percent of the dLGN occupied by ipsilateral fibers by dividing the area of the contralateral projection by the area of the ipsilateral projection. While this method of analysis may not reveal subtle deficits in eye-specific pathfinding, it does imply that Isl2's involvement in this process is negligible if present.

Isl2 is required for specification and/or survival of RGC subtypes

To determine whether *Isl2* is required for the specification of RGCs, I analyzed the expression of proteins that are (Foxp2, Zic1, Tusc5) and that are not (melanopsin) normally expressed in Isl2^{+} RGCs. I found reduced expression of all Isl2-RGC subtype

markers tested (**Fig. 3.4),** no effect on the expression of the ipRGC marker melanopsin (**Fig. 3.5A-D**), and a significant loss of RGCs (**Fig. 3.5B**) accompanied by increased apoptosis in the developing GCL (**Fig. 3.5 E-H)**. These results combined suggest that Isl2-RGC subtypes need Isl2 during development for their survival.

Foxp2 (forkhead box protein 2) is a transcription factor that is expressed in 5 RGC subtypes: F-mini-ON, F-mini-OFF, F-midi-ON, and F-midi-OFF (Rousso et al., 2016) were identified immunohistochemically and a novel F-RGC type was identified via RNAseq (cluster 32 [C32] in Tran et al., 2019). Isl2 is expressed in F-mini-ON (63.6%, C3), F-midi-ON (73%, C38), and the novel F-RGC type (76.6%, C32) (Tran et al., 2019). F-mini-ON RGCs are the most numerous F-RGC type, followed by F-mini-OFF RGCs, together accounting for ~13% of all RGCs. There is a 48% decrease in the density of Foxp2^{+} RGCs in *Isl1^{Cre};Isl2$^{flox/flox}$* retinas and a 44% decrease in *Chx10^{Cre};Isl2$^{flox/flox}$* retinas (**Fig. 3.4A-B, 3.4D**). Because Isl2 is not expressed in F-midi-OFF RGCs (C28) and lowly expressed in F-mini-OFF RGCs (38.9%, C4), I did not expect to see a complete loss of Foxp2-RGCs. It remains to be distinguished whether the majority of Foxp2-expressing RGCs in *Isl2^{CKO}* mice are these OFF types, but my analysis of Tusc5 expression (see below and **Fig. 3.4N**) does suggest they are. Additionally, some Foxp2-ON types may have been spared due to the incomplete knockout of Isl2.

Zic1 is a zinc-finger transcription factor that is expressed in only one subtype of RGCs, the W3B RGCs corresponding to cluster 6 (89%) from Tran et al.'s scRNAseq dataset and cluster 34 in Rheaume et al.'s scRNAseq dataset (Tran et al.,

2019; Rheaume et al., 2018). C6 happens to be the cluster that expresses the highest levels of *Isl2* according to this dataset. In addition to being expressed in W3B RGCs, Zic1 is expressed in the optic nerve, neural retina, and optic cup during development (Wan et al., 2019). There is a 58% reduction in Zic1^{+} RGC density in *Isl1^{Cre};Isl2$^{flox/flox}$* retinas (**Fig. 3.4F-H**) and a 27% reduction in *Chx10^{Cre};Isl2$^{flox/flox}$* retinas (**Fig. 3.4I-J**); Zic1 is expressed in 2.7% of RGCs in *Isl1^{Cre};Isl2$^{flox/flox}$* (**Fig. 3.4H**) retinas and in 5.4% of RGCs in retinas of their littermate controls whereas it is expressed in 5.5% of *Chx10^{Cre};Isl2$^{flox/flox}$* retinas and in 6% of RGCs in the retinas of their littermate controls (**Fig. 3.4J**). The greater defect observed in *Isl1$^{Cre/+}$;Isl2$^{flox/flox}$* could be due to the additional partial loss of *Isl1*, as Cre in this model disrupts the exon encoding the second LIM domain of *Isl1* (homozygous Isl1Cre mice are not viable) (Srinivas et al., 2001). W3B RGCs have small dendritic arbors and are high-definition 2 (HD2) cells (Zhang et al., 2012; Goetz et al., 2022). These belong to the object motion-sensitive functional group of RGCs which are responsible for distinguishing local motion in a visual scene from global motion (Kerschensteiner 2022).

Tusc5 (tumor suppressor candidate 5; also known as Trarg1—trafficking regulator of glut4) is an integral membrane protein with an intracellular C-terminus and extracellular N-terminus (Duan et al., 2018). It has been shown to regulate glucose transport in adipocytes in response to insulin by trafficking of the glucose transporter Glut4 (Beaton et al., 2015; Fazakerley et al., 2015). It is also expressed in primary somatosensory neurons (Oort et al., 2007). Interestingly, overexpression of a dominant-negative form of Isl2a in zebrafish sensory neurons has been shown to reduce

expression of Tusc5 in sensory neurons (Aoki et al., 2014). Additionally, morpholino knockdown of Tusc5 caused a reduction in peripheral and central axon extension as well as loosened fascicles. Because of its expression in dendrites and in several RGC subtypes (~15 RNAseq clusters; Tran et al., 2019), quantifying Tusc5^{+} cells in retinal flatmounts proved to be difficult, thus I assessed Tusc5 expression in retina sections. I found that *Isl1*^{Cre}*;Isl2*$^{flox/flox}$ have fewer RGCs that express Tusc5 than controls, but not to a degree that is statistically significant (**Fig. 3.4N**). However, there is a significant and specific loss of Tusc5-expressing RGC dendrites in S3 of the IPL, corresponding to where Isl2-RGC dendrites localize (Triplett et al., 2014) (**Fig. 3.4M**); Tusc5^{+} dendrites in the strictly OFF sublamina (S1) are unaffected in *Isl2*^{CKO}. Tusc5 is expressed in ~9 Isl2^{+} RGC subtypes including in Foxp2-expressing F-mini-ON RGCs and in the Zic1-expressing W3B class (Tran et al., 2019; Goetz et al., 2022). Loss of Tusc5 expression in S3 in the mutants is likely partly due to the loss of F-mini-ON and W3B RGCs. Tusc5 is also expressed in the Foxp2-expressing F-mini-OFF RGCs that express low levels of Isl2 (Tran et al., 2019; Goetz et al., 2022). The persistence of Tusc5-expressing dendrites in the OFF S1 sublamina in *Isl2*^{CKO} mice likely reflects the survival of F-mini-OFF RGCs and other non-Isl2-expressing Tusc5-RGCs.

In conclusion, this study uncovers the importance of a developmentally required transcription factor, Isl2, in RGC development and survival. Despite being long-known to be expressed in RGCs and predicted to be important for subtype specification, it was only ever studied in *Isl2*$^{-/-}$ mice who fail to develop to maturity.

3.5 Materials and Methods

3.5.1 Mice

The conditional Isl2 allele ($Isl2^{flox}$) was generated by Cyagen via CRISPR/Cas9 to insert loxP sites that flank exons 4-6 (**Fig. 1A**). The guide RNAs (gRNAs) to *Isl2* gene, the donor vector containing loxP sites, and Cas9 mRNA were co-injected into fertilized mouse eggs to generate targeted conditional knockout offspring. F0 founder animals were identified by PCR followed by sequence analysis and were bred to wildtype mice to test germline transmission and F1 animal generation. Guide RNA sequences used: Forward strand: gRNA-F1: ACTAGCCTAGGCGATCCCTT-AGG; gRNA-F2: TCCTGCAGCCGCGATCCTAG-CGG; Reverse strand: gRNA-R1: CTGCTCCTAAGGGATCGCCT-AGG; gRNA-R2: CTGCAGCCGCGATCCTAGCG-GGG. Primers used for PCR genotyping detect the first loxP site: Forward primer: 5'-GTCCTAGTCCGAGAGTGTTCCTAA-3' ; Reverse primer: 5'-TTAGAGGAAGAGGTGGAAATCGAA-3'; Product sizes: Targeted allele: 228 bp; Wildtype allele: 166 bp. Cyagen delivered us heterozygous $Isl2^{+/flox}$ mice. I bred the $Isl2^{+/flox}$ mice with each other to obtain homozygous $Isl2^{flox/flox}$ mice. I then bred the homozygotes to Isl1-Cre and Chx10-Cre mice to obtain heterozygous $Isl1^{Cre};Isl2^{+/flox}$ and $Chx10^{Cre};Isl2^{+/flox}$ progeny. These were then bred with $Isl2^{flox/flox}$ mice to generate mutant and control mice for experiments.

The Isl1-Cre mouse line (Srinivas et al., 2001) was acquired from Dr. Eric Ullien (UCSF, Department of Ophthalmology). Primers used for PCR genotyping are

as follows: Forward primer: 5'-ACCAGAGACGGAAATCCATCG-3'; Reverse primer: 5'-TGCCACGACCAAGTGACAGCAATG-3'.

The Chx10-Cre mouse line was acquired from the Jackson Laboratory (JAX stock #005105; Rowan and Cepko 2004). Primers used for PCR genotyping are as follows: Forward primer: 5'-GTCTCCTAGCCTTTGCGTTCAGAC-3'; Reverse primer: 5'-TTCGGCTATACGTAACAGGG-3'

Genotyping was performed using genomic DNA extracted from tail clippings using standard techniques.

Both female and male mice were used in this study and no significant differences were observed between them. For each experiment, 3 or more mice were used (number of mice used for each experiment is noted in the figure legends). Adult mice used in this study were between P40-P100.

All experimental procedures were performed in accordance with protocols approved by the Institutional Animal Care and Use Committee at the University of California, Santa Cruz.

3.5.2 RT-PCR

Mice were anesthetized with isoflurane and their eyes were immediately removed and placed into a dish containing ice cold 1X phosphate buffered saline (PBS; pH 7.4). Retinas were dissected out of the eyes and immediately placed into a tube containing lysis buffer (buffer RLT) from Qiagen's RNeasy Mini Kit (74104). Total RNA was subsequently extracted from the retinas using this kit. The RNA was then transcribed into cDNA using Superscript III Reverse Transcriptase (18080-044,

Invitrogen) with oligo(dT)$_{20}$ primers. PCR was performed using the following primers recognizing an exon-exon spanning region between exons 5 and 6 of Isl2: Forward: 5'-CGCCTTTCAACAGCTGGTTTC-3' (spans a region including exon 5 and exon 6) Reverse: 5'-TTCAGAGCTGGAATGGCCTG-3' (located in exon 6). Product size: 217 bp. For GAPDH, primers detect a 105 bp region between exons 5 and 6 of GAPDH: Forward: 5'-CATGGCCTTCCGTGTTCTTA-3' (located in exon 5); Reverse: 5'-CCTGCTTCACCACCTTCTTGAT-3' (located in exon 6). RT-PCR band intensities were quantified in FIJI using analyze->gels->plot lanes. The area of Isl2 peaks were normalized to those of GAPDH peaks for each sample.

3.5.3 Fluorescent in situ hybridization (FISH)

Single molecule FISH was performed with RNAscope Multiplex Fluorescent Reagent Kit V2 (Advanced Cell Diagnostics 323136) using a probe that targets Isl2 mRNA (1224951-C2 (Mm_Isl2-O1-C2) or 885511-C2 (Mm_Isl2-C2). The assay was carried out according to the manufacturer's instructions. Briefly, after intracardial perfusion with ice cold 1X PBS (pH 7.4) followed by perfusion with ice cold freshly prepared 4% paraformaldehyde (PFA), eyes were harvested and fixed in 4% PFA for 18-24 hours at 4°C. A hole was made in the cornea with fine forceps (Dumont #55) prior to immersion in PFA to allow for improved retinal fixation. After the fixation period, eyes were transferred to 30% sucrose in 1X PBS overnight (4°C) for cryoprotection. The eyes were then frozen in Tissue Plus™ O.C.T. compound (Fisher HealthCare) using dry ice. The frozen eyes were sectioned 14µm thick via cryostat (Leica cm 3050s) onto SuperFrost Plus slides (Fisher Scientific). Slides were placed in

the freezer for at least 2 hours before proceeding with the protocol. Next, slides were pretreated, probes were hybridized, amplified, and signal was developed. TSA vivid fluorophore 520 and TSA vivid fluorophore 570 were used (Tocris 323271 and 323272, respectively). Slides were coverslipped with ProLong™ Gold Antifade Mountant (invitrogen P10144).

3.5.4 Retinogeniculate axon tracing

For adult retinogeniculate tracing, mice were anesthetized with isoflurane and a hole was created at the corneal-scleral junction of each eye with a 26 gauge BD Precisionglide® needle (BD-305110). The vitreous humor was gently massaged out with a cotton swab in order to minimize back-pressure upon injection of virus. A pulled glass pipette preloaded with CTB was inserted into the hole and a Picospritzer III (Parker) was used to administer ~1 µl of CTB-488 (8mg/mL in 1x PBS; invitrogen C22841) or CTB-594 (8mg/mL in 1x PBS; invitrogen C22842) . Mice were sacrificed 3 days after bilateral anterograde tracer injections. Mice were anesthetized with isoflurane and then intracardially perfused with PBS followed by perfusion with 4% PFA. Brains were harvested and fixed in 4% PFA for 24 hours (4°C) and subsequently cryopreserved in 30% sucrose in 1X PBS for at least 24 hours (4°C). 100µM thick coronal sections were obtained using a freezing sliding microtome (ThermoFisher microm hm430). Sections were mounted onto SuperFrost Plus slides (Fisher Scientific) and coverslipped with Fluoromount-G (SouthernBiotech).

For P0 retinogeniculate tracing, pups were anesthetized on ice, their eyelids were cut, and CTB injections were performed as described above for adult tracing. Pups

were warmed in a 37°C incubator and allowed to recover prior to being reintroduced to their mother. They were sacrificed 24 hours later on P1 where they were re-anesthetized on ice and intracardially perfused with 4% PFA. Brains were dissected out of skulls under a dissecting microscope using fine forceps (Dumont #55). Fixation, cryopreservation, sectioning, and mounting of sections were all performed as described above for adult brains.

3.5.5 Immunohistochemistry

Eyes were harvested from mice after intracardial perfusion with PBS followed by perfusion with 4% PFA. For retinal wholemount staining, retinas were dissected out of the eye in PBS and subsequently fixed in 4% PFA for 1 hour at room temperature. For retina sections, a hole was made in the cornea with forceps before immersing eyes in 4% PFA for 1 hour at room temperature. Eyes were subsequently transferred to 30% sucrose for 24 hours (4°C) before being frozen in O.C.T. using dry ice. 20 μm thick sections were obtained via cryostat (Leica cm 3050s) and collected onto SuperFrost Plus slides (Fisher Scientific).

Wholemount retinas were incubated in blocking solution (5% donkey serum, 0.25% TritonX-100 in PBS) for 3 hours at room temperature (RT), incubated in primary antibody for 2–3 days at 4°C, washed 3 times (2 hours each wash) with 0.1% PBST (PBS with TritonX- 100) at RT, incubated in secondary antibody overnight at 4°C, washed 3 times (2 hours each wash) with PBS at RT. They were then mounted retinal ganglion cell layer (GCL) side up onto SuperFrost Plus slides where relieving cuts were

made. Fluoromount-G tissue mounting medium (SouthernBiotech) was applied prior to coverslipping.

For retina sections, slides were incubated in blocking solution for 1 hour, incubated in primary antibody overnight at 4°C, washed 3 times (15 min each wash) in PBS at RT, incubated in secondary antibody for 1-3 hours at RT, incubated in DAPI (1:1000) for 10 min, washed 3 times (15 min each wash) in PBS at RT, and lastly covered with fluoromount-G (SouthernBiotech) and coverslipped.

The following antibodies were used in this study: primary antibodies: goat anti-Zic1(1:200; R&D Systems AF4978), guinea pig anti-RBPMS(1:250; PhosphoSolutions 1832-RBPMS), rabbit anti-melanopsin (1:500 wholemount, 1:1000 sections; Advanced Targeting Systems AB-N39), goat anti-ChAT(1:200; Millipore AB144P), mouse anti-Tusc5(1:200; Santa Cruz Biotechnology sc-377025), rabbit anti-foxp2(1:1000; Abcam ab16046), goat anti-foxp2(1:500; Abcam ab1307); secondary antibodies: all secondaries used in this study were raised in donkey against the appropriate host species and were conjugated to Alexa Fluor (AF) 488, AF555, AF568, AF594, or AF647 (each was used at 1:1000; Invitrogen or Jackson ImmunoResearch).

3.5.6 Image acquisition

An Olympus BX51 fluorescence microscope equipped with a Qimaging Retiga EXi Fast 1394 camera was used to obtain images. Field of view (FOV) dimensions: 4X, 2223.63 µm x 1661.34 µm;10X, 890.6 µm x 665.39 µm; 20X, 446.15 µm × 333.33 µm).

3.5.7 Data analysis

For quantification of cells expressing *Isl2* mRNA, images of retina sections were taken at 40X and FIJI's multi-point tool was used to count $Isl2^+$ cells in the GCL. $DAPI^+$ nuclei in the GCL containing 4 or more $Isl2^+$ puncta (as detected by RNAscope probes) were considered $Isl2^+$ without regard to their fluorescence intensity. 300 or more cells were quantified per animal.

For adult retinogeniculate tracing, images of the LGN were taken under 4X magnification. 5 sequential sections spanning the same region along the rostrocaudal axis were analyzed in each mouse, with section 1 being rostral and 5 caudal. The area of the dLGN was measured in FIJI by tracing the contralateral projection using the freehand selection tool. The area of the ipsilateral projection was also measured with this tool and the proportion of the dLGN innervated by ipsilateral axons was calculated (ipsilateral area/ dLGN area). The average ipsilateral innervation ratio was calculated across the 5 sections for each animal.

For P0 retinogeniculate tracing, images of the LGN were taken under 10X magnification. 4 sequential sections spanning the same region along the rostrocaudal axis were analyzed in each mouse, with section 1 being rostral and 4 caudal. Measurements and analyses across the 4 sections were performed as described above for adult tracing.

For quantification of cell density in wholemount retinas, FIJI's multi-point tool was used to count cells in 4-12 FOVs per retina under 20X magnification. For each experiment, the same relative regions of the retina were quantified across animals and included 1-3 FOVs per retina quadrant. One retina was quantified per mouse.

To determine the IPL lamination depths of Tusc5$^+$ and ChAT$^+$ dendrites, images of retina sections were obtained using the 20X objective and analyzed using FIJI's IPLaminator plugin (Li et al., 2016). Straight regions of the IPL were selected for analysis using the rectangle tool, with boundaries at the edge of DAPI$^+$ nuclei in the GCL and INL. 5-6 regions (3000 μm^2 or greater each) were analyzed per mouse, including regions from 3 or more sections. The "n Equal boundaries" method was used to divide the INL regions into 10 equal layers. The layer of the IPL closest to the GCL corresponds to layer 1 and the layer closest to the INL corresponds to layer 10. The plugin measured the normalized fluorescence intensities of each marker within each layer. For each retina, the average fluorescence intensity across all 5 or 6 regions was calculated for each layer.

Statistical analyses and graph generation were performed using GraphPad's Prism 9 software. Statistical tests and number of animals used for each experiment are indicated in the figure legends.

3.6 Supplementary Figures

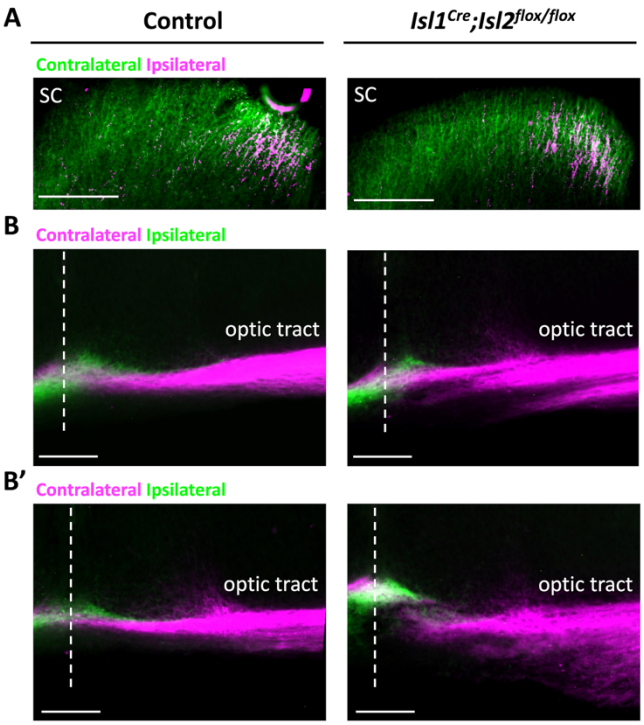

Figure S3.1 Eye-specific RGC axon tracing to the SC and through the optic tract

(A) Coronal sections of the anterior SC of a control (left) and *Isl1*^{Cre}*;Isl2*$^{flox/flox}$ (right) mouse at P1 (same mice as **Fig. 3.3**). Ipsilateral RGC axons are displayed in magenta and contralateral axons are in green; scale bars= 200 µm. The SC does not display increased ipsilateral innervation in *Isl1*^{Cre}*;Isl2*$^{flox/flox}$. **(B,B')** Coronal sections showing the contralateral optic tract in magenta of control (left) and *Isl1*^{Cre}*;Isl2*$^{flox/flox}$ (right) mice; scale bars= 100 µm. Dashed lines indicate the midline. Sections in **(B)** and **(B')** are from different animals (2 examples shown for each genotype). *Isl1*^{Cre}*;Isl2*$^{flox/flox}$ mice display increased defasciculation in the contralateral optic tract.

3.7 Bibliography

Al-Khindi T, Sherman MB, Kodama T, Gopal P, Pan Z, Kiraly JK, Zhang H, Goff LA, du Lac S, Kolodkin AL. 2022. The transcription factor Tbx5 regulates direction-selective retinal ganglion cell development and image stabilization. Curr Biol. 32(19):4286-4298.e5. doi:10.1016/j.cub.2022.07.064.

Aranda ML, Schmidt TM. 2021. Diversity of intrinsically photosensitive retinal ganglion cells: circuits and functions. Cell Mol Life Sci. 78:887–907. doi:10.1007/s00018-020-03641-5.

Assali A, Gaspar P, Rebsam A. 2014. Activity dependent mechanisms of visual map formation-From retinal waves to molecular regulators. Semin Cell Dev Biol. 35:136–146. doi:10.1016/j.semcdb.2014.08.008.

Baden T, Berens P, Franke K, Román Rosón M, Bethge M, Euler T. 2016. The functional diversity of retinal ganglion cells in the mouse. Nature. 529(7586):345–350. doi:10.1038/nature16468.

Bae JA, Mu S, Kim JS, Turner NL, Tartavull I, Kemnitz N, Jordan CS, Norton AD, Silversmith WM, Prentki R, et al. 2018. Digital Museum of Retinal Ganglion Cells with Dense Anatomy and Physiology. Cell. 173(5):1293-1306.e19. doi:10.1016/j.cell.2018.04.040.

Ballesteros JM, Van Der List DA, Chalupa LM. 2005. Formation of eye-specific retinogeniculate projections occurs prior to the innervation of the dorsal lateral geniculate nucleus by cholinergic fibers. Thalamus Relat Syst. 3(2):157–163. doi:10.1017/S1472928807000167.

Beaton N, Rudigier C, Moest H, Müller S, Mrosek N, Röder E, Rudofsky G, Rülicke T, Ukropec J, Ukropcova B, et al. 2015. TUSC5 regulates insulin-mediated adipose tissue glucose uptake by modulation of GLUT4 recycling. Mol Metab. 4(11):795–810. doi:10.1016/j.molmet.2015.08.003

Berson DM, Dunn FA, Takao M. 2002. Phototransduction by retinal ganglion cells that set the circadian clock. Science. 295(5557):1070–1073. doi:10.1126/science.1067262.

Burmeister M, Novak J, Liang M, Basu S, Ploder L, Hawes NL, Vidgen D, Hoover F, Goldman D, Kalnins VI, et al. 1996. Ocular retardation mouse caused by Chx10 homeobox null allele: impaired retinal progenitor proliferation and bipolar cell differentiation. Nat Genet. 12(April):376–384. doi:10.1038/ng0496-376.

Chen C, Kiyama T, Weber N, Whitaker CM, Pan P, Badea TC, Massey SC, Mao C. 2021. Characterization of Tbr2-expressing retinal ganglion cells. J Comp Neurol.:1–20. doi:10.1002/cne.25208.

Chowdary PD, Che DL, Cui B. 2012. Neurotrophin signaling via long-distance axonal transport. Annu Rev Phys Chem. 63:571–594. doi:10.1146/annurev-physchem-032511-143704.

Damiani D, Alexander JJ, O'Rourke JR, McManus M, Jadhav AP, Cepko CL, Hauswirth WW, Harfe BD, Strettoi E. 2008. Dicer inactivation leads to progressive functional and structural degeneration of the mouse retina. J Neurosci. 28(19):4878–4887. doi:10.1523/JNEUROSCI.0828-08.2008.

Dräger UC. 1985. Birth dates of retinal ganglion cells giving rise to the crossed and uncrossed optic projections in the mouse. Proc R Soc London - Biol Sci. 224(1234):57–77. doi:10.1098/rspb.1985.0021.

Duan X, Krycer JR, Cooke KC, Yang G, James DE, Fazakerley DJ. 2018. Membrane Topology of Trafficking Regulator of GLUT4 1 (TRARG1). Biochemistry. 57(26):3606–3615. doi:10.1021/acs.biochem.8b00361.

Elshatory Y, Deng M, Xie X, Gan L. 2007. Expression of the LIM-Homeodomain Protein Isl1 in the Developing and Mature Mouse Retina. J Comp Neurol. 503(October 2007):182–197. doi:10.1002/cne.

Fazakerley DJ, Naghiloo S, Chaudhuri R, Koumanov F, Burchfield JG, Thomas KC, Krycer JR, Prior MJ, Parker BL, Murrow BA, et al. 2015. Proteomic analysis of GLUT4 storage vesicles reveals tumor suppressor candidate 5 (TUSC5) as a novel regulator of insulin action in adipocytes. J Biol Chem. 290(39):23528–23542. doi:10.1074/jbc.M115.657361.

Godement P, Salaün J, Imbert M. 1984. Prenatal and postnatal development of retinogeniculate and retinocollicular projections in the mouse. J Comp Neurol. 230(4):552–575. doi:10.1002/cne.902300406.

Goetz J, Jessen ZF, Jacobi A, Mani A, Cooler S, Greer D, Kadri S, Segal J, Shekhar K, Sanes J, et al. 2022. Unified Classification of Mouse Retinal Ganglion Cells Using Function, Morphology, and Gene Expression. Cell Rep. 40(111040):1–17. doi:10.2139/ssrn.3867730. Doi: 10.1016/j.celrep.2022.111040.

Hattar S, Liao HW, Takao M, Berson DM, Yau KW, Heller HC, O'Hara BF. 2002. Melanopsin-Containing Retinal Ganglion Cells: Architecture, Projections, and Intrinsic Photosensitivity. Science. 295(5557):1065–1070. doi:10.1126/science.1069609.

Herrera E, Brown L, Aruga J, Rachel RA, Dolen G, Mikoshiba K, Brown S, Mason CA. 2003. Zic2 patterns binocular vision by specifying the uncrossed retinal projection. Cell. 114(5):545–557. doi:10.1016/S0092-8674(03)00684-6.

Kerschensteiner D. 2022. Feature Detection by Retinal Ganglion Cells. Annu Rev Vis Sci. 8:135–169. doi:10.1146/annurev-vision-100419-112009.

Kiyama T, Long Y, Chen C-K, Whitaker CM, Shay A, Wu H, Badea TC, Mohsenin A, Parker-Thornburg J, Klein WH, et al. 2019. Essential Roles of Tbr1 in the Formation and Maintenance of the Orientation-Selective J-RGCs and a Group of OFF-Sustained RGCs in Mouse. Cell Rep. 27(3):900-915.e5. doi:10.1016/j.celrep.2019.03.077.

Liu ISC, Chen J de, Ploder L, Vidgen D, van der Kooy D, Kalnins VI, Mclnnes RR. 1994. Developmental expression of a novel murine homeobox gene (Chx10): Evidence for roles in determination of the neuroretina and inner nuclear layer. Neuron. 13(2):377–393. doi:10.1016/0896-6273(94)90354-9.

Lyu J, Mu X. 2021. Genetic control of retinal ganglion cell genesis. Cell Mol Life Sci. 78(9):4417–4433. doi:10.1007/s00018-021-03814-w.

Mao C-A, Kiyama T, Pan P, Furuta Y, Hadjantonakis A-K, Klein WH. 2008. Eomesodermin, a target gene of Pou4f2, is required for retinal ganglion cell and optic nerve development in the mouse. Development. 135(2):271–280. doi:10.1242/dev.009688.

Mao C-A, Li H, Zhang Z, Kiyama T, Panda S, Hattar S, Ribelayga CP, Mills SL, Wang SW. 2014. T-box Transcription Regulator Tbr2 Is Essential for the Formation and Maintenance of Opn4/Melanopsin-Expressing Intrinsically Photosensitive Retinal Ganglion Cells. J Neurosci. 34(39):13083–13095. doi:10.1523/JNEUROSCI.1027-14.2014.

Marler KJ, Suetterlin P, Dopplapudi A, Rubikaite A, Adnan J, Maiorano NA, Lowe AS, Thompson ID, Pathania M, Bordey A, et al. 2014. BDNF promotes axon branching of retinal ganglion cells via miRNA-132 and p250GAP. J Neurosci. 34(3):969–979. doi:10.1523/JNEUROSCI.1910-13.2014.

Marcos S, Nieto-Lopez F, Sandonìs A, Cardozo MJ, Di Marco F, Esteve P, Bovolenta P. 2015. Secreted frizzled related proteins modulate pathfinding and fasciculation of mouse retina ganglion cell axons by direct and indirect mechanisms. J Neurosci. 35(11):4729–4740. doi:10.1523/JNEUROSCI.3304-13.2015.

Martin P.R. 1986. The projection of different retinal ganglion cell classes to the dorsal lateral geniculate nucleus in the hooded rat. Exp Brain Res. 62(1986):77–88. doi:10.1007/BF00237404.

Mikkelsen JD. 1992. Visualization of efferent retinal projections by immunohistochemical identification of cholera toxin subunit B. Brain Res Bull. 28:619–623. doi:10.1016/0361-9230(92)90112-B.

Oort PJ, Warden CH, Baumann TK, Knotts TA, Adams SH. 2007. Characterization of Tusc5, an adipocyte gene co-expressed in peripheral neurons. Mol Cell Endocrinol. 276(1–2):24–35. doi:10.1016/j.mce.2007.06.005.

Ozturk H, Cingoz H, Tufan T, Yang J, Adair SJ, Tummala KS, Kuscu C, Kinali M, Comertpay G, Nagdas S, et al. 2022. ISL2 is a putative tumor suppressor whose epigenetic silencing reprograms the metabolism of pancreatic cancer. Dev Cell. 57(11):1331-1346.e9. doi:10.1016/j.devcel.2022.04.014.

Pak W, Hindges R, Lim YS, Pfaff SL, O'Leary DDM. 2004. Magnitude of binocular vision controlled by islet-2 repression of a genetic program that specifies laterality of retinal axon pathfinding. Cell. 119(4):567–578. doi:10.1016/j.cell.2004.10.026.

Peng YR, Tran NM, Krishnaswamy A, Kostadinov D, Martersteck EM, Sanes JR. 2017. Satb1 Regulates Contactin 5 to Pattern Dendrites of a Mammalian Retinal Ganglion Cell. Neuron. 95(4):869-883.e6. doi:10.1016/j.neuron.2017.07.019.

Qi L, Wang ZY, Shao XR, Li M, Chen SN, Liu XQ, Yan S, Zhang B, Zhang Xu Dong, Li X, et al. 2020. ISL2 modulates angiogenesis through transcriptional regulation of ANGPT2 to promote cell proliferation and malignant transformation in oligodendroglioma. Oncogene. 39(37):5964–5978. doi:10.1038/s41388-020-01411-y.

Rachel RA, Dölen G, Hayes NL, Lu A, Erskine L, Nowakowski RS, Mason CA. 2002. Spatiotemporal Features of Early Neuronogenesis Differ in Wild-Type and Albino Mouse Retina. J Neurosci. 22(11):4249–4263. doi:10.1523/jneurosci.22-11-04249.2002.

Rheaume BA, Jereen A, Bolisetty M, Sajid MS, Yang Y, Renna K, Sun L, Robson P, Trakhtenberg EF. 2018. Single cell transcriptome profiling of retinal ganglion cells identifies cellular subtypes. Nat Commun. 9(2759):1–17. doi:10.1038/s41467-018-05134-3.

Rodriguez AR, Perez De Sevilla Muller L, Brecha NC. 2014. The RNA Binding Protein RBPMS is a Selective Marker of Ganglion Cells in the Mammalian Retina. J Comp Neurol. 522:1411–1443. doi:10.1002/cne.23521.

Rousso DL, Qiao M, Kagan RD, Yamagata M, Palmiter RD, Sanes JR. 2016. Two Pairs of ON and OFF Retinal Ganglion Cells Are Defined by Intersectional Patterns of Transcription Factor Expression. Cell Rep. 15(9):1930–1944. doi:10.1016/j.celrep.2016.04.069.

Rowan S, Cepko CL. 2004. Genetic analysis of the homeodomain transcription factor Chx10 in the retina using a novel multifunctional BAC transgenic mouse reporter. Dev Biol. 271(2):388–402. doi:10.1016/j.ydbio.2004.03.039.

Sanes JR, Masland RH. 2015. The Types of Retinal Ganglion Cells: Current Status and Implications for Neuronal Classification. Annu Rev Neurosci. 38(1):221–246. doi:10.1146/annurev-neuro-071714-034120.

Schmitt AM, Shi J, Wolf AM, Lu CC, King LA, Zou Y. 2006. Wnt-Ryk signalling mediates medial-lateral retinotectal topographic mapping. Nature. 439(7072):31–37. doi:10.1038/nature04334.

Srinivas S, Watanabe T, Lin CS, William CM, Tanabe Y, Jessell TM, Costantini F. 2001. Cre reporter strains produced by targeted insertion of EYFP and ECFP into the ROSA26 locus. BMC Dev Biol. 1:1–8. doi:10.1186/1471-213X-1-4.

Srinivasan A, Roth KA, Sayers RO, Shindler KS, Wong AM, Fritz LC, Tomaseili KJ. 1998. In situ immunodetection of activated caspase-3 in apoptotic neurons in the developing nervous system. Cell Death Differ. 5(12):1004–1016. doi:10.1038/sj.cdd.4400449.

Stael S, Miller LP, Fernandez-Fernandez AD, Van Breusegem F. 2022. Detection of Damage-Activated Metacaspase Activity by Western Blot in Plants Simon. In: Plant Proteases and Plant Cell Death: Methods and Protocols. Vol. 2447. p. 127–137.

Sweeney NT, Tierney H, Feldheim DA. 2014. Tbr2 Is Required to Generate a Neural Circuit Mediating the Pupillary Light Reflex. J Neurosci. 34(16):5447–5453. doi:10.1523/JNEUROSCI.0035-14.2014.

Sweeney NT, James KN, Nistorica A, Lorig-Roach RM, Feldheim DA. 2017. Expression of transcription factors divides retinal ganglion cells into distinct classes. J Comp Neurol.(December 2016):1–11. doi:10.1002/cne.24172.

Thaler JP, Koo SJ, Kania A, Lettieri K, Andrews S, Cox C, Jessell TM, Pfaff SL. 2004. A Postmitotic Role for Isl-Class LIM Homeodomain Proteins in the Assignment of Visceral Spinal Motor Neuron Identity. Neuron. 41(3):337–350. doi:10.1016/S0896-6273(04)00011-X.

Tran NM, Shekhar K, Whitney IE, Jacobi A, Benhar I, Hong G, Yan W, Adiconis X, Arnold ME, Lee JM, et al. 2019. Single-cell profiles of retinal neurons differing in resilience to injury reveal neuroprotective genes. Neuron. 104:1–17. doi:10.1016/j.neuron.2019.11.006.

Triplett JW, Wei W, Gonzalez C, Sweeney NT, Huberman AD, Feller MB, Feldheim DA. 2014. Dendritic and axonal targeting patterns of a genetically-specified class of retinal ganglion cells that participate in image-forming circuits. Neural Dev.:1–13.

Wan Y, White C, Robert N, Rogers MB, Szabo-Rogers HL. 2019. Localization of Tfap2β, Casq2, Penk, Zic1, and Zic3 Expression in the Developing Retina, Muscle, and Sclera of the Embryonic Mouse Eye. J Histochem Cytochem. 67(12):863–871. doi:10.1369/0022155419885112.

Zhang Y, Kim IJ, Sanes JR, Meister M. 2012. The most numerous ganglion cell type of the mouse retina is a selective feature detector. Proc Natl Acad Sci U S A. 109(36):E2391–E2398. doi:10.1073/pnas.1211547109.